MARCELA ULI PEIXOTO ARAUJO

PHYSIOLOGICAL AND BIOCHEMICAL ASPECTS OF SILICON AND MAGNESIUM INTERACTION AND OF THE ACIDS BETA-AMINOBUTYRIC AND GAMMA-AMINOBUTYRIC IN THE POTENTIATION OF WHEAT RESISTANCE AGAINST BLAST

Thesis presented to the Universidade Federal de Viçosa, as part of the requirements of the Graduate Program in Plant Pathology, to obtain the title of *Doctor Scientiae*.

Advisor: Fabrício de Ávila Rodrigues

VIÇOSA - MINAS GERAIS
2021

Ficha catalográfica elaborada pela Biblioteca Central da Universidade Federal de Viçosa - Campus Viçosa

T
A663p
2021

Araujo, Marcela Uli Peixoto, 1990-
Physiological and biochemical aspects of silicon and magnesium interaction and of the acids beta-aminobutyric and gamma-aminobutyric in the potentiation of wheat resistance against blast / Marcela Uli Peixoto Araujo. – Viçosa, MG, 2021.
1 tese eletrônica (132 f.): il. (algumas color.).

Orientador: Fabrício de Ávila Rodrigues.
Tese (doutorado) - Universidade Federal de Viçosa, Departamento de Fitopatologia, 2021.
Inclui bibliografia.
DOI: https://doi.org/10.47328/ufvbbt.2021.169
Modo de acesso: World Wide Web.

1. Plantas - Resistência a doenças e pragas. 2. Aminoácidos. 3. Fungos fitopatogênicos. 4. Plantas - Nutrição. 5. Stress oxidativo. 6. Plantas - Efeito dos minerais. 7. Fisiologia vegetal. I. Rodrigues, Fabrício de Ávila, 1974-. II. Universidade Federal de Viçosa. Departamento de Fitopatologia. Programa de Pós-Graduação em Fitopatologia. III. Título.

CDD 22. ed. 632.46

Bibliotecário(a) responsável: Renata de Fátima Alves CRB6/2578

MARCELA ULI PEIXOTO ARAUJO

PHYSIOLOGICAL AND BIOCHEMICAL ASPECTS OF SILICON AND MAGNESIUM INTERACTION AND OF THE ACIDS BETA-AMINOBUTYRIC AND GAMMA-AMINOBUTYRIC IN THE POTENTIATION OF WHEAT RESISTANCE AGAINST BLAST

Thesis presented to the Universidade Federal de Viçosa, as part of the requirements of the Graduate Program in Plant Pathology, to obtain the title of *Doctor Scientiae*.

APPROVED: October 22, 2021

Assent:

Marcela Uli Peixoto Araujo
Marcela Uli Peixoto Araujo
Author

Fabrício Ávila Rodrigues
Fabrício de Ávila Rodrigues
Advisor

I dedicate to my parents, Eliomar Silva Araujo and Ana Maria Peixoto Araujo, and my fiance, Eluardo Marques, for the love and unconditional support in all stages of this achievement.

ACKNOWLEDGMENTS

First of all, I thank God for the blessings and opportunities.

I want to express my sincere thanks to:

My parents, Eliomar Silva Araujo and Ana Maria Peixoto Araujo, and my fiance, Eluardo Marques, for their support, trust, love, words of encouragement, understanding, and all their efforts for the accomplishment of this new phase of my professional life.

Professor Fabrício Ávila Rodrigues, a great professor and researcher, for his great guidance, support, and understanding.

My colleagues from Laboratory of Host-Pathogen Interaction for their friendship, knowledge sharing, and contribution to this research.

All my friends that support me during this journey.

UFV employees, especially Mr. Mário, Mr. Daniel, Mr. Delfim, Mr.Bruno, and Mrs. Sara.

Thanks are due to Universidade Federal de Viçosa (UFV), Department of Plant Pathology, Laboratory of Host-Pathogen Interaction, and the Postgraduate Program in Plant Pathology for providing me all the necessary conditions for the development of this research.

I thank the Coordenação de Aperfeiçoamento de Pessoal de Nível Superior (CAPES) for the financial support.

I thank all whom contributed directly or indirectly to this research.

THANK YOU!

BIOGRAPHY

MARCELA ULI PEIXOTO ARAUJO, daughter of Eliomar Silva Araujo and Ana Maria Peixoto Araujo, was born on May 25, 1990, in São Luís, Maranhão, Brazil.

In March 2015, she graduated from Universidade Estadual do Maranhão with a Bachelor in Agronomy. In July 2017, she obtained the *Master Scientiae* in Plant Pathology at Universidade Federal de Viçosa (UFV). In August 2017, she started the doctoral degree in the Plant Pathology Program at UFV under the guidance of Professor Fabrício Ávila Rodrigues defending her Thesis on October 22, 2021.

You may never know what results come of your actions, but if you do nothing, there will be no results.

Mahatma Gandhi

ABSTRACT

ARAUJO, Marcela Uli Peixoto, D.Sc., Universidade Federal de Viçosa, October, 2021. **Physiological and Biochemical Aspects of Silicon and Magnesium Interaction and of the Acids beta-Aminobutyric and gamma-Aminobutyric in the Potentiation of Wheat Resistance against Blast**. Adviser: Fabrício de Ávila Rodrigues.

Epidemics of blast, caused by *Pyricularia oryzae*, have caused great yield losses in wheat and disease control has relied on using resistant cultivars combined with fungicides spray. Other control strategies need to be investigated and the use of inducers of host resistance may become an environmentally friendly and viable strategy for blast management. In the first study, the hypothesis that wheat plants with higher foliar concentrations of silicon (Si) and magnesium (Mg) could had their resistance against blast maximized was tested. An in-depth analysis of the photosynthetic apparatus (parameters of chlorophyll (Chl) *a* fluorescence and pool of photosynthetic pigments) and changes in enzymes activities involved in host defense and in the antioxidant metabolism in the leaves of wheat plants non-supplied (0 mM) or supplied (2 mM) with Si combined to lower (0.25 mM) or adequate (0.6 mM) Mg rates and challenged with *P. oryzae* were investigated. Blast symptoms were reduced for Si-supplied plants due to higher foliar Si concentration. Magnesium or its possible synergistic effect with Si did not contribute to reduce blast severity even though there was higher foliar Mg concentration for plants supplied with 0.6 mM Mg compared to 0.25 mM Mg. Higher values of variable-to-maximum chlorophyll *a* fluorescence ratio (F_v/F_m), photochemical yield (Y(II)), and yield for dissipation by down-regulation (Y(NPQ)) parameters, great Chl *a+b* concentration, and less production of malondialdehyde (MDA), hydrogen peroxide (H_2O_2), and superoxide anion radical ($O_2^{\bullet-}$) were noticed for Si-supplied and infected plants due to less blast symptoms. In general, Si-supplied and infected plants, regardless of Mg rate, displayed higher activities of defense (chitinase (CHI), β-1,3-glucanase (GLU), phenylalanine ammonia-lyase (PAL), peroxidase (POX), and polyphenoloxidase (PPO)) and antioxidative (ascorbate peroxidase (APX), catalase (CAT), glutathione reductase (GR), and superoxide dismutase (SOD)) enzymes as well as more lignin concentration reconfirming, therefore, the potential of Si to increase wheat resistance against blast. No evidence of synergism between Si and Mg or a possible effect of higher foliar Mg concentration to maximize wheat resistance to blast, linked to antioxidative metabolism robustness, was obtained as illustrated by the three independent groups (0.25 mM Mg +Si; 0.6 mM Mg +Si; as well as 0.25 mM Mg -Si and 0.6 mM Mg -Si) generated from principal

component analysis. The fact that Mg was not able to reduce blast symptoms cannot discard its indirect and barely participation in the potentiation of host defense responses considering its key functions in plant metabolism even though the physiological and biochemical analysis performed were not able to bring this up for discussion. In the second study, the potential of using *β*-aminobutyric acid (BABA) and γ-aminobutyric acid (GABA) to induce wheat resistance against blast was investigated. This goal was achieved by performing Chl *a* fluorescence measurements, determining Chl *a*+*b* and carotenoids concentrations, host defense responses (CHI, GLU, POX, PAL, PPO, and LOX activities along with concentrations of phenolics and lignin), antioxidative metabolism (SOD, CAT, APX, and GR activities) as well as oxidative stress (concentrations of MDA, H_2O_2, and $O_2^{\bullet-}$) of non-inoculated and inoculated plants from cultivar BRS Guamirim (susceptible to blast) sprayed with water or with solutions (100 mM) of BABA and GABA. Plants were sprayed with BABA and GABA solutions at 48 h before inoculation with *B. oryzae*. Blast progressed much faster for water and GABA-sprayed plants than for BABA-sprayed plants. The area under blast progress curve was significantly higher by 52 and 47% for plants from control and GABA treatments, respectively, compared to BABA-sprayed plants. Values of Chl *a* fluorescence parameters F_v/F_m, Y(II), and Y(NPQ)) linked to Chl *a*+*b* and carotenoids concentrations were higher for BABA-sprayed plants than for those of control and GABA treatments. Activities of CHI, GLU, PAL, PPO, and LOX were more remarkable for BABA-sprayed plants than for those from control and GABA treatments. Greater APX, CAT, and SOD activities for BABA-sprayed plants helped to alleviate the stress imposed by higher H_2O_2 and $O_2^{\bullet-}$ concentrations in contrast from control and GABA treatments. Taken together, the results of the present study allowed to conclude that supplying BABA to wheat plants increased their resistance against blast in a scenario where the photosynthetic apparatus was preserved along with a boosted defense response and a more robust antioxidative metabolism to counteract the harmful effect imposed by *P. oryzae* infection.

Keywords: Amino acids. Antioxidative metabolism. Fungal disease. Hemibiotrophic pathogen. Host defense responses. Induced resistance. Plant nutrition. Reactive oxygen species.

RESUMO

ARAUJO, Marcela Uli Peixoto, D.Sc., Universidade Federal de Viçosa, outubro de 2021. **Aspectos Fisiológicos e Bioquímicos da Interação do Silício e Magnésio e dos Ácidos beta-Aminobutírico e gama-Aminobutírico na Potencialização da Resistência do Trigo contra à Brusone**. Orientador: Fabrício de Ávila Rodrigues.

Epidemias de brusone, causadas por *Pyricularia oryzae*, têm ocasionado grandes perdas na produção do trigo e o controle dessa doença tem ocorrido com o uso de cultivares resistentes combinado com a pulverização de fungicidas. Outras estratégias de controle precisam ser investigadas e o uso de indutores de resistência pode se tornar uma estratégia ambientalmente amigável e viável para o manejo da brusone. No primeiro estudo, foi testada a hipótese de que plantas de trigo com maiores concentrações foliares de silício (Si) e magnésio (Mg) poderiam ter a resistência à brusone maximizada. Uma análise aprofundada do aparato fotossintético (parâmetros da fluorescência da clorofila (Chl) *a* e pigmentos fotossintéticos) e alterações nas atividades das enzimas de defesa e do metabolismo antioxidativo em folhas de plantas de trigo não supridas (0 mM) ou supridas (2 mM) com Si em combinação com baixa (0,25 mM) ou adequada (0,6 mM) concentração de Mg e infectadas com *P. oryzae* foi investigada. Os sintomas da brusone foram reduzidos nas plantas supridas com Si devido à maior concentração foliar de Si. O Mg ou seu possível efeito sinergístico com o Si não contribuíram para reduzir a severidade da brusone, embora ocorreu maior concentração foliar de Mg para as plantas supridas com 0,6 mM de Mg em comparação com 0,25 mM de Mg. Maiores valores da eficiência quântica máxima do fotossistema II (F_v/F_m), rendimento fotoquímico (Y(II)) e rendimento quântico de dissipação regulada (Y(NPQ)), alta concentração de Chl *a*+*b* e menor produção de aldeído malônico (MDA), peróxido de hidrogênio (H_2O_2) e radical ânion superóxido ($O_2^{\bullet-}$) foram observados para as plantas supridas com Si e infectadas devido a menor severidade da brusone. Em geral, as plantas supridas com Si e infectadas, independentemente da dose do Mg, apresentaram maiores atividades das enzimas de defesa (quitinase (QUI), *β*-1,3-glucanase (GLU), fenilalanina amônia-liase (FAL), peroxidase (POX) e polifenoloxidase (PFO)) e do metabolismo antioxidativo (ascorbato peroxidase (APX), catalase (CAT), glutationa redutase (GR) e superóxido dismutase (SOD)), bem como maior concentração de lignina reconfirmando, portanto, o potencial do Si em aumentar a resistência do trigo à brusone. Nenhuma evidência de sinergismo entre o Si e Mg ou um possível efeito da maior concentração foliar de Mg para maximizar a resistência do trigo à brusone, ligada à robustez do metabolismo

antioxidante, foi obtida como mostrado pelos três grupos independentes (0,25 mM Mg +Si; 0,6 mM Mg +Si; bem como 0,25 mM Mg -Si e 0,6 mM Mg -Si) obtidos pela análise dos componentes principais. O fato do Mg não ter sido capaz de reduzir os sintomas da brusone não descarta sua possível participação mesmo que indireta na potencialização das respostas de defesa do trigo considerando suas importantes funções no metabolismo vegetal, embora as análises fisiológicas e bioquímicas realizadas não tenham sido capazes de trazer isso à discussão. No segundo estudo, foi investigado o potencial dos ácidos *β*-aminobutírico (BABA) e *γ*-aminobutírico (GABA) em induzir a resistência do trigo à brusone. Este objetivo foi alcançado analisando o desempenho fotossintético (medições da fluorescência da clorofila (Chl) *a* e concentrações de pigmentos fotossintéticos (Chl *a*+*b*) e carotenoides), resposta de defesa (atividades da quitinase (QUI), *β*-1,3-glucanase (GLU), peroxidase (POX), fenilalanina amônia-liase (FAL), polifenoloxidase (PFO), lipoxigenase (LOX) e concentrações de compostos fenólicos e lignina), metabolismo antioxidativo (atividades da superóxido dismutase (SOD), catalase (CAT), ascorbato peroxidase (APX) e glutationa redutase (GR)), assim como o estresse oxidativo (concentrações de aldeído malônico (MDA), peróxido de hidrogênio (H_2O_2) e ânion superóxido ($O_2^{\bullet-}$)) de plantas não inoculadas ou inoculadas da cultivar BRS Guamirim (suscetível à brusone) pulverizadas com água ou com soluções (100 mM) de BABA e GABA. As plantas foram pulverizadas com soluções de BABA e GABA às 48 h antes da inoculação com *P. oryzae*. A brusone progrediu muito mais rápido nas plantas pulverizadas com água e GABA do que nas plantas pulverizadas com BABA. A área abaixo da curva do progresso da brusone foi significativamente maior em 52 e 47% para as plantas dos tratamentos controle e GABA, respectivamente, em comparação com as plantas pulverizadas com BABA. Os valores dos parâmetros da fluorescência da Chl *a* F_v/F_m, Y(II) e Y(NPQ) e as concentrações de Chl *a*+*b* e carotenoides foram maiores para as plantas pulverizadas com BABA em comparação com as plantas dos tratamentos controle e GABA. As atividades da QUI, GLU, FAL, PFO e LOX foram mais notáveis para as plantas pulverizadas com BABA do que para aquelas dos tratamentos controle e GABA. Maiores atividades da APX, CAT e SOD para as plantas pulverizadas com BABA ajudaram no alívio do estresse imposto pelas altas concentrações de H_2O_2 e $O_2^{\bullet-}$ em contraste com os tratamentos controle e GABA. Levando tudo isso em consideração, os resultados do presente estudo permitem concluir que o fornecimento de BABA às plantas de trigo aumentou a resistência à brusone em um cenário onde o aparato fotossintético foi preservado juntamente com uma maior resposta de defesa e um metabolismo antioxidativo mais robusto para reduzir o efeito negativo imposto pela infecção por *P. oryzae*.

Palavras-chave: Aminoácidos. Doença fúngica. Espécies reativas de oxigênio. Metabolismo antioxidativo. Nutrição de plantas. Patógeno hemibiotrófico. Resistência induzida. Respostas de defesa do hospedeiro.

SUMMARY

Chapter I

PHYSIOLOGICAL AND BIOCHEMICAL ASPECTS OF SILICON AND MAGNESIUM INTERACTION IN THE POTENTIATION OF WHEAT RESISTANCE AGAINST BLAST

Resumo

ARAUJO, Marcela Uli Peixoto, Dsc., Universidade Federal de Viçosa, Outubro, 2021. **Aspectos Fisiológicos e Bioquímicos da Interação do Silício e Magnésio na Potencialização da Resistência do Trigo à Brusone**. Orientador: Fabrício Ávila Rodrigues.

A brusone, causada por *Pyricularia oryzae*, tem afetado negativamente a produtividade do trigo e a qualidade dos grãos. Neste estudo, foi testada a hipótese de que plantas de trigo com maiores concentrações foliares de silício (Si) e magnésio (Mg) poderiam ter a resistência à brusone maximizada. Uma análise aprofundada do aparato fotossintético (parâmetros da fluorescência da clorofila (Chl) *a* e pigmentos fotossintéticos) e alterações nas atividades das enzimas de defesa e do metabolismo antioxidativo em folhas de plantas de trigo não supridas (0 mM) ou supridas (2 mM) com Si combinadas com baixa (0,25 mM) ou adequada (0,6 mM) concentração de Mg e infectadas com *P. oryzae* foram investigados. Os sintomas da brusone foram reduzidos nas plantas supridas com Si devido à maior concentração foliar de Si. O Mg ou seu possível efeito sinergístico com o Si não contribuíram para reduzir a severidade da brusone, embora ocorreu maior concentração foliar de Mg para as plantas supridas com 0,6 mM Mg em comparação com 0,25 mM Mg. Maiores valores dos parâmetros da fluorescência da Chl *a* (eficiência quântica máxima do fotossistema II, rendimento fotoquímico e rendimento quântico de dissipação regulada), alta concentração de clorofilas *a+b* e menor produção de aldeído malônico, peróxido de hidrogênio e ânion superóxido foram observados para plantas supridas com Si e infectadas devido a menor severidade da brusone. Em geral, as plantas supridas com Si e infectadas, independentemente do Mg, apresentaram maiores atividades das enzimas de defesa (quitinase, β-1,3-glucanase, fenilalanina amônia-liase, peroxidase e polifenoloxidase) e antioxidantes (ascorbato peroxidase, catalase, glutationa redutase e superóxido dismutase), bem como maior concentração de lignina reconfirmando, portanto, o potencial do Si em aumentar a

resistência do trigo à brusone. Nenhuma evidência de sinergismo entre o Si e Mg ou um possível efeito da maior concentração foliar de Mg para maximizar a resistência do trigo à brusone, ligada à robustez do metabolismo antioxidante, foi obtida conforme obtido pelos três grupos independentes (0,25 mM Mg +Si; 0,6 mM Mg +Si; bem como 0,25 mM Mg -Si e 0,6 mM Mg -Si) na análise de componentes principais. O fato de o Mg não ter sido capaz de reduzir os sintomas da brusone não descarta a sua possível ou indireta participação na potencialização das respostas de defesa do trigo considerando suas importantes funções no metabolismo vegetal, embora as análises fisiológicas e bioquímicas realizadas não tenham sido capazes de trazer isso à discussão.

Palavras-chave: doença fúngica, espécies reativas de oxigênio, metabolismo antioxidativo, nutrição mineral de plantas, patógeno hemibiotrófico, respostas de defesa do hospedeiro.

Abstract

ARAUJO, Marcela Uli Peixoto, Dsc., Universidade Federal de Viçosa, October, 2021. **Physiological and Biochemical Aspects of Silicon and Magnesium Interaction in the Potentiation of Wheat Resistance against Blast**. Adviser: Fabrício Ávila Rodrigues.

Blast, caused by *Pyricularia oryzae*, has negatively impacted wheat yield and grains quality. In this study, the hypothesis that wheat plants with higher foliar concentrations of silicon (Si) and magnesium (Mg) could had their resistance against blast maximized was tested. An in-depth analysis of photosynthetic apparatus (parameters of chlorophyll (Chl) *a* fluorescence and pool of photosynthetic pigments) and changes in enzymes activities involved in host defense and in the antioxidant metabolism in the leaves of wheat plants non-supplied (0 mM) or supplied (2 mM) with Si combined to lower (0.25 mM) or adequate (0.6 mM) Mg rates and challenged with *P. oryzae* were investigated. Blast symptoms were reduced for Si-supplied plants due to higher foliar Si concentration. Magnesium or its possible synergistic effect with Si did not contribute to reduce blast severity even though there was higher foliar Mg concentration for plants supplied with 0.6 mM Mg compared to 0.25 mM Mg. Higher values of Chl *a* fluorescence (variable-to-maximum chlorophyll *a* fluorescence ratio, photochemical yield, and yield for dissipation by down-regulation) parameters, great total chlorophylls *a+b* concentration, and less production of malondialdehyde, hydrogen peroxide, and superoxide anion radical were noticed for Si-supplied and infected plants due to less blast symptoms. In general, Si-supplied and infected plants, regardless of Mg rate, displayed higher activities of defense (chitinase, β-1,3-glucanase, phenylalanine ammonia-lyase, peroxidase, and polyphenoloxidase) and antioxidative (ascorbate peroxidase, catalase, glutathione reductase, and superoxide dismutase) enzymes as well as more lignin concentration reconfirming, therefore, the potential of Si to increase wheat resistance against blast. No evidence of synergism between Si and Mg or a

possible effect of higher foliar Mg concentration to maximize wheat resistance to blast, linked to antioxidative metabolism robustness, was obtained as illustrated by the three independent groups (0.25 mM Mg +Si; 0.6 mM Mg +Si; as well as 0.25 mM Mg -Si and 0.6 mM Mg -Si) generated from principal component analysis. The fact that Mg was not able to reduce blast symptoms cannot discard its indirect and barely participation in the potentiation of host defense responses considering its key functions in plant metabolism even though the physiological and biochemical analysis performed were not able to bring this up for discussion.

Keywords: antioxidative metabolism, fungal disease, hemibiotrophic pathogen, host defense responses, plant nutrition, reactive oxygen species.

Introduction

Blast, caused by the hemibiotrophic fungus *Pyricularia oryzae* Cavara (teleomorph *Magnaporthe oryzae* (T. T. Hebert) M. E. Barr), is no doubt a very destructive disease in wheat grown in many countries in South America with intercontinental jumps to Bangladesh in South Asia and Zambia in Africa and potential to spread to other countries especially Europe, the United States, Australia, China, and India (Ceresini et al., 2018; Singh et al., 2021). The great impact of blast to cause yield losses up to 100% and reduce grains quality is an alarming situation for food security (Ceresini et al., 2018; Cruz and Valent, 2017). Some management strategies for wheat blast control such as using resistant cultivars, fungicides and inducers of resistance sprays, cultural management, and plant nutrition have been recommended (Rodrigues et al., 2017; Cruz et al., 2011; Ceresini et al., 2018; Singh et al., 2021). However, considering that *P. oryzae* is fast-evolving, highly aggressive, and with a wide range of alternative host (Ceresini et al., 2018; Singh et al., 2021), other sustainable methods for blast control need to be investigated.

Increased resistance of plants against diseases has been achieved through a balanced status of nutrients in their tissues. In the chloroplasts, chlorophylls (Chl) *a* and Chl *b* have magnesium (Mg) as the central atom in their tetrapyrrole ring so an effective light capture for photosynthetic carbon reduction reactions is maintained (Tian et al., 2021). Considering that photophosphorylation reactions in chloroplasts are affected by the Mg ions, this macronutrient can be related to CO_2 assimilation reactions (Marschner, 2011). Magnesium is important for proteins synthesis due to its involvement in structure, function, and stability of ribosomal particles, functionality of mitochondria as well as RNA formation in the nucleus (Marschner, 2011; Tian et al., 2021). Magnesium is directly involved in ATP and energy metabolism because many respiratory enzymes (*e.g.*, ATPases, carboxylases, and phosphatases) have this macronutrient as co-factor (Tian et al., 2021). Moreover, some enzymes related to lipid

metabolism (*e.g.*, acetic thiokinase and various phospholipid-synthesizing enzymes) need Mg in the enzymatic reactions and, therefore, cell membranes are greatly preserved (Marschner, 2011; Tian et al., 2021).

Many abiotic (*e.g.*, cold, drought, heat, mineral deficiency or toxicity, and salinity) and biotic (*e.g.*, herbivores and other pests as well as plant diseases) stresses faced by profitable crops, including wheat, are mitigated by silicon (Si) (Rodrigues et al., 2015). In wheat, the supply of Si has efficiently contributed to decrease the symptoms of blast as well as many other diseases such as powdery mildew (*Erysiphe graminis* f. sp. *graminis*), spot blotch (*Cochliobolus sativus*), septoria leaf spot (*Septoria nodorum*), leaf rust (*Puccinia triticina*), tan spot (*Pyrenophora tritici-repentis*), eyespot (*Oculimacula yallundae*), and bacterial leaf streak (*Xanthomonas translucens* pv. *undulosa*) (Debona et al., 2017). Avoiding or delaying pathogen penetration (increased incubation and latent periods) due to Si deposition below the cuticle or the potentiation of host defense responses (*e.g.*, enhanced transcription of defense-related genes, great activities of defense enzymes, and high production of phenolics and lignin) are the mechanisms underlining the effect of this element to decrease the intensities of diseases caused by pathogens of different lifestyles (Rodrigues et al., 2015; Debona et al., 2017). Interestingly, Si deposition in the cell wall may impair the outflow of effectors released by pathogens, especially those causing rusts, and haustoria functionality through a less efficient nutrients uptake and impedance for successful colonization of leaf tissues (Coskun et al., 2019).

Infection of plants by pathogens of different lifestyles are linked to irreversible damages on their photosynthetic apparatus (Rodrigues et al., 2020; Resende et al., 2012; Debona et al., 2014; Tatagiba et al., 2015). Photosynthesis is the major physiological process affected in wheat plants infected by *P. oryzae* (Debona et al., 2014; Aucique-Pérez et al., 2020; Rodrigues et al., 2020). However, wheat plants supplied with Si undergoing *P. oryzae* infection exhibited a better photosynthetic performance (higher values for net carbon assimilation rate, stomatal

conductance to water vapor, and transpiration rate linked with less degradation of photosynthetic pigments as well as great concentrations of amino acids, carbohydrates, and proteins) providing energy to be used in biochemical pathways related to host-defense responses besides a more robust antioxidative metabolism to alleviate the reactive oxygen species (ROS) generated due to oxidative damage to cell membrane and organelles (Rodrigues et al., 2015; Debona et al., 2017).

Based on the fact that Si and Mg have been used for plant diseases management, but their possible synergistic effect still missing in the literature, the present study hypothesized that wheat plants with higher foliar Si and Mg concentrations could had their resistance against blast maximized. This hypothesis was tested by carrying out a study that performed an in-depth analysis of the photosynthetic apparatus (parameters of Chl *a* fluorescence and pool of photosynthetic pigments) and a profile of changes in enzymes activities involved in both host defense and antioxidant metabolism in leaves of wheat plants non-supplied or supplied with Si combined to low or high Mg rates and challenged with *P. oryzae*.

Material and Methods

Nutrient solution preparation and plant growth

Wheat seeds from cultivar BRS Guamirim, susceptible to blast (Cruz et al., 2010), were surface sterilized in 10% (vol/vol) NaOCl for 2 min, rinsed in sterilized water for 3 min, and germinated on a sand substrate for seven days in a greenhouse. A total of five germinated seedlings were transferred to one plastic pot (20-cm in diameter) containing 5 L of half-strength Clark nutrient solution (Clark, 1975), with some modifications, which consisted of: 1.04 mM $Ca(NO_3)_2{\cdot}4H_2O$, 1 mM NH_4NO_3, 0.8 mM KNO_3, 0.6 mM $MgSO_4{\cdot}7H_2O$, 0.069 mM KH_2PO_4, 0.931 mM KCl, 19 µM H_3BO_3, 2 µM $ZnSO_4{\cdot}7H_2O$, 7 µM $MnCl_2{\cdot}4H_2O$, 0.6 µM $Na_2MoO_4.4H_2O$, 0.5 µM $CuSO_4{\cdot}5H_2O$, 90 µM $FeSO_4{\cdot}7H_2O$, and 90 mM ethylenediaminetetraacetic acid (EDTA) disodium for seven days. After this period, plants were divided into two groups and supplied with Mg rates of 0.25 mM (using 0.25 mM $MgSO_4.7H_2O$ and 0.25 mM Na_2SO_4 to provide the required sulfur for adequate plant growth; lower Mg rate) and 0.6 mM (using $MgSO_4.7H_2O$; adequate Mg rate). After two weeks growing plants in nutrient solutions containing lower and adequate Mg rates, they started to grow in nutrient solution non-supplied (0 mM) or supplied (2 mM) with Si. The monosilicic acid was obtained by passing potassium silicate (PQ Corporation, São Paulo, Brazil) through a column with a cation exchange resin (Amberlite IR-120B, H^+ form; Sigma-Aldrich, São Paulo, Brazil) (Ma et al., 2002). The nutrient solution was changed every four days and the pH was measured daily to be kept at 6.0 by using NaOH or HCl solutions (1 M) as needed. Plants were grown in a greenhouse with temperature of 25 ± 2°C, relative humidity of 70 ± 5%, and natural photosynthetically active radiation of 950 ± 50 µmol photons m^{-2} s^{-1}.

Inoculum production and plant inoculation

The isolate UFV/DFP *Po*-12 of *P. oryzae* obtained from spikes of wheat plants from cultivar BR-18 was used to inoculate the plants (Debona et al., 2012). Disks of filter paper containing fungal mycelia were transferred to Petri dishes containing oat-agar medium. After fungal mycelia growth, plugs of the medium containing fungal mycelia were transferred to new Petri dishes containing the same medium. The dishes were incubated in a growth chamber at 25°C with a 24 h photoperiod for eight days. After this period, conidia were carefully removed from the dishes with a soft bristle brush using water containing gelatin (1% wt/vol). The conidial suspension was calibrated with a hemacytometer to obtain a concentration of 1×10^5 conidia/ml. The conidial suspension was sprayed on the adaxial surface of the leaves of plants (Zadoks et al., 1974) with the aid of an VL Airbrush atomizer (Paasche Airbrush Co., Chicago, IL, USA). After inoculation, plants were kept in a mist chamber at 25°C for 24 h at darkness. Thereafter, plants were transferred to a greenhouse (temperature of 25 ± 3°C, relative humidity of 80 ± 5%, and photoperiod of 12 hours) until the end of experiments.

Experimental design

A 2 × 2 × 2 factorial experiment, consisting of plants supplied with lower (0.25 mM) and adequate (0.6 mM) Mg rates (refereed to as 0.25 mM Mg and 0.6 mM Mg plants thereafter), non-supplied or supplied with Si (refereed to as -Si and +Si plants thereafter), and non-inoculated or inoculated with *P. oryzae*, was arranged in a completely randomized design with five replications. Each experimental unit consisted of a plastic pot containing five plants. The experiment was conducted twice. A total of 200 plants were used in each experiment (25 plants per each treatment at each evaluation time).

Determining foliar Mg and Si concentrations

Leaf samples from plants from replications of each treatment were collected at 96 hours after inoculation (hai), dried at 65ºC for 72 h, and ground in a ball mill (TECNAL TE 350, Piracicaba, SP, Brazil) for 1 min. A total of 0.2 g of dried leaf tissues was digested with a nitric-perchloric acid solution and foliar Mg concentration was determined by optical emission spectrometry with inductively coupled plasma (ICP-OES) (DV8300, PerkinElmer) according to Mesquita et al. (2019). The foliar Si concentration was determined by colorimetric analysis of 0.1 g of dried and alkali-digested tissues (Korndörfer et al., 2004).

Blast assessments

Blast severity was assessed on fourth and fifth leaves, from base to top, of each plant per replication of each treatment at 48, 72, and 96 hai using the diagrammatic scale proposed by Rios et al. (2013).

Imaging and quantification of chlorophyll (Chl) *a* fluorescence parameters

Images and parameters of Chl *a* fluorescence were obtained from fourth leaf, from base to top, of each plant per replication of each treatment at 48, 72, and 96 hai using the MAXI version of the Imaging-PAM fluorometer and the Imaging Win software (Heinz Walz GmbH, Effeltrich, Germany). The Chl *a* fluorescence emission transients were captured by a CCD (charge-coupled device) camera with a resolution of 640 × 480 pixels in a visible sample area of 24 × 32 mm on each leaf. The leaves were initially adapted to darkness for 30 min, after which they were carefully and individually fixed in a support at a distance of 18.5 cm from the CCD camera. The leaves were then exposed to a weak, modulated measuring beam (0.5 μmol m^{-2} s^{-1}, 100 μs, 1 Hz) to determine the initial fluorescence (F_0) when all the photosystem II (PSII) reaction centers were “open”. Next, a saturating white light pulse of 2,400 μmol m^{-2} s^{-1} (10 Hz)

was applied for 0.8 s to ensure maximum fluorescence emission (F_m) when all the PSII reaction centers are expected to be "closed". From these initial measurements, the maximum PSII photochemical efficiency of the dark-adapted leaves was estimated through the variable-to-maximum Chl fluorescence ratio as follow: $F_v/F_m = [((F_m - F_0)/F_m)]$. The leaf tissues were subsequently exposed to actinic photon irradiance (110 μmol m^{-2} s^{-1}) for 120 s to obtain the steady-state fluorescence yield (F_s), after which a saturating white light pulse (2,400 μmol m^{-2} s^{-1}; 0.8 s) was applied to achieve the light-adapted maximum fluorescence (F'_m). Following the calculations of Kramer et al. (2004), the energy absorbed by the PSII for the following two yield components for dissipative processes was determined: the yield of photochemistry [YII = $((F'_m - F)/F'_m)$], the yield for dissipation by down-regulation [$Y(NPQ) = (F_s/F'_m) – (F_s/F_m)$], and the yield for other non-photochemical (non-regulated) losses [$Y(NO) = F_s/F_m$]. The parameters of Chl *a* fluorescence were determined by selecting the circular option on the Imaging Win software (area of ≈ 0.5 cm^2) on the leaves evaluated.

Determining Chl *a*, Chl *b*, and carotenoids concentrations

The concentrations of Chl *a*, Chl *b*, and carotenoids were determined using dimethyl sulfoxide (DMSO) as the solvent (Santos et al., 2008). Five leaf discs (1 cm^2 each) were obtained from fourth leaf, from base to top, of each plant per replication of each treatment at 48, 72, and 96 hai. The collected discs were immersed in glass tubes containing 5 ml of saturated DMSO solution and calcium carbonate ($CaCO_3$) (5 g/L) (Wellburn, 1994) and kept in the dark at room temperature for 24 h. The absorbances of the extracts were read at 480, 649, and 665 nm using a saturated solution of DMSO and $CaCO_3$ as a blank.

Biochemical assays

For all biochemical assays, fourth and fifth leaves, from base to top, of each plant per replication of each treatment were collected at 48, 72, and 96 hai. Leaves were also collected from non-inoculated plants at these same sampling times. Leaf samples were kept in liquid nitrogen during sampling and stored at -80ºC until further analysis.

Determining antioxidant enzymes activities

A total of 0.2 g of leaf tissues was ground into a fine powder using a vibration ball mill (Retsch, Haan, Germany) with liquid nitrogen for 5 min and homogenized in 2 ml of a solution containing 50 mM of potassium phosphate buffer (pH 6.8), 0.1 mM EDTA, 1 mM phenylmethylsulfonyl fluoride (PMSF), and 2% (w/v) polyvinylpyrrolidone (PVP) to determine the activities of ascorbate peroxidase (APX) (EC 1.11.1.11), catalase (CAT) (EC 1.11.1.6), peroxidase (POX) (EC 1.11.1.7), superoxide dismutase (SOD) (EC 1.15.1.1), and glutathione reductase (GR) (EC 1.8.1.7). The homogenized material was centrifuged at 12,000 *g* for 15 min at 4°C and the supernatant was used as the crude enzyme extract. The SOD activity was determined by measuring its ability to photochemically reduce nitroblue tetrazolium (NBT) as described by Beauchamp and Fridovich (1971). The reaction was initiated by adding the crude enzyme extract to a mixture containing 50 mM potassium phosphate buffer (pH 7.8), 14 mM methionine, 75 µM NBT, 0.1 mM EDTA, and 2 µM riboflavin. Samples were light-exposed for 7 min, and the production of formazan blue, resulting from the photoreduction of NBT, was measured at 560 nm with a spectrophotometer (Giannopolitis and Ries, 1977). Samples kept in the dark for 7 min served as a blank. One unit of SOD was defined as the amount of enzyme necessary to inhibit NBT photoreduction by 50%. The CAT activity was determined by adding the crude enzyme extract to a reaction mixture containing 50 mM potassium phosphate buffer (pH 7.0) and 20 mM hydrogen peroxide (H_2O_2). The determination

of CAT activity was based on the rate of H_2O_2 decomposition measured in the spectrophotometer at 240 nm for 1 min at 25°C (Cakmak and Marschner, 1992). An extinction coefficient of 36 M^{-1} cm^{-1} was used to calculate CAT activity (Anderson et al., 1995). The POX activity was assayed by determining the pyrogallol oxidation as proposed by Kar and Mishra (1976). The reaction was started after the addition of the crude enzyme extract to a reaction mixture containing 25 mM potassium phosphate (pH 6.8), 20 mM pyrogallol, and 20 mM H_2O_2. The POX activity was determined by the absorbance of colored purpurogallin recorded for 1 min at 420 nm at 25°C. The extinction coefficient of 2.47 mM^{-1} cm^{-1} (Chance and Maehly, 1955) was used to calculate POX activity. The APX activity assay followed that described by Nakano and Asada (1981). The crude enzyme extract was added to a mixture containing 50 mM phosphate buffer (pH 7.0), 0.5 mM ascorbic acid, and 0.1 mM H_2O_2. The rate of ascorbate oxidation was measured by recording the absorbance at 290 nm for 1 min. The extinction coefficient of 2.8 mM^{-1} cm^{-1} (Nakano and Asada, 1981) was used to calculate APX activity. In order to determine GR activity, the reaction was started after the addition of the crude enzyme extract to a mixture containing 50 mM potassium phosphate (pH 7.8), 1 mM oxidized glutathione (GSSG), and 0.75 mM NADPH prepared in 0.5 mM Tris-HCl buffer (pH 7.5) according to Carlberg and Mannervik (1985). The decrease in absorbance was determined at 340 nm for 1 min at 30°C. The extinction coefficient of 6.22 mM^{-1} cm^{-1} was used to calculate GR activity (Foyer and Halliwell, 1976). The activities of these enzymes were expressed in a protein-basis whose concentration was determined according to Bradford (1976).

Determining defense-related enzymes activities

A total of 0.2 g of leaf tissues was ground into a fine powder as described above for 5 min to determine the activities of chitinase (CHI) (EC 3.2.1.14), β-1,3-glucanase (GLU) (EC 3.2.1.39), phenylalanine ammonia-lyase (PAL) (EC 4.3.1.5), polyphenoloxidase (PPO), and lipoxygenase

(LOX) (EC 1.13.11.12). The fine powder was homogenized in 2 ml of a solution containing 50 mM potassium phosphate buffer (pH 6.8), 1 mM EDTA, 1 mM PMSF, and 2% (w/v) PVP. The homogenate was centrifuged at 12,000 *g* for 15 min at 4°C and the supernatant was collected to be used to determine enzymes activity. The CHI activity was determined by adding the crude enzyme extract to a reaction mixture containing 50 mM sodium acetate buffer (pH 5.0) and 0.1 mM *p*-nitrophenyl-β-*D*-*N*-*N'*-diacetylchitobiose (Harman et al., 1993). The reaction mixture was incubated in a water bath at 37°C for 2 h and the reaction was terminated by the addition of 0.2 M sodium carbonate. For the control samples, the sodium carbonate was added soon after the addition of the crude enzyme extract to the reaction mixture. The absorbance of the product released by CHI was measured at 410 nm. The extinction coefficient of 7×10^3 mM^{-1} cm^{-1} was used to calculate CHI activity. The GLU activity was determined after adding the crude enzyme extract to a reaction mixture containing 50 mM sodium acetate buffer (pH 5.0) and laminarin (1 mg/mL) (Lever, 1972). The reaction mixture was incubated in a water bath for 30 min at 45°C. Afterward, this mixture was added to a reaction mixture of dinitrosalicylic acid (DNS). This reaction mixture was then incubated in a water bath for 10 min at 90°C and then cooled in an ice bath until it reached 25°C. The absorbance was measured at 540 nm. A similar procedure was used for the control samples except that the first incubation was excluded. For PAL activity, the crude enzyme extract reacted with a reaction mixture containing 25 mM Tris-HCl buffer (pH 8.8) and 25 mM *L*-phenylalanine. The reaction mixture was incubated at 40°C for 3 h. For the control samples, the extract was replaced by the Tris-HCl buffer. The reaction was stopped by adding 6 N HCl. The absorbance of *trans*-cinnamic acid derivatives was recorded at 290 nm. The extinction coefficient of 100 M^{-1} cm^{-1} was used to calculate PAL activity (Guo et al., 2007). The PPO activity was determined using the same procedure as for POX, but H_2O_2 was omitted from the reaction mixture. The LOX activity was determined by adding the crude enzyme extract to a reaction mixture containing 50 mM sodium phosphate buffer (pH 6.5) and 50 µM

sodium linoleate. The reaction mixture was incubated at 25°C, and the absorbance of the product released by LOX for 1 min was measured at 234 nm. The extinction coefficient of 25000 M^{-1} cm^{-1} was used to calculate LOX activity (Axelrod et al., 1981). These enzyme activities were expressed on a protein basis and protein concentration was determined according to Bradford (1976).

Determining concentrations of total soluble phenolics (TSP) and lignin-thioglycolic acid (LTGA) derivatives

A total of 0.1 g of leaf tissues was ground into a fine powder as described above and homogenized in 1 mL of 80% (v/v) methanol solution. The crude extract was shaken at 300 rpm at 25°C for 2 h and the mixture was centrifuged at 17,000 *g* for 30 min. The TSP concentration was determined in the methanolic extract and the pellet was used to determine the LTGA derivatives concentration with a few modifications (Tatagiba et al., 2014).

Determining malondialdehyde (MDA) concentration

Oxidative damage in the leaf tissues was estimated as the concentration of total 2-thiobarbituric acid (TBA) reactive substances and expressed as equivalents of MDA (Cakmak and Horst, 1991). A total of 0.1 g of leaf tissues was ground into a fine powder as described above and homogenized in 2 ml of 0.1% (w/v) trichloroacetic acid (TCA) solution in an ice bath. The homogenate was centrifuged at 12,000 *g* for 15 min at 4°C. After centrifugation, a total of 250 µl of the supernatant was reacted with 750 µl of TBA solution (0.5% in 20% TCA) for 60 min in a boiling water bath at 95°C. After this period, the reaction was stopped in an ice bath. The non-specific absorbance was estimated at 600 nm and subtracted from the specific absorbance value. The extinction coefficient of 155 mM^{-1} cm^{-1} (Heath and Packer, 1968) was used to calculate MDA concentration.

Determining H_2O_2 concentration

A total of 0.1 g of leaf tissues was ground into a fine powder as described above and homogenized in 2 ml of 0.1% (w/v) of TCA. The homogenate was centrifuged at 12,000 *g* for 15 min at 4°C and the supernatant was used as the crude extract to determine H_2O_2 concentration. The supernatant was added to a reaction mixture containing 10 mM potassium buffer (pH 7.0) and 1 M of iodide solution and incubated for 10 min. The oxidation product formed was measure a 390 nm (Velikova et al., 2000). A standard curve for H_2O_2 (Sigma-Aldrich, São Paulo, Brazil) was used to determine H_2O_2 concentration.

Determining superoxide anion radical ($O_2^{\bullet-}$) concentration

A total of 0.2 g of leaf tissues was ground into a fine powder as described above and homogenized in 2 ml of a solution containing 100 mM sodium phosphate buffer (pH 7.2) and 1 mM sodium diethyldithiocarbamate (SDD). The homogenate was centrifuged at 22,000 *g* for 20 min at 4°C and the supernatant was used to determine the $O_2^{\bullet-}$ concentration according to Chaitanya and Naithani (1994).

Data analysis

Data for all variables and parameters evaluated were subjected to analysis of variance and the treatments means were compared by *F* test ($P \leq 0.05$). Linear correlation of Pearson (using data from inoculated plants at 96 hai) was used to determine relationships among foliar Si and Mg concentrations and blast severity as well as of these variables with Chl *a* fluorescence parameters, activities of defense and antioxidante enzymes, and concentrations of Chl *a*+*b*, carotenoids, MDA, H_2O_2, $O_2^{\bullet-}$, TSP, and LTGA derivatives. Principal components analysis (PCA) was performed aiming to determine the relationship between the variables and

parameters evaluated. Data were analyzed using the Minitab software (version 18, Minitab Corporation).

Results

Analysis of variance

Only the factor Si rates (Si) was significant for severity and AUBPC. The factors Si, Mg rates (Mg), and plant inoculation (PI) as well as the Si × Mg, Si × PI, Mg × PI, and Si × Mg × PI interactions were significant for most of the variables and parameters evaluated (Table 1).

Blast symptoms, severity, and AUBPC

In the absence of Si, blast symptoms (number and size of necrotic lesions, lesions coalescence, and chlorosis) were quite similar in the leaves of plants supplied with the two Mg rates. By contrast, in the leaves of plants supplied with Si, lesions were of reduced size, less coalesced, and in less number regardless of Mg rate (Fig. 1). At 48 hai, blast severity was significantly lower by 56% for 0.6 mM Mg +Si plants compared to 0.25 mM Mg +Si plants. Blast severity significantly decreased by 51 and 45% at 72 and 96 hai, respectively, for 0.25 mM Mg +Si plants and by 58, 35, and 52% at 48, 72, and 96 hai, respectively, for 0.6 mM Mg +Si plants compared to their counterparts (Fig. 2A-B). The AUBPC was significantly reduced by 43% for 0.25 mM Mg +Si plants and by 47% for 0.6 mM Mg +Si plants compared to 0.25 mM Mg -Si and 0.6 mM Mg -Si plants, respectively (Fig. 2C-D).

Foliar Si and macronutrients concentrations

For non-inoculated plants, foliar Si concentration significantly increased by 90% for 0.25 mM Mg +Si plants and by 86% for 0.6 mM Mg +Si plants compared to 0.25 mM Mg -Si and 0.6 mM Mg -Si plants, respectively (Fig. 3A). For inoculated plants, foliar Si concentration significantly increased by 85% for 0.25 mM Mg +Si plants and by 86% for 0.6 mM Mg +Si plants compared to 0.25 mM Mg -Si and 0.6 mM Mg -Si plants, respectively (Fig. 3B). Foliar

P concentration was significantly higher by 22% for non-inoculated 0.6 mM Mg -Si plants compared to non-inoculated 0.25 mM Mg -Si plants and significantly higher by 28% for inoculated 0.25 mM Mg -Si plants compared to inoculated 0.6 mM Mg -Si plants. At 0.6 mM Mg, foliar Mg concentration significantly increased by 26, 15, 17, and 13%, respectively, for plants of non-inoculated -Si, non-inoculated +Si, inoculated -Si, and inoculated +Si treatments compared to 0.25 mM Mg (Fig. 4A-D). Foliar K concentration was significantly higher by 18% for non-inoculated +Si plants compared to non-inoculated -Si plants at 0.25 mM Mg (Fig. 4A-B). Significant decreases of 15 and 26% for Mg foliar concentrations at 0.25 and 0.6 mM Mg rates, respectively, occurred for non-inoculated +Si plants compared to non-inoculated -Si plants. Foliar concentrations of N, P, and K were significantly lower by 14, 17, and 27%, respectively, for inoculated +Si plants compared to inoculated -Si plants at 0.25 mM Mg. Significant decreases of 18 and 14% for Mg foliar concentrations at 0.25 and 0.6 mM Mg, respectively, occurred for inoculated +Si plants compared to inoculated -Si plants (Fig. 4A-D). In the absence of Si and at 0.25 mM Mg, foliar concentrations of N, P, K, and Mg were significantly lower for non-inoculated plants compared to inoculated plants while Ca foliar concentration was significantly higher for non-inoculated plants compared to inoculated plants. At 0.6 mM Mg, N foliar concentration was significantly lower for non-inoculated -Si plants compared to inoculated -Si plants while P foliar concentration was significantly lower for inoculated -Si plants compared to non-inoculated -Si plants. Foliar Mg concentration significantly increased for inoculated +Si plants compared to non-inoculated +Si plants at 0.25 mM Mg (Fig. 4A-D).

Images of Chl *a* fluorescence parameters

Remarkable changes in the images for F_v/F_m, Y(II), Y(NPQ), and Y(NO), based on the darker areas, were noticed in the leaves of inoculated -Si plants compared to leaves of inoculated +Si

plants, at each Mg rate, starting at 72 hai (Fig. 5). In the absence of Si, there was no distinct difference in the color pattern of Chl *a* fluorescence images regardless of Mg rate. Less expressive changes in the images of the above-mentioned parameters were noticed in the leaves of 0.6 mM Mg plants compared to 0.25 mM Mg plants in the presence of Si (Fig. 5).

Parameters of Chl *a* fluorescence

Comparing Mg rates

At 48 hai, F_v/F_m was significantly higher by 7% for inoculated 0.6 mM Mg +Si plants compared to inoculated 0.25 mM Mg +Si plants (Fig. 6D). In the absence of Si, Y(NPQ) was significantly higher by 24% at 48 hai and Y(NO) was significantly lower by 40% at 72 hai for inoculated 0.6 mM Mg plants compared to inoculated 0.25 mM Mg plants (Fig. 6O).

Comparing -Si and +Si treatments for non-inoculated and inoculated plants

Non-inoculated plants

At 96 hai, Y(NPQ) and Y(NO) were significantly lower by 16 and 24%, respectively, for +Si plants compared to -Si plants at 0.6 mM Mg (Fig. 6I-J). Y(NO) significantly increased by 19% at 72 hai and by 8% at 48 hai for +Si plants at 0.25 and 0.6 mM Mg, respectively, compared to their counterparts (Fig. 6M-N).

Inoculated plants

At 0.25 mM Mg, F_v/F_m (8 and 25% at 72 and 96 hai, respectively), Y(II) (20, 28, and 66% at 48, 72, and 96 hai, respectively), and Y(NPQ) (23, 24, and 33% at 48, 72 and 96 hai, respectively) were significantly higher for +Si plants compared to -Si plants (Fig. 6C-D). At 0.6 mM Mg, F_v/F_m (3, 11, and 19% at 48, 72, and 96 hai, respectively), Y(II) (30, 23, and 56% at 48, 72, and 96 hai, respectively), and Y(NPQ) (22 and 33% at 72 and 96 hai, respectively)

were significantly higher for +Si plants compared to -Si plants (Fig. 6C-D). Y(NO) was significantly lower by 43 and 45% at 72 and 96 hai, respectively, at 0.25 mM Mg and by 28, 25, and 40% at 48, 72, and 96 hai, respectively, at 0.6 mM Mg for +Si plants compared to -Si plants (Fig. 6O-P).

Comparing non-inoculated and inoculated plants for -Si and +Si treatments

In the absence of Si, F_v/F_m, Y(II), and Y(NPQ) were significantly lower while Y(NO) was significantly higher for inoculated plants compared to non-inoculated plants from 48 to 96 hai regardless of Mg rate (Fig. 6A-D). In the presence of Si, F_v/F_m and Y(II) were significantly lower while Y(NO) was significantly higher for inoculated plants compared to non-inoculated plants from 48 to 96 hai regardless of Mg rate (Fig. 6A-D).

Photosynthetic pigments

Comparing Mg rates

Concentration of Chl *a*+*b* significantly increased for inoculated -Si plants (42, 46, and 66% at 48, 72, and 96 hai, respectively) and inoculated +Si plants (9, 38, and 34% at 48, 72, and 96 hai, respectively) at 0.6 mM Mg compared to 0.25 mM Mg (Fig. 7C-D).

Comparing -Si and +Si treatments for non-inoculated and inoculated plants

Non-inoculated plants

Significant increases for Chl *a*+*b* (13 and 15% at 48 and 72 hai, respectively, for 0.25 mM Mg and 12% at 96 hai for 0.6 mM Mg) and carotenoids (4% at 48 hai for 0.25 mM Mg) were obtained for +Si plants compared to -Si plants (Fig. 7A-B and E-F).

Inoculated plants

Concentrations of Chl *a*+*b* (53, 34, and 60% at 48, 72, and 96 hai, respectively, for 0.25 mM Mg and 26 and 24% at 48 and 72 hai, respectively, for 0.6 mM Mg) and carotenoids (46% at 48 hai for 0.25 mM Mg) were significantly higher for +Si plants compared to -Si plants (Fig. 7C-D and G-H).

Comparing non-inoculated and inoculated plants for -Si and +Si treatments

In the absence of Si, concentrations of Chl *a*+*b* and carotenoids were significantly lower for inoculated plants compared to non-inoculated plants from 48 to 96 hai regardless of Mg rate (Fig. 7A-H). In the presence of Si, concentrations of Chl *a*+*b* (72-96 hai at 0.25 mM Mg) and carotenoids (72-96 hai at 0.25 mM and 0.6 mM Mg) were significantly lower for inoculated plants compared to non-inoculated plants (Fig. 7A-H).

Concentrations of MDA, H_2O_2, and $O_2^{\bullet-}$

Comparing Mg rates

At 96 hai, MDA concentration significantly decreased by 24% for inoculated +Si plants at 0.6 mM Mg compared to 0.25 mM Mg (Fig. 8D). Concentrations of MDA and H_2O_2 were significantly lower and higher by 15 and 18% at 96 hai, respectively, for inoculated -Si plants at 0.6 mM Mg compared to 0.25 mM Mg (Fig. 8C and G). Concentration of $O_2^{\bullet-}$ was significantly lower by 24% at 72 hai and by 30% at 96 hai for non-inoculated -Si plants at 0.6 mM Mg compared to 0.25 mM Mg (Fig. 8I). For inoculated +Si plants, H_2O_2 and $O_2^{\bullet-}$ concentrations were significantly higher by 23% at 72 hai and by 27% at 96 hai, respectively, at 0.6 mM Mg compared to 0.25 mM Mg (Fig. 8H and L).

Comparing -Si and +Si treatments for non-inoculated and inoculated plants

Non-inoculated plants

Significant reductions in $O_2^{\bullet-}$ concentration of 45, 42, and 45% at 48, 72, and 96 hai, respectively, for 0.25 mM Mg, and of 47 and 27% at 48 and 96 hai, respectively, for 0.6 mM Mg occurred for +Si plants compared to -Si plants (Fig. 8I-J).

Inoculated plants

Concentrations of MDA (36% at 96 hai for 0.6 mM Mg), H_2O_2 (31 and 33% at 72 and 96 hai, respectively, for 0.25 mM Mg and 35% at 96 hai for 0.6 mM Mg), and $O_2^{\bullet-}$ (50% at 96 hai for 0.25 mM Mg) were significantly lower for +Si plants compared to -Si plants (Fig. 8C-D, G-H, and K-L).

Comparing non-inoculated and inoculated plants for -Si and +Si treatments

Concentrations of MDA (-Si plants: 48-96 hai for 0.25 mM Mg and 48 and 96 hai for 0.6 mM Mg; +Si plants: 48-96 hai for both 0.25 and 0.6 mM Mg), H_2O_2 (-Si plants: 48-96 hai for 0.25 mM Mg and 72-96 hai for 0.6 mM Mg; +Si plants: 48-96 hai for both 0.25 and 0.6 mM Mg), and $O_2^{\bullet-}$ (-Si plants: 96 hai for 0.25 mM Mg and 72-96 hai for 0.6 mM Mg; +Si plants: 72-96 hai for both 0.25 mM and 0.6 mM Mg) were significantly higher for inoculated plants compared to non-inoculated plants (Fig. 8A-L).

Activities of antioxidant enzymes

Comparing Mg rates

For inoculated +Si plants, SOD (11, 29, and 21% at 48, 72, and 96 hai, respectively), CAT (44% at 96 hai), APX (34, 29, and 44% at 48, 72, and 96 hai, respectively), and GR (20, 24, and 26% at 48, 72, and 96 hai, respectively) were significantly higher at 0.6 mM Mg compared to 0.25 mM Mg (Fig. 9C, H, and P). Activities of APX at 96 hai and GR at 72 hai were

significantly lower by 43 and 22%, respectively, for inoculated -Si plants at 0.6 mM Mg compared to 0.25 mM Mg (Fig. 9K and O).

Comparing -Si and +Si treatments for non-inoculated and inoculated plants

Inoculated plants

Activities of SOD (47 and 13% at 72 and 96 hai, respectively, for 0.25 mM Mg), CAT (19, 26, and 22% at 48, 72, and 96 hai, respectively, for 0.25 mM Mg), APX (30 and 44% at 48 and 96 hai, respectively, for 0.25 mM Mg), and GR (18, 22, and 31% at 48, 72, and 96 hai, respectively, for 0.25 mM Mg) were significantly lower for +Si plants compared to -Si plants (Fig. 9C-D, G-H, K-L, and O-P). For +Si plants, activities of CAT and APX (34 and 43% at 96 hai, respectively, for 0.6 mM Mg) and GR (23% at 72 hai for 0.6 mM Mg) were significantly higher compared to -Si plants (Fig. 9G-H, K-L, and O-P).

Comparing non-inoculated and inoculated plants for -Si and +Si treatments

Activities of SOD (-Si plants: 72-96 hai for both 0.25 and 0.6 mM Mg; +Si plants: 48 hai for 0.25 mM Mg and 48-96 hai for 0.6 mM Mg), CAT (-Si plants: 72 hai for 0.25 mM Mg and 48 and 72 hai for 0.6 mM Mg; +Si plants: 96 hai for 0.6 mM Mg), APX (-Si plants: 48-96 hai for 0.25 mM Mg and 48 and 72 hai for 0.6 mM Mg; +Si plants: 72 hai for 0.25 mM Mg and 48-96 hai for 0.6 mM Mg), and GR (-Si plants: 48 hai for 0.6 mM Mg; +Si plants: 72 hai for 0.6 mM Mg) were significantly higher for inoculated plants compared to non-inoculated plants (Fig. 9A-P).

Activities of defense enzymes

Comparing Mg rates

For non-inoculated +Si plants, PAL (67 and 83% at 72 and 96 hai, respectively) and LOX (69% at 48 hai) activities were significantly higher for 0.6 mM Mg compared to 0.25 mM Mg (Fig. 10N and V). At 96 hai, PPO activity was significantly lower for non-inoculated +Si plants at 0.6 mM Mg compared to 0.25 mM Mg (Fig. 10R). For inoculated -Si plants, GLU (28% at 72 hai), POX, and PAL (37 and 48%, respectively, at 96 hai), and PPO (27 and 18% at 48 and 72 hai, respectively) activities were significantly higher for 0.6 mM Mg compared to 0.25 mM Mg (Fig. 10G, K, O, and S). At 48 hai, GLU activity was significantly lower for inoculated -Si plants at 0.6 mM Mg compared to 0.25 mM Mg (Fig. 10G). For inoculated +Si plants, CHI (49% at 96 hai), GLU (27 and 39% at 72 and 96 hai, respectively), POX, and LOX (38 and 37%, respectively, at 96 hai), and PAL (44 and 47% at 48 and 96 hai, respectively) activities were significantly higher for 0.6 mM Mg compared to 0.25 mM Mg (Fig. 10D, H, L, and X). At 72 hai, PAL activity was significantly lower for inoculated +Si plants at 0.6 mM Mg compared to 0.25 mM Mg (Fig. 10P).

Comparing -Si and +Si treatments for non-inoculated and inoculated plants

Non-inoculated plants

Activities of POX (55 and 35% at 72 and 96 hai, respectively, for 0.25 mM Mg), PPO (28% at 72 hai for 0.6 mM Mg), and LOX (72% at 48 hai for 0.25 mM Mg) were significantly lower for +Si plants compared to -Si plants (Fig. 10I-J, Q-R, and U-V). For +Si plants, PAL activity was significantly higher by 61% at 96 hai compared to -Si plants at 0.6 mM Mg (Fig. 10M-N).

Inoculated plants

For +Si plants, activities of CHI (26% at 96 hai for 0.25 mM Mg), POX (40 and 33% at 48 and 72 hai, respectively, for 0.25 mM Mg and 45% at 48 hai for 0.6 mM Mg), PAL (37% at 72 hai for 0.6 mM Mg), and LOX (51% at 48 hai for 0.25 mM Mg) were significantly lower compared to -Si plants (Fig. 10C-D, K-L, O-P, and W-X). Activities of CHI (40% at 48 hai for 0.25 mM Mg and 27, 29, and 31% at 48, 72, and 96 hai, respectively, for 0.6 mM Mg), GLU (41% at 72 hai for 0.25 mM Mg and 52 and 40% at 48 and 72 hai, respectively, for 0.6 mM Mg), PAL (58 and 73% at 48 hai, respectively, for 0.25 and 0.6 mM Mg), PPO (27 and 38% at 72 and 96 hai, respectively, for 0.25 mM Mg and 30% at 96 hai for 0.6 mM Mg), and LOX (28 and 22% at 72 and 96 hai, respectively, for 0.25 mM Mg and 36 and 43% at 72 and 96 hai, respectively, for 0.6 mM Mg) were significantly higher for +Si plants compared to -Si plants (Fig. 10C-D, G-H, K-L, O-P, S-T, and W-X).

Comparing non-inoculated and inoculated plants for -Si and +Si treatments

Activities of CHI (-Si plants: 72-96 hai for 0.25 mM Mg; +Si plants: 48-72 hai for 0.25 mM and 48-96 hai for 0.6 mM Mg), GLU (-Si plants: 48-72 hai for 0.25 mM Mg and 72-96 hai for 0.6 mM Mg; +Si plants: 48-72 hai for 0.25 mM Mg and 48-96 hai for 0.6 mM Mg), POX (-Si plants: 48-96 for both 0.25 mM and 0.6 mM Mg; +Si plants: 72-96 hai for both 0.25 and 0.6 mM Mg), PAL (-Si plants: 72-96 hai for both 0.25 and 0.6 mM Mg; +Si plants: 72-96 hai for 0.25 mM Mg and 48-96 hai for 0.6 mM Mg), PPO (-Si plants: 72-96 hai for 0.25 mM Mg and 48-96 hai for 0.6 mM Mg; +Si plants: 48-96 hai for 0.25 mM Mg and 72-96 hai for 0.6 mM Mg), and LOX (-Si plants: 48-96 hai for both 0.25 and 0.6 mM Mg; +Si plants: 48-96 hai for 0.25 mM Mg and 72-96 hai for 0.6 mM Mg) were significantly higher for inoculated plants compared to non-inoculated plants (Fig. 10A-X).

TSP and LTGA derivatives concentrations

Comparing Mg rates

Concentration of TSP was significantly lower by 54% at 72 hai and by 29% at 96 hai, for plants of inoculated -Si and inoculated +Si treatments at 0.6 mM Mg, respectively, compared to 0.25 mM Mg (Fig. 11C-D). Concentration of LTGA derivatives was significantly higher by 29 and 36% at 72 and 96 hai, respectively, for inoculated +Si plants at 0.6 mM Mg compared to 0.25 mM Mg (Fig. 12D).

Comparing -Si and +Si treatments for non-inoculated and inoculated plants

For inoculated +Si plants, TSP concentration was significantly lower by 59% at 72 hai and 0.25 mM Mg compared to inoculated -Si plants (Fig. 11D). At 96 hai and 0.6 mM Mg, LTGA derivatives concentration was significantly higher by 30% for inoculated +Si plants compared to inoculated -Si plants (Fig. 12D).

Comparing non-inoculated and inoculated plants for -Si and +Si treatments

Concentrations of TSP (-Si plants: 72-96 hai for 0.25 mM Mg and 96 hai for 0.6 mM Mg; +Si plants: 96 hai for both 0.25 mM and 0.6 mM Mg) and LTGA derivatives (+Si plants: 48-96 hai for 0.6 mM Mg) were significantly higher for inoculated plants compared to non-inoculated plants (Fig. 11C-D and 12C-D).

Pearson correlation analysis

Foliar Si concentration was negatively correlated with foliar Mg concentration and severity while foliar Mg concentration was negatively correlated with foliar Si concentration and positively with severity (Table 2). Foliar Si concentration was positively correlated with F_v/F_m, Y(II), Y(NPQ), Chl *a*+*b*, Car, PPO, and LOX, but negatively correlated with Y(NO), MDA,

H_2O_2, and $O_2^{\bullet-}$. Foliar Mg concentration was positively correlated with Y(NO), SOD, GLU, POX, and H_2O_2, but negatively correlated with F_v/F_m, Y(II), and Y(NPQ). Blast severity was positively correlated with Y(NO), MDA, H_2O_2, and $O_2^{\bullet-}$, but negatively correlated with F_v/F_m, Y(II), Y(NPQ), Chl *a*+*b*, Car, PPO, and LOX (Table 2).

PCA analysis

Distinct separation occurred between non-inoculated and inoculated plants as well as for inoculated plants from 0.25 mM Mg -Si, 0.6 mM Mg -Si, 0.25 mM Mg +Si, and 0.6 mM Mg +Si treatments (Fig. 13A-B). One principal component (PC) explained most of data variation (59 and 15% for PC1 and PC2, respectively) (Fig. 13A-B). According to cluster analysis with complete linkage and Pearson distance, four clusters (C) were generated: C1 (non-inoculated plants for the 0.25 mM Mg -Si, 0.6 mM Mg -Si, 0.25 mM Mg +Si, and 0.6 mM Mg +Si treatments), C2 (inoculated plants for the 0.25 mM Mg -Si and 0.6 mM Mg -Si treatments), C3 (inoculated plants for the 0.25 mM Mg +Si treatment), and C4 (inoculated plants for the 0.6 mM Mg +Si treatment) (Fig. 13A). The first PC was characterized by negative scores for photosynthetic parameters (foliar Si concentration, F_v/F_m, Y(NPQ), and Y(II)), photosynthetic pigments (Chl *a*+*b* and Car), and GR activity. Positive scores were obtained for Mg foliar concentration, disease severity, Y(NO), antioxidant (APX, CAT, and SOD) and defense (CHI, GLU, POX, PPO, LOX, and PAL) enzymes activities, and concentrations of metabolites (MDA, H_2O_2, and $O_2^{\bullet-}$), TSP, and LTGA derivatives (Fig. 13B).

Discussion

In line with the current trends toward unraveling the role played by Si for plant diseases management (Rodrigues et al., 2015; Debona et al., 2017), the current study not only bring support to the concept that this element was able to increase wheat resistance to blast (Xavier Filha et al., 2011; Aucique-Pérez et al., 2014), but provides novel insights at biochemical and physiological levels of its interaction with Mg. Interestingly, while higher foliar Si concentration contributed to reduce the foliar blast symptoms on Si-supplied wheat plants in agreement with previously reports (Xavier Filha et al., 2011; Aucique-Pérez et al., 2014), the same trend was not obtained for Mg. Even though higher foliar Mg concentration occurred for plants supplied with 0.6 mM Mg compared to those supplied with 0.25 mM Mg, blast development was quite similar in plants from these treatments. Moreover, no significance of Si × Mg interaction for blast severity and AUBPC indicated independence of these two elements in modulate wheat response against *P. oryzae* infection. The literature is rich in reports showing the positive effect of Si in reducing diseases intensity (Debona et al., 2017; Araújo et al., 2019) in contrast to Mg. Some studies report that Mg can increase the resistance of some profitable crops against fungal diseases while others do not bring positive response (Rodrigues et al., 2019). Schurt et al. (2014) reported an increase on rice resistance to sheath blight associated with higher Mg concentration on sheaths. Brown spot severity decreased in rice plants supplied with high Mg rate in the soil (Jones and Huber, 2007). According to Tatagiba et al. (2016), leaf scald symptoms on rice leaves were reduced for plants supplied with 1.5 mM Mg compared to 0.5 mM Mg. Cotton and peanut plants grown under low Mg concentration in the soil were more susceptible to *Rhizoctonia solani* (Csinos and Bell, 1989). Debona et al. (2016) reported that blast severity in wheat increased as the Mg rates in the nutrient solution increased from 0.25 to 4 mM. According to the authors, reduced Ca uptake partially explained the increased susceptibility of wheat plants to blast supplied with 4 mM Mg. In contrast to Si and Mg, the

nutritional status of wheat plants regarding N, P, K, Ca, and S were quite similar between non-infected and infected plants regardless of Si and Mg supplies. In rice plants supplied with Si and infected by *P. oryzae*, foliar concentrations of N, P, K, Ca, Mg, Cu, and B were significantly lower and of Zn, Fe, and Mn were significantly higher compared to -Si infected plants (Domiciano et al., 2019).

It is well documented in the literature that plants infected by pathogens of different lifestyles have their photosynthetic process drastically impaired (Silveira et al., 2019; Tatagiba et al., 2016; Bermúdez-Cardona et al., 2015; Rodrigues et al., 2017, 2020). Interestingly, changes on the photosynthetic machinery caused by pathogen infections were attenuated on Si-supplied plants (Resende et al., 2012; Aucique-Pérez et al., 2014; Tatagiba et al., 2016; Debona et al., 2017). Considering the fact that great part of the absorbed energy by the photosynthetic pigments in plants not exposed to stress is allocated to photochemical processes of photosynthesis while under stress the photosynthetic efficiency dramatically decreases, exploring the parameters related to Chl *a* fluorescence become very informative to attest the correct functioning of the photosynthetic apparatus (Lichtenthaler and Miehé, 1997). Consistent with previous findings for wheat-*P. oryzae* interaction (Aucique-Pérez et al., 2014; Debona et al., 2014), as blast symptoms developed, the use of light energy through photochemical reactions become less efficient. In comparison to non-infected plants, in general, F_v/F_m, Y(II), and Y(NPQ) values were lower while Y(NO) values were higher for infected plants regardless of Si and Mg rates. However, for +Si infected plants, F_v/F_m, Y(II), and Y(NPQ) values were higher while the Y(NO) values were lower compared to -Si infected plants regardless of Mg rate indicating attenuation of damages caused in the photosynthetic apparatus mainly in the PS II. The F_v/F_m reflects the quantum efficiency of PSII and has been used as an indicator of the physiological status of stressed plants (Maxwell and Johnson, 2000). Photoprotection and photoinhibition mechanisms are promptly activated in plant tissues when the energy from the

absorbed light is greater than its utilization in the photochemical processes (Demmig-Adams and Adams, 1992). Changes in Y(NPQ) and Y(NO) indicate regulation of non-used energy in the photosynthetic processes (Maxwell and Jonhson, 2000; Klughammer and Schreiber, 2008). Regardless of Mg rate, higher Y(NPQ) values for +Si infected plants compared to -Si infected plants contributed to preventing damage to PSII by releasing energy as heat. On the other hand, lower Y(NO) values for +Si infected plants compared to -Si infected plants indicated that the photoprotection and photoinhibition mechanisms were operative independently of Mg supply. Higher Y(NO) values indicate inefficient photochemical energy conversion and protective regulatory mechanisms of plants exposed to stressed and is generally accompanied by lower Y(NPQ) values (Klughammer and Schreiber, 2008). Both Y(NPQ) and Y(NO) were quite unresponsive to Mg supply during *P. oryzae* infection process regardless of Si supply. Collectively, these responses are consistent with a greater use of photochemical excitation energy to drive the higher carbon fixation rates for infected +Si plants in agreement with previously reports (Aucique-Pérez et al., 2014; Debona et al., 2014). Despite the participation of Mg in many steps of the photosynthetic process of plants (Marschner, 2011; Tian et al., 2021), in the present study, its higher foliar concentration for plants supplied with 0.6 mM Mg compared to 0.25 mM Mg did not contribute to improving the photosynthetic performance of non-infected wheat plants. On the other hand, higher values of F_v/F_m and Y(NPQ) were noticed for +Si and -Si infected plants, respectively, at 48 hai, supplied with 0.6 mM Mg compared to 0.25 mM indicating a barely impact of Mg in the alleviation of the stress imposed by *P. oryzae* infection on photosynthesis. According to Tatagiba et al. (2016), photosynthetic impairments in rice leaves infected by *M. albescens* were associated with photochemical and biochemical dysfunctions at the chloroplast level (*e.g.*, continuous loss of light energy allocated to photochemical reactions) and lower photosynthetic pigments concentration for plants supplied with 1.5 mM Mg compared to 0.5 mM Mg. Photosynthetic pigments responsible for capturing

light energy in plant leaves are Chl *a*, Chl *b*, and Car being Chl *a* the most widely distributed and playing the major role for light absorption and energy supply for all photochemical processes involved in photosynthesis (Wang and Grimm, 2021). Reductions in photosynthesis, stomatal conductance, transpiration, and photosynthetic pigment concentrations decreased more pronounced for infected plants grown with 4 mM Mg than for those grown with 0.25 mM Mg (Debona et al., 2016). Higher internal CO_2 concentration, invertase activity, and malondialdehyde concentration were recorded for infected plants grown with 4 mM Mg compared to those grown with 0.25 mM Mg. In the present study, concentration of Chl *a+b* was kept higher for +Si infected plants compared to -Si infected plants and also for plants supplied with 0.6 mM Mg compared to 0.25 mM Mg regardless of Si supply contributing for maintenance of photosynthetic process especially for Si-supplied plants. During the infection process of *P. oryzae* on wheat leaves, especially in susceptible cultivars, concentrations of Chl *a*, Chl *b*, and carotenoids are lowered and photosynthesis was impaired profoundly (Aucique-Pérez et al., 2014; Debona et al., 2014; Rodrigues et al., 2017, 2020). For the wheat-*P. oryzae* and rice-*M. albescens* interactions, infected plants supplied with Si showed higher concentration of photosynthetic pigments compared to -Si infected plants (Aucique-Pérez et al., 2014; Tatagiba et al., 2016). Lower Chl *a+b* concentration as a result of *P. oryzae* infection in -Si plants implies that the photosynthetic apparatus became most vulnerable against the saturating light resulting in a photooxidative environment inside the infected leaf tissues and loss of photosynthetic apparatus functionality.

Intense production of ROS (*e.g.*, H_2O_2, $^1O_2$, $O_2^{\bullet-}$, and OH) in plant tissues infected by pathogens need the activation of a wealth of enzymes and synthesized compounds to prevent or alleviate the cellular damage caused by them (Debona et al., 2012; Fortunato et al., 2015). The SOD is involved in $O_2^{\bullet-}$ removal by converting $O_2^{\bullet-}$ into O_2 and H_2O_2 while APX, CAT, and POX act in the H_2O_2 detoxification (Sharma et al., 2012; Das and Roychoudhury, 2014).

In the ascorbate-glutathione cycle, the GR uses NADPH as a reductant to catalyze the reduction of GSSG to GSH, which is essential to the scavenging of H_2O_2 (Sharma et al., 2012; Das and Roychoudhury, 2014). In the present study, wheat plants displayed increased APX, CAT, GR, and SOD activities in response to *P. oryzae* infection, but more pronounced in the absence of Si supply. For infected Si-supplied plants at 0.6 mM Mg compared to 0.25 mM Mg, APX, GR, and SOD (from 48 to 96 hai) and CAT (at 96 hai) activities were great. It is plausible to postulate that APX, GR, POX, and SOD activities modulated by Si, and to a less extension by Mg, played a role in alleviating the oxidative stress imposed by *P. oryzae*. Debona et al. (2012) reported that SOD, POX, APX, and GST activities increased for plants of wheat cultivars susceptible and partially resistant to blast infected by *P. oryzae*. Considering that photosynthesis was dramatically depressed in *P. oryzae*-infected wheat plants in the absence of Si, the energy surplus should be dissipated by alternative ways such as photosynthetic reduction of $O_2^{\bullet-}$ through Mehler-peroxidase reactions to produce H_2O_2 (Biehler and Fock, 1996). Accumulation of ROS and the associated cellular damage is a well-documented phenomenon in wheat leaves infected by *P. oryzae* (Debona et al., 2012). For +Si infected plants, in general, H_2O_2 (72 hai, 0.25 mM Mg; 96 hai for 0.25 and 0.6 mM Mg) and $O_2^{\bullet-}$ (96 hai, 0.25 mM Mg) concentrations were lower compared to -Si infected plants. Less production of MDA, a widely used biochemical marker of oxidative lipid damage in cellular membrane (Davey et al., 2005), for +Si infected plants, especially at 0.6 mM Mg, at 96 hai, indirectly indicated less extensive colonization of leaf tissues by *P. oryzae* (reduced release of hydrolytic enzymes and non-host selective toxins) and, therefore, less obtainment of nutrients for fungal nutrition resulting in less blast symptoms. Taken together, this finding indicates a major participation of Si and a discreet effect of Mg to reduce the cellular damage provoked by *P. oryzae* infection where a more robust antioxidative metabolism to lower H_2O_2 and $O_2^{\bullet-}$ concentrations generated by *P. oryzae* infection played a major role.

Host defense responses (*e.g.*, increased expression of pathogenesis-related genes, higher activities of defense-related enzymes, and great production of phenolics, phytoalexins, and lignin) against pathogen infections are potentiated by Si (Debona et al., 2017). The lytic enzymes CHI and GLU are responsible for acting directly on chitin and *β*-1,3-glucan, respectively, present in the cell walls of pathogens leading to the release of elicitors that maximizes the host defense responses (Stintzi et al., 1993). The PPO is also another important defense-related enzyme for promoting the oxidation of phenolics with the consequent release of quinones that are extremely toxic against pathogens (Mayer and Staples, 2002; Mayer, 2006). The PAL is a key enzyme involved in the phenylpropanoid pathway for being responsible for catalyzing *L*-phenylalanine to *trans*-cinnamic acid that originates other types of phenolics, flavonoids, phytoalexins, and lignin (Schuster and Rétey, 1995*;* Campbell and Sederoff, 1996). In general, CHI, GLU, PAL, PPO, and LOX activities were greater for +Si infected plants compared to -Si infected ones. In the absence of Si, GLU (72 hai), POX and PAL (96 hai), and PPO (48 hai) activities were higher at 0.6 mM Mg rate compared to 0.25 mM Mg. Meanwhile, in the presence of Si, CHI, POX, and LOX at 96 hai as well as GLU (from 72 to 96 hai) and PAL (at 48 and 96 hai) increased in activities at the rate of 0.6 mM Mg compared to 0.25 mM Mg. For several host-pathogen interactions, activities of defense enzymes and expression of their correspondent genes were higher for Si-supplied plants (Debona et al., 2017; Rodrigues et al., 2019). Tatagiba et al. (2016) reported great activities of PPO, POX, PAL, and LOX, but not of CHI and GLU, in rice leaves of plants supplied with 1.5 mM Mg compared to 0.5 mM Mg during the infection process of *M. albescens*.

In the present study, TSP production was quite similar between non-infected and infected plants regardless of Si and Mg supplies. By contrast, LTGA derivatives concentration was kept higher for +Si infected compared to -Si infected plants at 96 hai without any potentiation by Mg. At 96 hai, LTGA derivatives concentration was great for infected +Si plants supplied with

0.6 mM Mg than for infected +Si plants supplied with 0.25 mM Mg. In this scenario, the pool of soluble phenolics were used for lignin production due to Si potentiation linked to great PAL and PPO activities. It is known that lignin is covalently bound to polysaccharides and hemicelluloses and provides mechanical strength to host cell wall and affects diffusion of hydrolytic enzymes and non-host selective toxins produced by pathogens during the colonization process (Chabannes et al., 2001). According to Resende et al. (2013), TSP concentration was similar in sorghum plants non-supplied or supplied with Si throughout the infection process of *C. sublineolum*. Rodrigues et al. (2005) reported great lignin production by rice plants from a susceptible cultivar non-supplied with Si and infected by *P. grisea*. Great PAL activity and higher TSP and LTGA derivatives concentrations on leaves of rice plants supplied with 1.5 mM Mg compared to 0.5 mM Mg reduced leaf scald symptoms (Tatagiba et al., 2016). Increases in POX activity during host-pathogen interactions was closely associated with a progressive incorporation of phenolics in cell wall (Fink et al., 1991).

In conclusion, results of the present study reconfirm the importance of Si to potentiate wheat resistance against blast mainly through great activities of defense enzymes, more robust antioxidative metabolism, and preservation of the photosynthetic machinery with less biochemical and physiological impairments. No evidence of synergism between Si and Mg or even the expected effect of Mg to increase wheat resistance to blast linked to the robustness of the antioxidative metabolism was obtained. This finding was clearly illustrated by the three independent groups (-Mg +Si; +Mg +Si; as well as -Mg -Si and +Mg -Si) generated in the PCA analysis. However, the fact that Mg was not able to reduce blast symptoms cannot discard its important functions in plant metabolism (*e.g.*, constituent of chlorophylls, component of middle lamella, participation in carbohydrate metabolism, oxidative phosphorylation, energy transfer reactions, respiration, DNA and RNA formation as well as cofactor for numerous enzymes (Marschner, 2011; Tian et al., 2021) that could be useful at some extend for host defense

responses even though the physiological and biochemical analysis carried out in the present study were not able to attest.

References

Anderson MD, Prasad TK, Stewart CR (1995) Changes in isozyme profiles of catalase, peroxidase, and glutathione reductase during acclimation to chilling in mesocotyls of maize seedlings. Plant Physiology 109:1247-1257.

Araújo MUP, Rios JA, Silva ET, Rodrigues FA (2019) Silicon alleviates changes in the source-sink relationship of wheat plants infected by *Pyricularia oryzae*. Phytopathology 109:1129-1140.

Aucique-Pérez CE, Rios VS, Neto LBC, Rios JA, Martins SCV, Rodrigues FA (2020) Photosynthetic changes in wheat cultivars with contrasting levels of resistance to blast. Journal of Phytopathology 168:721-729.

Aucique Pérez CE, Rodrigues FA, Moreira WR, DaMatta FM (2014) Leaf gas exchange and chlorophyll *a* fluorescence in wheat plants supplied with silicon and infected with *Pyricularia oryzae*. Phytopathology 104:143-149.

Axelrod B, Cheesbrough TM, Laasko S (1981) Lipoxygenases from soybeans. Methods in Enzymology 71:441-451.

Beauchamp C, Fridovich I (1971) Superoxide dismutase: improved assays and an assay applicable to acrylamide gels. Analytical Biochemistry 44:276-287.

Bermúdez-Cardona MB, Wordell Filho JA, Rodrigues FA (2015) Leaf gas exchange and chlorophyll *a* fluorescence in maize leaves infected with *Stenocarpella macrospora*. Phytopathology 105:26-34.

Biehler K, Fock HP (1996) Evidence for the contribution of the Mehler peroxidase reaction in dissipation of excess electrons in drought stressed wheat. Plant Physiology 112:265-272.

Bradford MN (1976) A rapid and sensitive method for the quantitation of microgram quantities of protein utilizing the principle of protein-dye binding. Analytical Biochemistry 72:248-254.

Cakmak I, Horst WJ (1991) Effect of aluminium on lipid peroxidation, superoxide dismutase, catalase, and peroxidase activities in root tips of soybean (*Glycine max*). Physiologia Plantarum. 83:463-468.

Cakmak I, Marschner H (1992) Magnesium deficiency and high light intensity enhance activities of superoxide dismutase, ascorbate peroxidase, and glutathione reductase in bean leaves. Plant Physiology 98:1222-1227.

Campbell MM, Sederoff RR (1996) Variation in lignin content and composition. Plant Physiology 110:3-13.

Carlberg I, Mannervik B (1985) Glutathione reductase. Methods in Enzymology 113:484-490.

Ceresini PC, Castroagudín VL, Rodrigues FA, Rios JA, Aucique-Pérez CE, Moreira SI, Alves E, Croll D, Maciel JLN (2018) Wheat blast: past, present, and future. Annual Review of Phytopathology 56:427-456.

Chaitanya KSK, Naithani SC (1994) Role of superoxide, lipid peroxidation and superoxide dismutase in membrane perturbation during loss of viability in seeds of *Shorea robusta* Gaertn. f. New Phytologist 126:623-627.

Chance B, Maehly AC (1955) Assay of catalase and peroxidase. Methods in Enzymology 2:764-775.

Clark RB (1975) Characterization of phosphates in intact maize roots. Journal of Agricultural and Food Chemistry 23:458-460.

Chabannes M, Ruel K, Yoshinaga A (2001) In situ analysis of lignins in transgenic tobacco reveals a differential impact of individual transformations on the spatial patterns of lignin deposition at the cellular and subcellular levels. The Plant Journal 28:271-282.

Coskun D, Deshmukh R, Sonah H, Menzies JG, Reynolds O, Ma JF, Kronzucker HJ, Bélanger RR (2019) The controversies of silicon's role in plant biology. New Phytologist 221:67-85.

Cruz CD, Valent B (2017) Wheat blast disease: danger on the move. Tropical Plant Pathology 42:210-222.

Cruz MFA, Diniz APC, Rodrigues FA, Barros EG (2011) Foliar application of products on the reduction of blast severity on wheat. Tropical Plant Pathology 36:424-428.

Cruz MFA, Prestes AR, Maciel JL, Scheeren P (2010) Resistência parcial à brusone de genótipos de trigo comum e sintético nos estádios de planta jovem e de planta adulta. Tropical Plant Pathology 25:24-25.

Csinos AS, Bell DK (1989) Pathology and nutrition in the peanut pod rot complex. In: Engelhard AW (Eds.). Soilborne plant pathogens: management of diseases with macro and microelements. APS Press, St. Paul. pp. 124-136.

Das K, Roychoudhury A (2014) Reactive oxygen species (ROS) and response of antioxidants as ROS-scavengers during environmental stress in plants. Frontiers in Environmental Science 2:53.

Davey MW, Stals E, Panis B, Keulemans J, Swennen RL (2005) High-throughput determination of malondialdehyde in plant tissues. Analytical Biochemistry 347:201-207.

Debona D, Rios JA, Nascimento KJT, Silva LC, Rodrigues FA (2016) Influence of magnesium on physiological responses of wheat infected by *Pyricularia oryzae*. Plant Pathology 65:114-123.

Debona D, Rodrigues FA, Datnoff LE (2017) Silicon's role in abiotic and biotic plant stresses. Annual Review of Phytopathology 55:85-107.

Debona D, Rodrigues FA, Rios JA, Nascimento KJT (2012) Biochemical changes in the leaves of wheat plants infected by *Pyricularia oryzae*. Phytopathology 102:1121-1129.

Debona D, Rodrigues FA, Rios JA, Nascimento KJT, Silva LC (2014) The effect of silicon on antioxidant metabolism of wheat leaves infected by *Pyricularia oryzae*. Plant Pathology 63:581-589.

Demmig-Adams B, Adams WW (1992) Photoprotection and other responses of plants to high light stress. Annual Review of Plant Physiology and Plant Molecular Biology 43:599-626.

Domiciano GP, Araujo L, Duarte HSS, Freitas CC, Einhardt AM, Rodrigues FA (2019) Nutritional status of rice plants supplied with silicon in response to *Pyricularia oryzae* infection. Bragantia 78:573-578.

Fink W, Deising H, Mendgen K (1991) Early defense responses of cowpea (*Vigna sinensis* L.) induced by non-pathogenic rust fungi. Planta 185:246-254.

Fortunato AA, Debona D, Bernardeli AMA, Rodrigues FA (2015) Changes in the antioxidant system in soybean leaves infected by *Corynespora cassiicola*. Phytopathology 105:1050-1058.

Foyer CH, Halliwell B (1976) The presence of glutathione and glutathione reductase in chloroplasts: a proposed role in ascorbic acid metabolism. Planta 133:21-25.

Giannopolitis CN, Ries SK (1977) Superoxide dismutases I. Occurrence in higher plants. Plant Physiology 59:309-314.

Guo Y, Liu L, Zhao J, Bi Y (2007) Use of silicon oxide and sodium silicate for controlling *Trichothecium roseum* postharvest rot in Chinese cantaloupe (*Cucumis melo* L.). International Journal of Food Science & Technology 42:1012-1018.

Harman GE, Hayes CK, Lorito M, Broadway RM, Di Pietro A, Peterbauer C, Tronsmo A (1993) Chitinolytic enzymes of *Trichoderma harzianum*: purification of chitobiosidase and endochitinase. Phytopathology 83:313-318.

Heath RL, Packer L (1968) Photoperoxidation in isolated chloroplasts I. Kinetics and stoichiometry of fatty acid peroxidation. Archives of Biochemistry and Biophysics 125:189-198.

Jones JB, Huber DM (2007) Magnesium and plant disease. In: Datnoff LE, Elmer WH, Huber DM (Eds.). Mineral Nutrition and Plant Disease. APS Press, St. Paul. pp. 95-100.

Kar M, Mishra D (1976) Catalase, peroxidase, and polyphenoloxidase activities during rice leaf senescence. Plant Physiology 57: 315-319.

Klughammer C, Schreiber U (2008) Saturation pulse method for assessment of energy conversion in PS I. PAM Application Notes 1:11-14.

Korndörfer GH, Pereira HS, Nola A (2004) Análise de Silício: Solo, Planta e Fertilizante. Uberlândia, MG. Grupo de Pesquisa em Silício/ICIAG/Universidade Federal de Uberlândia. (Boletim Técnico 1).

Kramer DM, Johnson G, Kiirats O, Edwards GE (2004) New fluorescence parameters for the determination of Q_A redox state and excitation energy fluxes. Photosynthesis Research 79:209-218.

Lever M (1972) A new reaction for colorimetric determination of carbohydrates. Analytical Biochemistry 47:273-279.

Lichtenthaler HK, Miehé JA (1997) Fluorescence imaging as a diagnostic tool for plant stress. Trends in Plant Science 2:316-320.

Ma JF, Tamai K, Ichii M, Wu GF (2002) A rice mutant defective in Si uptake. Plant Physiology 130:2111-2117.

Marschner P (2011) Marschner's Mineral Nutrition of Higher Plants. 3th Ed. Academic, London, 651 p.

Maxwell K, Johnson GN (2000) Chlorophyll fluorescence - a practical guide. Journal of Experimental Botany 51:659-668.

Mayer AM (2006) Polyphenol oxidases in plants and fungi: going places? A review. Phytochemistry 67:2318-2331.

Mayer AM, Staples RC (2002) Laccase: new functions for an old enzyme. Phytochemistry 60:551-565.

Mesquita GL, Tanaka FAO, Zambrosi FCB, Chapola R, Cursi D, Habermann G, Massola Junior NS, Ferreira VP, Gaziola SA, Azevedo RA (2019) Foliar application of manganese increases sugarcane resistance to orange rust. Plant Pathology 68:1296-1307.

Nakano Y, Asada K (1981) Hydrogen peroxide is scavenged by ascorbate-specific peroxidase in spinach chloroplasts. Plant and Cell Physiology 22:867-880.

Resende RS, Rodrigues FA, Cavatte PC, Martins SCV, Moreira RM, Chaves ARM, DaMatta FM (2012) Leaf gas exchange and oxidative stress in sorghum plants supplied with silicon and infected by *Colletotrichum sublineolum*. Phytopathology 102:892-898.

Resende RS, Rodrigues FA, Gomes RJ, Nascimento KJT (2013) Microscopic and biochemical aspects of sorghum resistance to anthracnose mediated by silicon. Annals of Applied Biology 163:114-123.

Rios JA, Debona D, Duarte HSS, Rodrigues FA (2013) Development and validation of a standard area diagram set to assess blast severity on wheat leaves. European Journal of Plant Pathology 136:603-611.

Rodrigues FA, Aucique-Pérez CE, Debona D, Rios JA (2020) Effect of blast on wheat physiology. In: Kumar S, Kashyap PL, Singh GP (Eds.). Wheat Blast. CRC Press, Boca Raton. pp. 131-148.

Rodrigues FA, Dallagnol LJ, Duarte HSS, Datnoff LE (2015) Silicon control of foliar diseases in monocots and dicots. In: Rodrigues FA, Datnoff LE (Eds.). Silicon and Plant Diseases. Springer International Publishing, Switzerland. pp. 67-108.

Rodrigues FA, Einhardt AM, Rios JA, Silveira PR, Elmer WH, Datnoff LE (2019) Nutrição Mineral no Manejo das Doenças de Plantas. In: Flores RA, Cunha PP, Marchão RL, Morais MF (Eds.) Nutrição e Adubação de Grandes Culturas na Região do Cerrado. Gráfica Universidade Federal de Goiás, Goiânia. pp. 36-76.

Rodrigues FA, Jurick WM, Datnoff LE, Jones JB, Rollins JA (2005) Silicon influences cytological and molecular events in compatible and incompatible rice-*Magnaporthe grisea* interactions. Physiological and Molecular Plant Pathology 66:144-159.

Rodrigues FA, Rios JA, Debona D, Aucique-Pérez CE (2017) *Pyricularia oryzae*-wheat interaction: physiological changes and disease management using mineral nutrition and fungicides. Tropical Plant Pathology 42:223-229.

Santos RP, Cruz, ACF, Iarema L, Kuki KN, Otoni WC (2008) Protocolo para extração de pigmentos foliares em porta-enxertos de videira micropropagados. Ceres 55:356-364.

Schurt DA, Lopes UP, Duarte HSS, Rodrigues FA (2014) Effect of magnesium on the development of sheath blight in rice. Journal of Phytopathology 162:617-620.

Schuster B, Rétey J (1995) The mechanism of action of phenylalanine ammonia-lyase: the role of prosthetic dehydro- alanine. Proceedings of the National Academy of Sciences of the United States of America 92:8433-8437.

Sharma P, Jha AB, Dubey RS, Pessarakli M (2012) Reactive oxygen species, oxidative damage, and antioxidative defense mechanism in plants under stressful conditions. Journal of Botany 2012:217037.

Silveira PR, Milagres PO, Correa EF, Aucique-Pérez CE, Filho JA, Rodrigues FA (2019) Changes in leaf gas exchange, chlorophyll *a* fluorescence, and antioxidants in maize leaves infected by *Exserohilum turcicum*. Biologia Plantarun. 63:643-653.

Singh PK, Gahtyari NC, Roy C, Roy KK, He X, Tembo B, Xu K, Juliana P, Sonder K, Kabir MR, Chawade A (2021) Wheat blast: a disease spreading by intercontinental jumps and its management strategies. Frontiers in Plant Science 12:710707.

Stintzi A, Heitz T, Prasad V, Wiedemann-Merdinoglu S, Kauffmann S, Geoffroy P, Legrand M, Fritig B (1993) Plant 'pathogenesis-related' proteins and their role in defense against pathogens. Biochimie 75:687-706.

Tatagiba SD, DaMatta FM, Rodrigues FA (2016) Magnesium decreases leaf scald symptoms on rice leaves and preserves the photosynthetic performance. Plant Physiology and Biochemistry 108:49-56.

Tatagiba SD, Rodrigues FA, DaMatta FM (2015) Leaf gas exchange and chlorophyll *a* fluorescence imaging of rice leaves infected with *Monographella albescens*. Phytopathology 105:180-188.

Tatagiba SD, Rodrigues FA, Filippi MCC, Silva GB, Silva LC (2014) Physiological responses of rice plants supplied with silicon to *Monographella albescens* infection. Journal of Phytopathology 162:596-606.

Tian XY, He DD, Bai S, Zeng W-Z, Wang Z, Wang M, Wu L-Q, Chen Z-C (2021) Physiological and molecular advances in magnesium nutrition of plants. Plant Soil (in press).

Velikova V, Yordanov I, Edreva A (2000) Oxidative stress and some antioxidant systems in acid rain-treated bean plants: protective role of exogenous polyamines. Plant Science 151:59-66.

Wang P, Grimm B (2021) Connecting chlorophyll metabolism with accumulation of the photosynthetic apparatus. Trends in Plant Science 26:484-495.

Wellburn AR (1994) The spectral determination of chlorophylls *a* and *b,* as well as total carotenoids, using various solvents with spectrophotometers of different resolution. Journal of Plant Physiology 144:307-313.

Xavier Filha MS, Rodrigues FA, Domiciano GP, Oliveira HV, Silveira PR, Moreira WR (2011) Wheat resistance to leaf blast mediated by silicon. Australasian Plant Pathology 40:28-38.

Zadoks JC, Chang TT, Konzak CF (1974) A decimal code for the growth stages of cereals. Weed Research 14:415-421.

Tables and Figures

Table 1. Analysis of variance for the effects of silicon rates (Si), magnesium rates (Mg), plant inoculation (PI), and the Si × Mg, Si × PI, Mg × PI, and Si × Mg × PI interactions for blast severity (Sev), area under blast progress curve (AUBPC), foliar concentrations of silicon (Si) and six macronutrients (N, P, K, Ca, Mg, and S), chlorophyll *a* fluorescence parameters (variable-to-maximum chlorophyll *a* fluorescence ratio (F_v/F_m), photochemical yield (Y(II)), yield for dissipation by down-regulation (Y(NPQ)), yield for non-regulated dissipation (Y(NO))), concentrations of chlorophylls *a*+*b* (Chl *a*+*b*) and carotenoids (Car), activities of superoxide dismutase (SOD), catalase (CAT), ascorbate peroxidase (APX), glutathione reductase (GR), chitinase (CHI), *β*-1,3-glucanase (GLU), peroxidase (POX), phenylalanine ammonia-lyase (PAL), polyphenoloxidase (PPO), and lipoxygenase (LOX) as well as concentrations of malondialdehyde (MDA), hydrogen peroxide (H_2O_2), superoxide anion radical ($O_2^{\bullet-}$), total soluble phenolics (TSP), and lignin-thioglycolic acid (LTGA) derivatives.

Variables/Parameters	Si	Mg	PI	Si × Mg	Si × PI	Mg × PI	Si × Mg × PI
Sev	**0.001**	0.343	-	0.880	-	-	-
AUBPC	**0.001**	0.196	-	0.855	-	-	-
Si	**< 0.001**	0.165	0.766	0.496	0.504	0.674	0.766
N	0.676	0.901	**0.006**	0.939	**< 0.001**	0.769	0.816
P	0.432	0.826	**< 0.001**	0.139	0.622	**< 0.001**	**< 0.001**
K	0.696	0.139	0.051	0.101	**< 0.001**	0.113	**0.002**
Ca	**0.004**	0.240	0.214	0.102	0.656	0.105	0.139
Mg	**< 0.001**	**< 0.001**	0.057	0.066	0.832	0.089	0.993
S	0.619	**0.031**	0.561	0.738	0.962	0.065	0.315
F_v/F_m	**0.007**	0.834	**< 0.001**	0.817	**0.014**	0.989	0.875
Y(II)	**< 0.001**	**0.028**	**< 0.001**	0.774	**0.006**	0.066	0.714
Y(NPQ)	**0.041**	0.177	**0.002**	0.063	**< 0.001**	0.848	0.644
Y(NO)	**< 0.001**	0.152	**< 0.001**	0.964	**< 0.001**	0.059	**0.017**
Chl *a*+*b*	**< 0.001**	**< 0.001**	**< 0.001**	0.090	**< 0.001**	**< 0.001**	0.331
Car	**0.003**	**0.023**	**< 0.001**	**0.004**	**0.013**	0.964	0.640
SOD	**0.001**	0.161	**< 0.001**	0.066	**0.026**	0.771	**0.028**
CAT	0.061	**0.001**	**< 0.001**	**0.006**	0.575	**0.004**	**0.016**
APX	0.137	**0.015**	**< 0.001**	**0.001**	0.870	0.415	**< 0.001**
GR	0.120	0.074	0.138	**0.001**	0.690	0.810	**0.004**
CHI	**0.002**	**0.001**	**< 0.001**	0.060	**0.001**	0.338	**0.027**
GLU	0.103	0.089	**< 0.001**	0.441	**0.009**	0.069	0.243
POX	**0.025**	0.213	**< 0.001**	0.676	0.279	0.117	0.883
PAL	0.632	**0.013**	**< 0.001**	0.648	0.881	0.763	0.688
PPO	**0.001**	0.208	**< 0.001**	0.056	**0.001**	0.443	0.189
LOX	0.224	0.169	**< 0.001**	0.224	**0.037**	0.356	0.514
MDA	0.233	0.291	**< 0.001**	0.290	0.255	0.478	0.459
H_2O_2	0.109	0.071	**< 0.001**	0.272	0.139	0.140	0.244
$O_2^{\bullet-}$	**< 0.001**	0.191	**< 0.001**	**0.026**	0.277	0.889	0.485
TSP	0.279	0.598	**0.002**	0.509	0.262	0.089	0.694
LTGA derivatives	0.879	0.173	**< 0.001**	0.351	0.139	0.073	0.163

[a] Bold values are significant ($P \leq 0.05$).

Table 2. Pearson correlation coefficients among foliar concentrations of silicon (Si) and magnesium (Mg), and blast severity (Sev) as well as of these variables with chlorophyll *a* fluorescence parameters (variable-to-maximum chlorophyll *a* fluorescence ratio (F_v/F_m), photochemical yield (Y(II)), yield for dissipation by down-regulation (Y(NPQ)), yield for non-regulated dissipation (Y(NO))), concentrations of chlorophylls *a*+*b* (Chl *a*+*b*) and carotenoids (Car), activities of antioxidant (superoxide dismutase (SOD), catalase (CAT), ascorbate peroxidase (APX), glutathione reductase (GR)) and defense (chitinase (CHI), *β*-1,3-glucanase (GLU), peroxidase (POX), phenylalanine ammonia-lyase (PAL), polyphenoloxidase (PPO), and lipoxygenase (LOX)) enzymes and concentrations of metabolites (malondialdehyde (MDA), hydrogen peroxide (H_2O_2), superoxide anion radical ($O_2^{\bullet-}$)), total soluble phenolics (TSP), and lignin-thioglycolic acid (LTGA) derivatives).

Variables/Parameters[a]	Si	Mg	Sev
Si	-	**-0.62**	**-0.88**
Mg	**-0.62**	-	**0.56**
F_v/F_m	**0.83**	**-0.69**	**-0.72**
Y(II)	**0.92**	**-0.69**	**-0.87**
Y(NPQ)	**0.79**	**-0.69**	**-0.64**
Y(NO)	**-0.95**	**0.56**	**0.87**
Chl *a*+*b*	**0.58**	0.11	**-0.55**
Car	**0.57**	-0.08	**-0.55**
SOD	-0.17	**0.54**	0.21
CAT	0.30	0.01	-0.16
APX	0.06	-0.17	0.09
GR	-0.34	0.14	0.31
CHI	0.26	0.16	-0.27
GLU	-0.43	**0.66**	0.31
POX	0.01	**0.57**	-0.14
PAL	0.14	0.48	-0.26
PPO	**0.88**	-0.49	**-0.77**
LOX	**0.70**	-0.22	**-0.72**
MDA	**-0.50**	0.27	**0.54**
H_2O_2	**-0.53**	**0.55**	**0.59**
$O_2^{\bullet-}$	**-0.86**	0.29	**0.87**
TSP	0.31	-0.41	-0.18
LTGA derivatives	0.31	0.17	-0.41

Bold values are significant ($P \leq 0.05$).

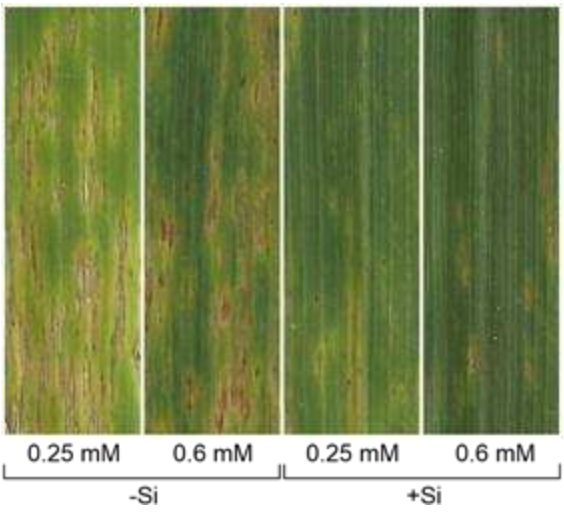

Figure 1. Blast symptoms on the leaves of wheat plants grown in hydroponic culture containing the rates of 0.25 and 0.6 mM magnesium (Mg) in the absence (-Si) or presence (+Si) of silicon (Si) at 96 hours after inoculation with *Pyricularia oryzae*.

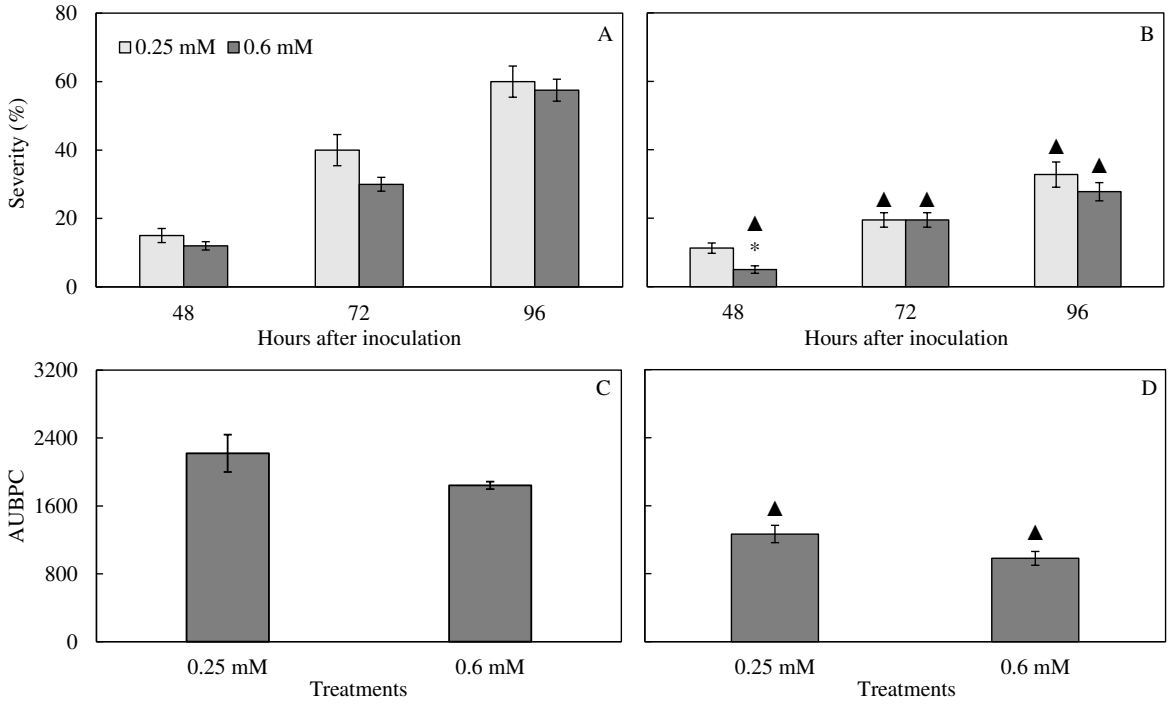

Figure 2. Severity of blast (A and B) and area under blast progress curve (AUBPC) (C and) determined on the leaves of wheat plants grown in hydroponic culture containing the rates of 0.25and 0.6 mM magnesium (Mg) in the absence (-Si) (A and C) or presence (+Si) (B and D) of silicon (Si). The symbol filled triangle (▲) indicates differences between -Si and +Si treatments, at each Mg rate and evaluation time (graphics A and B only), according to *F* test. Bars represent the standard error of the means. $n = 4$.

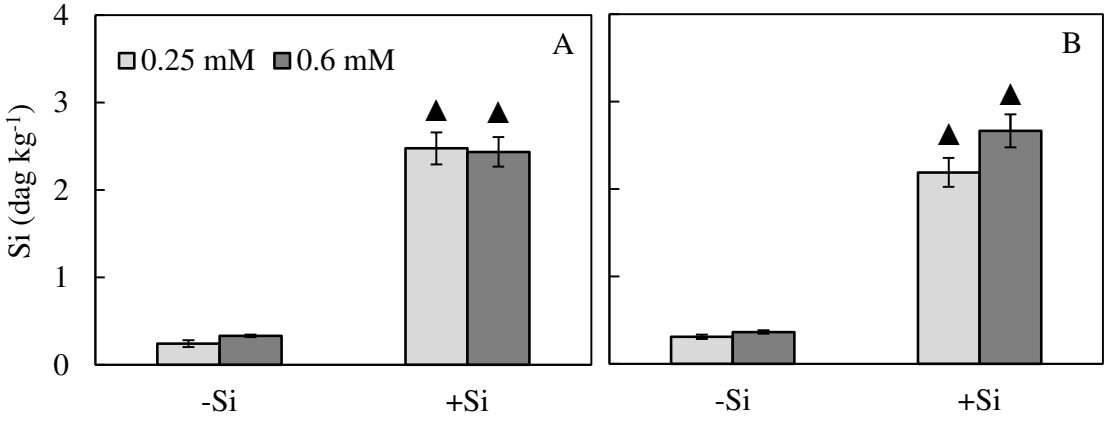

Figure 3. Foliar concentration of silicon (Si) for wheat plants grown in hydroponic culture containing the rates of 0.25 and 0.6 mM magnesium (Mg) in the absence (-Si) or presence (+Si) of Si and either non-inoculated (A) or inoculated (B) with *Pyricularia oryzae*. The symbol filled triangle (▲) indicates differences between 0.25 mM and 0.6 mM Mg rates, at each Si treatment, for non-inoculated and inoculated plants according to *F* test. Bars represent the standard errors of the means. $n = 4$.

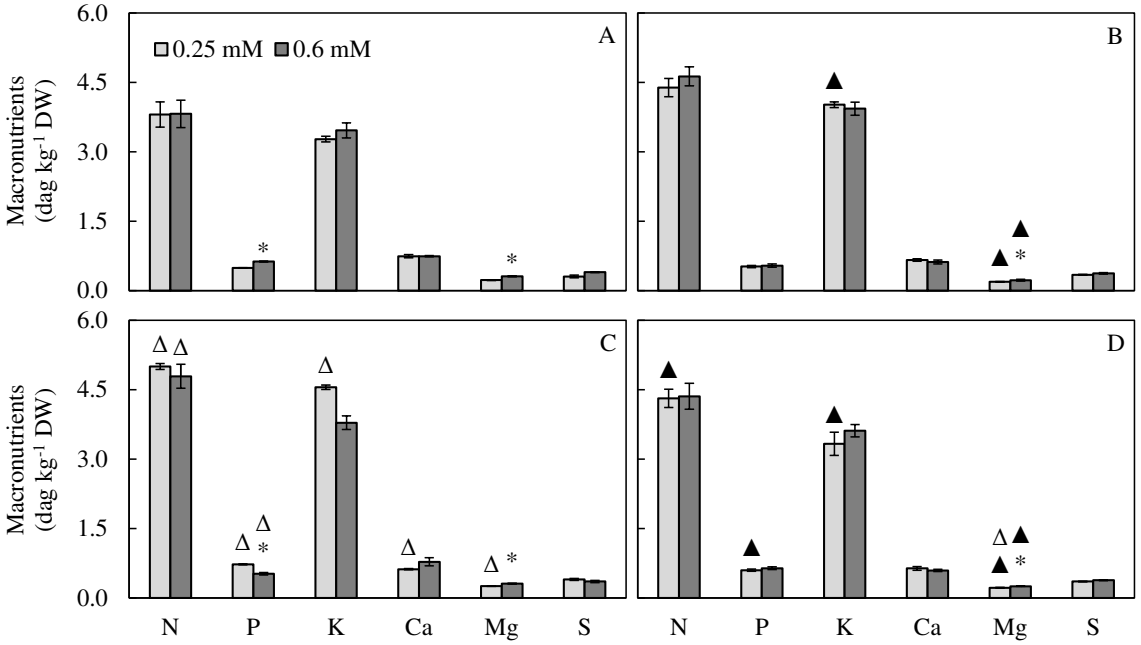

Figure 4. Foliar concentrations of nitrogen (N), phosphorus (P), potassium (K), calcium (Ca), magnesium (Mg), and sulfur (S) for wheat plants grown in hydroponic culture containing the rates of 0.25 and 0.6 mM magnesium (Mg) in the absence (-Si) (A and C) or presence (+Si) (B and D) of silicon (Si) and either non-inoculated (A and B) or inoculated (C and D) with *Pyricularia oryzae*. Means for 0.25 and 0.6 mM Mg, at each evaluation time, followed by an asterisk (*) are significantly different ($P \leq 0.05$) according to *F* test. The symbol filled triangle (▲) indicates differences between -Si and +Si plants for non-inoculated and inoculated treatments, at each Mg rate, according to *F* test. The symbol empty triangle (Δ) indicates differences between non-inoculated and inoculated plants for -Si and +Si treatments, at each Mg rate, according to *F* test. Bars represent the standard errors of the means. DW = dry weight. $n = 4$.

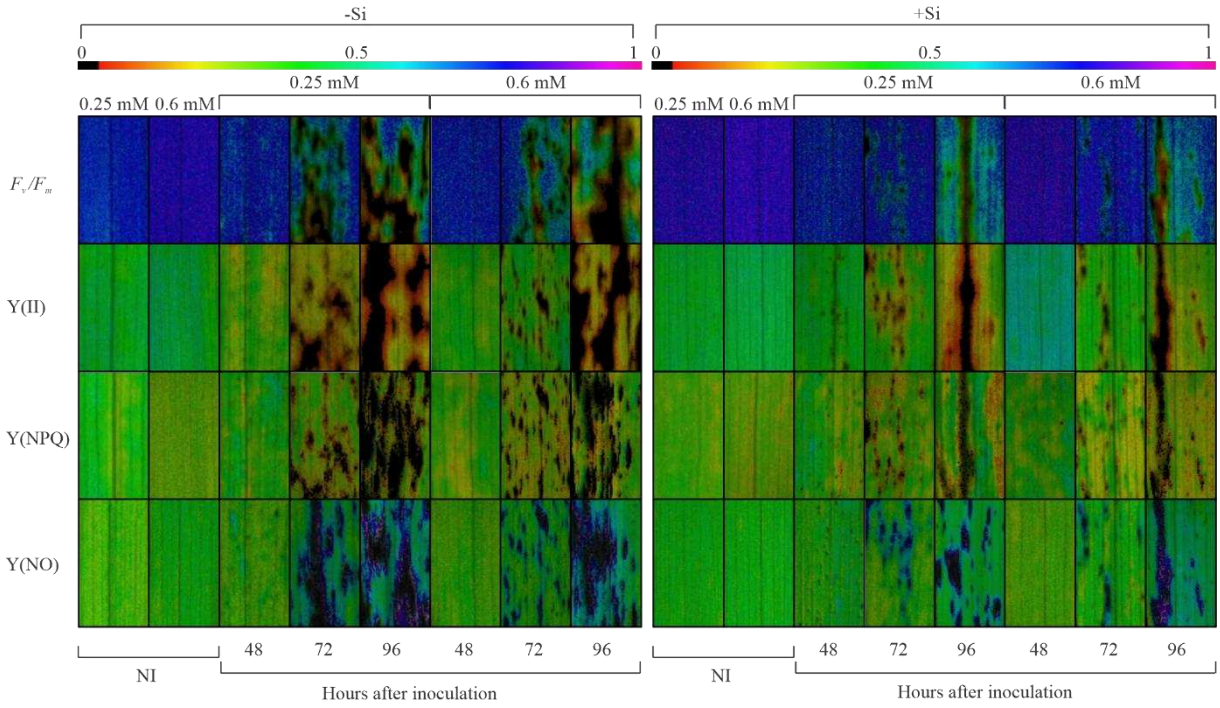

Figure 5. Images of chlorophyll *a* fluorescence parameters: variable-to-maximum chlorophyll a fluorescence ratio (F_v/F_m), photochemical yield (Y(II)), yield for dissipation by downregulation (Y(NPQ)), and yield for non-regulated dissipation (Y(NO)) determined on the leaves of wheat plants grown in hydroponic culture containing the rates of 0.25 and 0.6 mM magnesium (Mg) in the absence (-Si) or presence (+Si) of silicon (Si) and either non-inoculated (NI) or at 48, 72, and 96 hours after inoculation with *Pyricularia oryzae*.

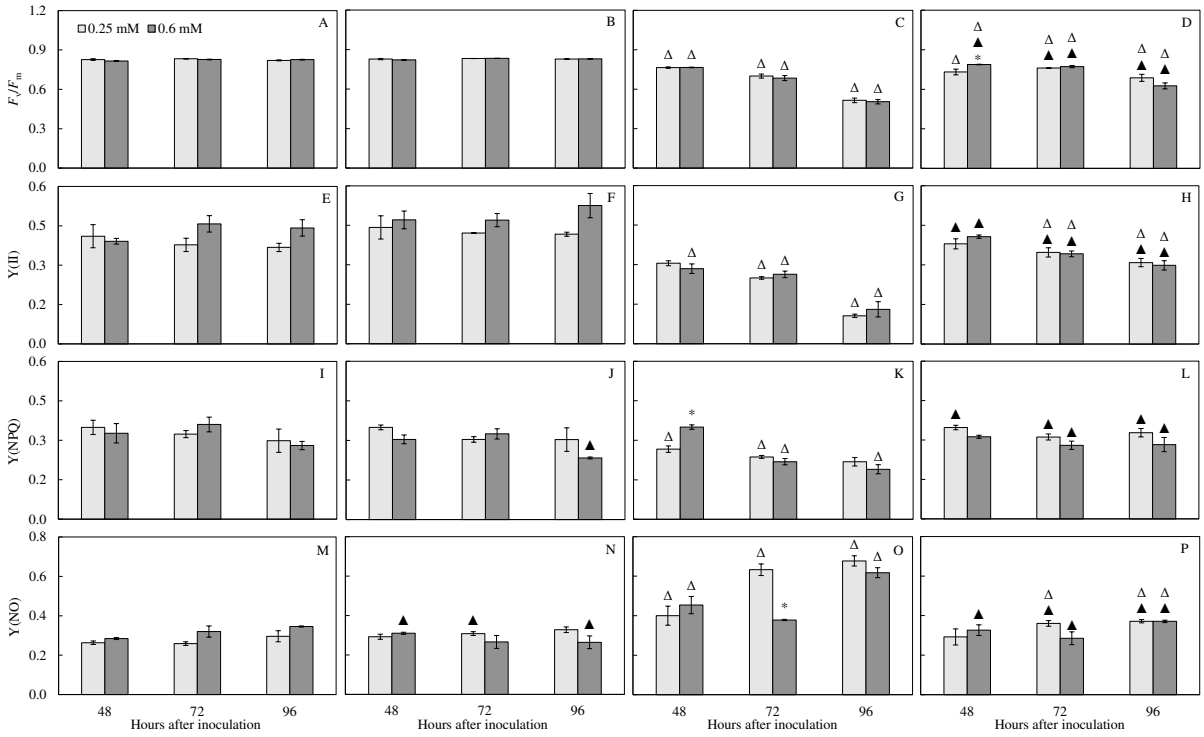

Figure 6. Quantification of chlorophyll *a* parameters: variable-to-maximum chlorophyll *a* fluorescence ratio (F_v/F_m) (A-D), photochemical yield (Y(II)) (E-H), yield for dissipation by down-regulation (Y(NPQ)) (I-L), and yield for non-regulated dissipation (Y(NO)) (M-P) on the leaves of wheat plants grown in hydroponic culture containing the rates of 0.25 and 0.6 mM magnesium (Mg) in the absence (-Si) (A, C, E, G, I, K, M, and O) or presence (+Si) (B, D, F, H, J, L, N, and P) of silicon (Si) and either non-inoculated (A-B, E-F,I-J, and M-N) or inoculated (C-D, G-H, K-L, and O-P) with *Pyricularia oryzae*. Means for 0.25 and 0.6 mM Mg, at each evaluation time, followed by an asterisk (*) are significantly different ($P \leq 0.05$) according to *F* test. The symbol filled triangle (▲) indicates differences between -Si and +Si plants for non-inoculated and inoculated treatments, at each Mg rate, according to *F* test. The symbol empty triangle (Δ) indicates differences between non-inoculated and inoculated plants for -Si and +Si plants treatments, at each Mg rate, according to *F* test. Bars represent the standard errors of the means. $n = 4$.

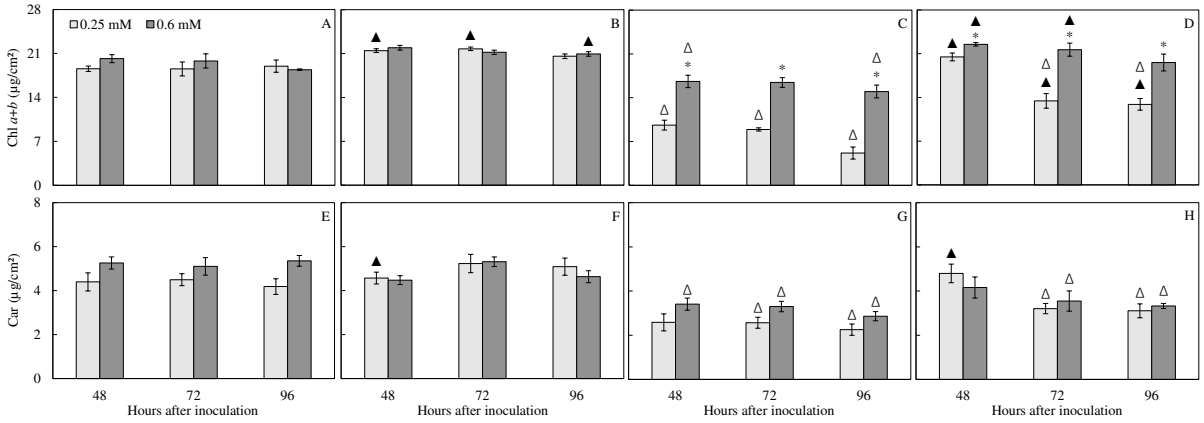

Figure 7. Concentrations of chlorophylls *a*+*b* (Chl *a*+*b*) (A-D) and carotenoids (Car) (E-H) determined on the leaves of wheat plants grown in hydroponic culture containing the rates of 0.25 and 0.6 mM magnesium (Mg) in the absence (-Si) (A, C, E, and G) or presence (+Si) (B, D, F, and H) of silicon (Si) and either non-inoculated (A-B and E-F) or inoculated (C-D and G-H) with *Pyricularia oryzae*. Means for 0.25 and 0.6 mM Mg, at each evaluation time, followed by an asterisk (*) are significantly different ($P \leq 0.05$) according to *F* test. The symbol filled triangle (▲) indicates differences between -Si and +Si plants for non-inoculated and inoculated treatments, at each Mg rate, according to *F* test. The symbol empty triangle (Δ) indicates differences between non-inoculated and inoculated plants for -Si and +Si plants treatments, at each Mg rate, according to *F* test. Bars represent the standard errors of the means. $n = 4$.

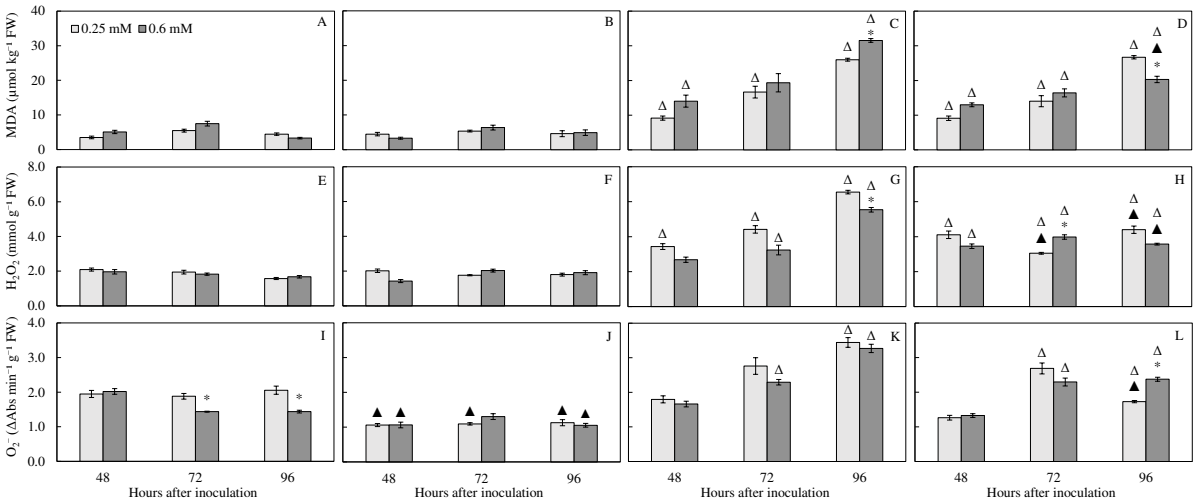

Figure 8. Concentrations of malondialdehyde (MDA) (A-D), hydrogen peroxide (H_2O_2) (E-H), and superoxide anion radical ($O_2^{\bullet-}$) (I-L) determined on the leaves of wheat plants grown in hydroponic culture containing the rates of 0.25 and 0.6 mM magnesium (Mg) in the absence (-Si) (A, C, E, G, I, and K) or presence (+Si) (B, D, F, H, J, and L) of silicon (Si) and either non-inoculated (A-B, E-F, and I-J) or inoculated (C-D, G-H, and K-L) with *Pyricularia oryzae*. Means for 0.25 and 0.6 mM Mg, at each evaluation time, followed by an asterisk (*) are significantly different ($P \leq 0.05$) according to *F* test. The symbol filled triangle (▲) indicates differences between -Si and +Si plants for non-inoculated and inoculated treatments, at each Mg rate, according to *F* test. The symbol empty triangle (Δ) indicates differences between non-inoculated and inoculated plants for -Si and +Si treatments, at each Mg rate, according to *F* test. Bars represent the standard errors of the means. FW = fresh weight $n = 4$.

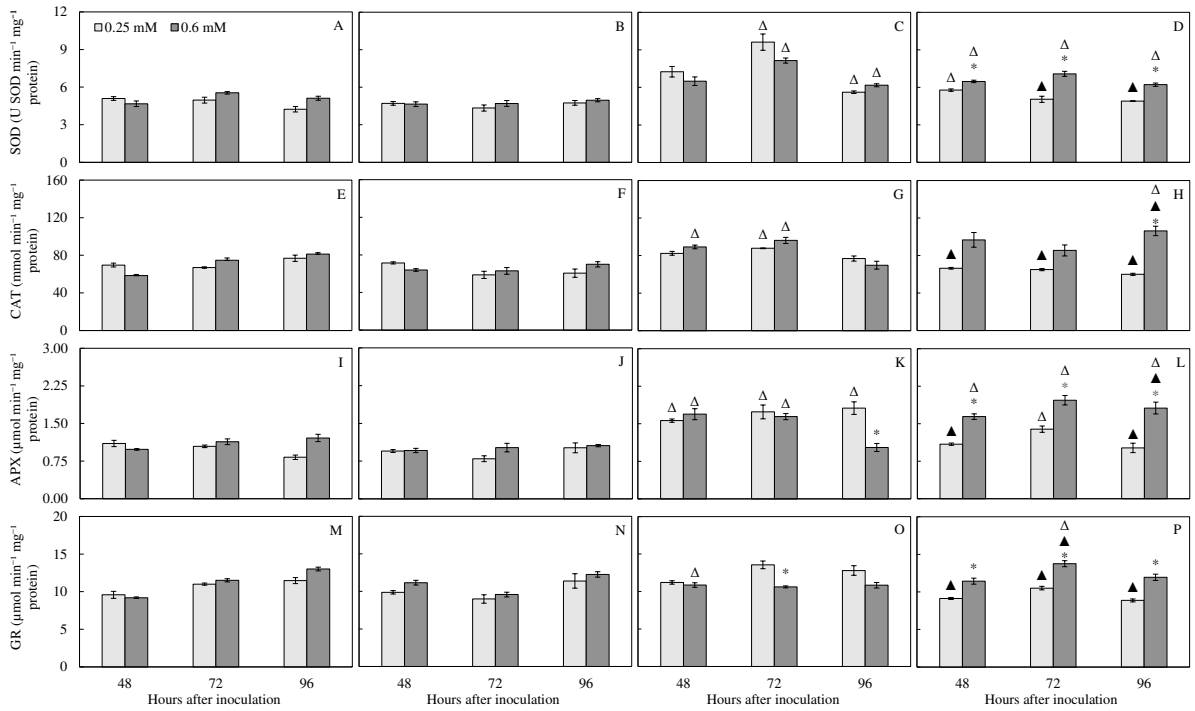

Figure 9. Activities of superoxide dismutase (SOD) (A-D), catalase (CAT) (E-H), ascorbate peroxidase (APX) (I-L), and glutathione reductase (GR) (M-P) determined on the leaves of wheat plants grown in hydroponic culture containing the rates of 0.25 and 0.6 mM magnesium (Mg) in the absence (-Si) (A, C, E, G, I, K, M, and O) or presence (+Si) (B, D, F, H, J, L, N, and P) of silicon (Si) and either non-inoculated (A-B, E-F, I-J, and M-N) or inoculated (C-D, G-H, K-L, and O-P) with *Pyricularia oryzae*. Means for 0.25 and 0.6 mM Mg, at each evaluation time, followed by an asterisk (*) are significantly different ($P \leq 0.05$) according to *F* test. The symbol filled triangle (▲) indicates differences between -Si and +Si plants for non-inoculated and inoculated treatments, at each Mg rate, according to *F* test. The symbol empty triangle (Δ) indicates differences between non-inoculated and inoculated plants for -Si and +Si treatments, at each Mg rate, according to *F* test. Bars represent the standard errors of the means. $n = 4$.

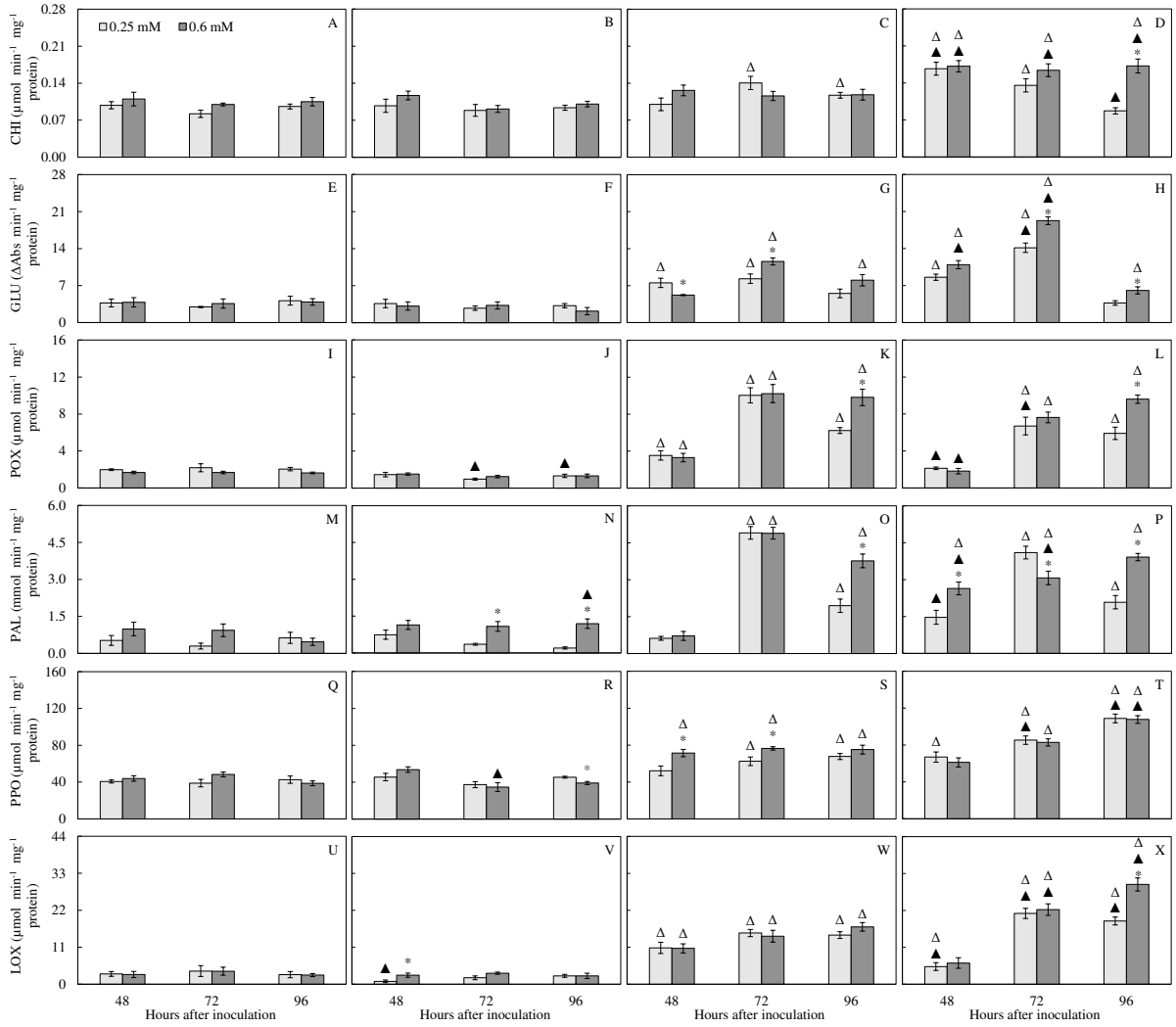

Figure 10. Activities of chitinase (CHI) (A-D), *β*-1,3-glucanase (GLU) (E-H), peroxidase (POX) (I-L), phenylalanine ammonia-lyase (PAL) (M-P), polyphenoloxidase (PPO) (Q-T), and lipoxygenase (LOX) (U-X) determined on the leaves of wheat plants grown in hydroponic culture containing the rates of 0.25 and 0.6 mM magnesium (Mg) in the absence (-Si) (A, C, E, G, I, K, M, O, Q, S, U, and W) or presence (+Si) (B, D, F, H, J, L, N, P, R, T, V, and X) of silicon (Si) and either non-inoculated (A-B, E-F, I-J, M-N, Q-R, and U-V) or inoculated (C-D, G-H, K-L, O-P, S-T, and W-X) with *Pyricularia oryzae*. Means for 0.25 and 0.6 mM Mg, at each evaluation time, followed by an asterisk (*) are significantly different ($P \leq 0.05$) according to *F* test. The symbol filled triangle (▲) indicates differences between -Si and +Si plants for non-inoculated and inoculated treatments, at each Mg rate, according to *F* test. The symbol empty triangle (Δ) indicates differences between non-inoculated and inoculated plants for -Si

and +Si treatments, at each Mg rate, according to *F* test. Bars represent the standard errors of the means. $n = 4$.

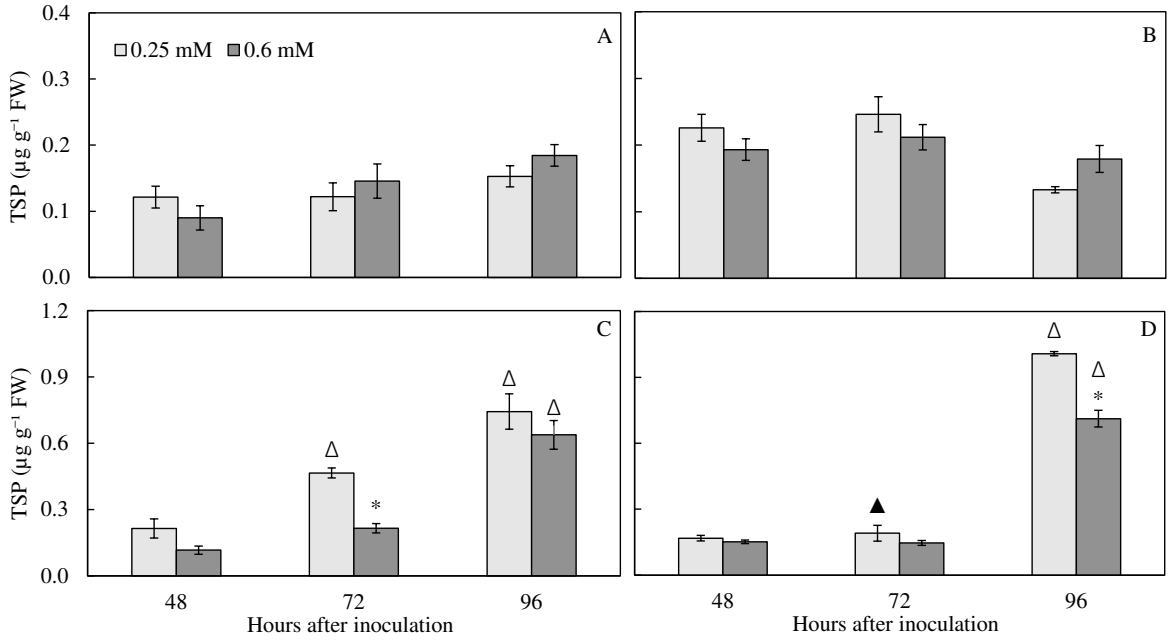

Figure 11. Concentration of total soluble phenolics (TSP) determined on the leaves of wheat plants grown in hydroponic culture containing the rates of 0.25 and 0.6 mM magnesium (Mg) in the absence (-Si) (A and C) or presence (+Si) (B and D) of silicon (Si) and either non-inoculated (A and B) or inoculated (C and D) with *Pyricularia oryzae*. Means for 0.25 and 0.6 mM Mg, at each evaluation time, followed by an asterisk (*) are significantly different ($P \leq 0.05$) according to *F* test. The symbol filled triangle (▲) indicates differences between -Si and +Si plants for non-inoculated and inoculated treatments, at each Mg rate, according to *F* test. The symbol empty triangle (Δ) indicates differences between non-inoculated and inoculated plants for -Si and +Si treatments, at each Mg rate, according to *F* test. Bars represent the standard errors of the means. FW = fresh weight. $n = 4$.

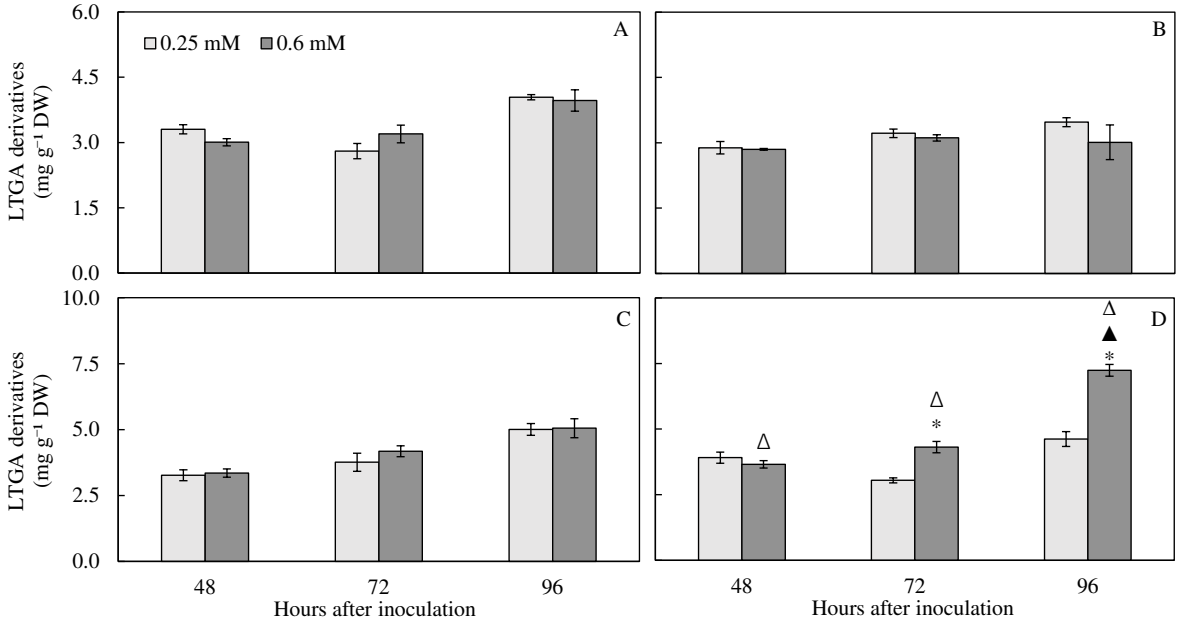

Figure 12. Concentration of lignin-thioglycolic acid (LTGA) derivatives determined on the leaves of wheat plants grown in hydroponic culture containing the rates of 0.25 and 0.6 mM magnesium (Mg) in the absence (-Si) (A and C) or presence (+Si) (B and D) of silicon (Si) and either non-inoculated (A and B) or inoculated (C and D) with *Pyricularia oryzae*. Means for 0.25 and 0.6 mM Mg, at each evaluation time, followed by an asterisk (*) are significantly different ($P \leq 0.05$) according to *F* test. The symbol filled triangle (▲) indicates differences between -Si and +Si plants for non-inoculated and inoculated treatments, at each Mg rate, according to *F* test. The symbol empty triangle (Δ) indicates differences between non-inoculated and inoculated plants for -Si and +Si treatments, at each Mg rate, according to *F* test. Bars represent the standard errors of the means. DW = dry weight. $n = 4$.

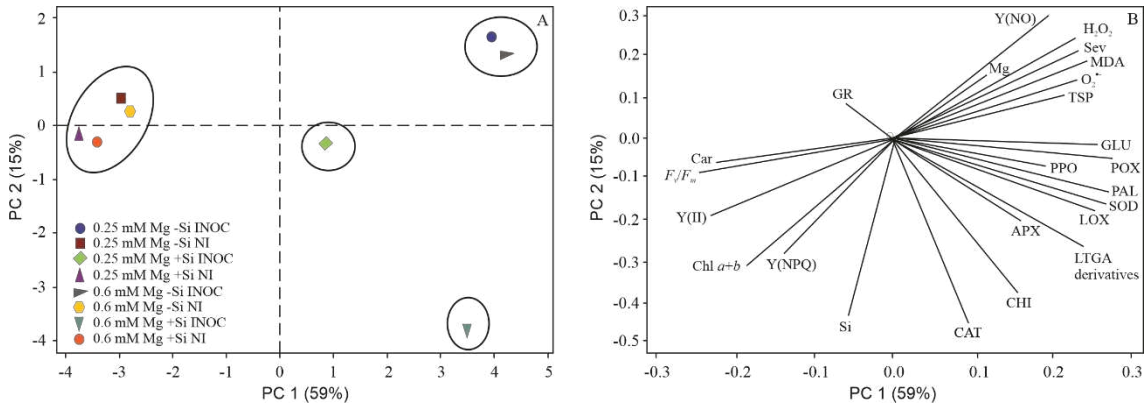

Figure 13. Principal components analysis showing score plot (a) and loading values (b) in the principal component analysis for foliar silicon (Si) and magnesium (Mg) concentrations, severity (Sev), chlorophyll *a* fluorescence parameters, defense and antioxidant enzymes, and concentrations of metabolites, total soluble phenolics (TSP), and lignin-thioglycolic acid (LTGA) derivatives for wheat plants grown in hydroponic culture containing the rates of 0.25 and 0.6 mM magnesium (Mg) in the absence (-Si) or presence (+Si) of silicon (Si) and either non-inoculated (NI) or inoculated (INOC) with *Pyricularia oryzae*. Chlorophyll *a* fluorescence parameters: maximum PSII quantum efficiency (F_v/F_m), effective photosystem II quantum yield (Y(II)), quantum yield of regulated energy dissipation (Y(NPQ)) and quantum yield of non-regulated energy dissipation (Y(NO)). Concentrations of photosynthetic pigments: chlorophylls *a*+*b* (Chl *a*+*b*) and carotenoids (CAR). Activities of antioxidant (ascorbate peroxidase (APX), catalase (CAT), glutathione reductase (GR), peroxidase (POX), superoxide dismutase (SOD)) and defense (chitinase (CHI), *β*-1,3-glucanase (GLU), peroxidase (POX), polyphenoloxidase (PPO), lipoxygenase (LOX), and phenylalanine ammonia-lyase (PAL)) enzymes. Concentrations of metabolites: malondialdehyde (MDA), hydrogen peroxide (H_2O_2), and superoxide anion radical ($O_2^{\bullet-}$). Groups were generated from cluster analysis with complete linkage and Pearson distance.

Chapter II

ACIDS *β*-AMINOBUTYRIC AND *γ*-AMINOBUTYRIC IN THE POTENTIATION OF WHEAT RESISTANCE AGAINST BLAST

Resumo

ARAUJO, Marcela Uli Peixoto, Dsc., Universidade Federal de Viçosa, Outubro, 2021. **Ácidos *β*-aminobutírico e *γ*-aminobutírico na Potencialização da Resistência do Trigo à Brusone**. Orientador: Fabrício Ávila Rodrigues.

Epidemias de brusone, causadas por *Pyricularia oryzae*, têm ocasionado grandes perdas na produção do trigo e o controle dessa doença depende do uso de cultivares resistentes combinada com a pulverização de fungicidas. Outras estratégias de controle precisam ser investigadas e o uso de indutores de resistência pode se tornar uma estratégia ambientalmente amigável e viável para o manejo da brusone. Nesse contexto, foi investigado o potencial dos ácidos *β*-aminobutírico (BABA) e *γ*-aminobutírico (GABA) em induzir a resistência do trigo à brusone. Este objetivo foi alcançado analisando o desempenho fotossintético (medições da fluorescência da clorofila (Chl) *a* e concentrações de pigmentos fotossintéticos (Chl *a*+*b*) e carotenoides), resposta de defesa (atividades da quitinase (QUI), *β*-1,3-glucanase (GLU), peroxidase (POX), fenilalanina amônia-liase (FAL), polifenoloxidase (PFO), lipoxigenase (LOX) e concentrações de compostos fenólicos e lignina), metabolismo antioxidativo (atividades da superóxido dismutase (SOD), catalase (CAT), ascorbato peroxidase (APX) e glutationa redutase (GR)), assim como o estresse oxidativo (concentrações de aldeído malônico (MDA), peróxido de hidrogênio (H_2O_2) e ânion superóxido ($O_2^{\bullet -}$)) de plantas não inoculadas ou inoculadas da cultivar BRS Guamirim (suscetível à brusone) pulverizadas com água ou com soluções (100 mM) de BABA e GABA. As plantas foram pulverizadas com soluções de BABA e GABA às 48 h antes da inoculação com *P. oryzae*. A brusone progrediu muito mais rápido nas plantas pulverizadas com água e GABA do que nas plantas pulverizadas com BABA. A área abaixo da curva do progresso da brusone foi significativamente maior em 52 e 47% para plantas dos tratamentos controle e GABA, respectivamente, em comparação com as plantas pulverizadas

com BABA. Os valores dos parâmetros da fluorescência da Chl *a* (eficiência quântica máxima do fotossistema II, rendimento fotoquímico e rendimento quântico de dissipação regulada) e as concentrações de Chl *a*+*b* e carotenoides foram maiores para as plantas pulverizadas com BABA em comparação as plantas dos tratamentos controle e GABA. As atividades da QUI, GLU, FAL, PFO e LOX foram mais notáveis para as plantas pulverizadas com BABA do que para aquelas dos tratamentos controle e GABA. Maiores atividades da APX, CAT e SOD para as plantas pulverizadas com BABA ajudaram no alívio do estresse imposto pelas altas concentrações de H_2O_2 e $O_2^{\bullet-}$ em contraste com os tratamentos controle e GABA. Levando tudo isso em consideração, os resultados do presente estudo permitem concluir que o fornecimento de BABA às plantas de trigo aumentou a resistência à brusone em um cenário onde o aparato fotossintético foi preservado juntamente com uma maior resposta de defesa e um metabolismo antioxidativo mais robusto para reduzir o efeito negativo imposto pela infecção por *P. oryzae*.

Palavras-chave: aminoácidos, doença fúngica, espécies reativas de oxigênio, metabolismo antioxidativo, patógeno hemibiotrófico, resistência induzida, respostas de defesa do hospedeiro.

Abstract

ARAUJO, Marcela Uli Peixoto, Dsc., Universidade Federal de Viçosa, October, 2021. **Acids *β*-aminobutyric and *γ*-aminobutyric in the Potentiation of Wheat Resistance against Blast**. Adviser: Fabrício Ávila Rodrigues.

Epidemics of blast, caused by *Pyricularia oryzae*, have caused great yield losses in wheat and disease control has relied on using resistant cultivars combined with fungicides spray. Other control strategies need to be investigated and the use of inducers of host resistance may become an environmentally friendly and viable strategy for blast management. In this context, the potential of using the acids *β*-aminobutyric (BABA) and γ-aminobutyric (GABA) to induce wheat resistance against blast was investigated. This goal was achieved by examining the photosynthetic performance (fluorescence of chlorophyll (Chl) *a* measurements and photosynthetic pigments pools (Chl *a*+*b* and carotenoids), host defense responses (activities of chitinase (CHI), *β*-1,3-glucanase (GLU), peroxidase (POX), phenylalanine ammonia-lyase (PAL), polyphenoloxidase (PPO), and lipoxygenase (LOX) as well as concentrations of phenolics and lignin), antioxidative metabolism (activities of superoxide dismutase (SOD), catalase (CAT), ascorbate peroxidase (APX), and glutathione reductase (GR)) as well as oxidative stress (concentrations of malondialdehyde (MDA), hydrogen peroxide (H_2O_2), and superoxide anion radical ($O_2^{\bullet-}$)) of non-inoculated and inoculated plants from cultivar BRS Guamirim (susceptible to blast) sprayed with water or with solutions (100 mM) of BABA and GABA. Plants were sprayed with BABA and GABA solutions at 48 h before inoculation with *B. oryzae*. Blast progressed much faster for water and GABA-sprayed plants than for BABA-sprayed plants. The area under blast progress curve was significantly higher by 52 and 47% for plants from control and GABA treatments, respectively, compared to BABA-sprayed plants. Values of Chl *a* fluorescence (variable-to-maximum Chl *a* fluorescence ratio, photochemical

yield, and yield for dissipation by down-regulation) parameters linked to Chl *a*+*b* and carotenoids concentrations were higher for BABA-sprayed plants than for those of control and GABA treatments. Activities of CHI, GLU, PAL, PPO, and LOX were more remarkable for BABA-sprayed plants than for those from control and GABA treatments. Greater APX, CAT, and SOD activities for BABA-sprayed plants helped to alleviate the stress imposed by higher H_2O_2 and $O_2^{\bullet-}$ concentrations in contrast from control and GABA treatments. Taken together, the results of the present study allowed to conclude that supplying BABA to wheat plants increased their resistance against blast in a scenario where photosynthetic apparatus was preserved along with a boosted defense response and a more robust antioxidative metabolism to counteract the harmful effect imposed by *P. oryzae* infection.

Keywords: amino acids, antioxidative metabolism, fungal disease, hemibiotrophic pathogen, host defense responses, induced resistance, reactive oxygen species.

Introduction

Wheat (*Triticum aestivum* L.) is the second most cereal cultivated worldwide and a very important source of proteins for both human and animal feed (FAO, 2020). Many fungal diseases affect the achievement of high wheat yield and, therefore, threaten world food security (Fisher et al., 2012). Blast, caused by hemibiotrophic fungus *Pyricularia oryzae* Cavara (teleomorph *Magnaporthe oryzae* (T. T. Hebert) M. E. Barr), stands out as one of the most destructive and yield-limiting diseases on wheat grown in warm and humid regions worldwide (Rodrigues et al., 2017; Ceresini et al., 2018). Although blast symptoms occur in all above-ground parts of wheat plants (*e.g.*, elliptical to round necrotic lesions on leaves), they become more expressive in the spikes, which become bleached after rachis or the base of spikes are infected by *P. oryzae* (Urashima et al., 2009; Ceresini et al., 2018). Genetic breeding for wheat resistance against blast became a reliable option for disease control even though few effective resistance genes have been identified (Anh et al., 2018; Ceresini et al., 2018; Wang et al., 2018). Available fungicides in the market are not efficient to slow blast epidemic rate and if intensively used may impose pressure against pathogen population resulting in rapid development of resistance mechanisms (Castroagudín et al., 2015; Ceresini et al., 2018). Therefore, the need of using integrated wheat blast management strategies is of detrimental importance considering the potential of this disease to decrease yield and grain quality, the broad host range of *P. oryzae*, and the inefficiency of using control methods separately (Pagani et al., 2014; Ceresini et al., 2018).

A sustainable environmentally friendly alternative to reduce the impact imposed by diseases on crop yield and quality relies on the use of different types of induced resistance stimulus (*e.g.*, abiotic or biotic) to prime or elicit plants to defend themselves (rapid and stronger activation of defense responses: increased production of phenolics, phytoalexins, and lignin along well with a great expression of pathogenesis-related genes), either local or systemically,

against pathogens infection (Jones and Dangl, 2006; Spoel and Dong, 2012; Mauch-Mani et al., 2017; Reglinski et al., 2007; Kesel et al., 2021; Conrath et al., 2015). To date, wheat resistance to blast has been potentiated by supplying silicon and calcium to plants as well as spraying them with phosphites, potassium silicate, or ethephon (Rodrigues et al., 2017). The non-proteinogenic amino acids β-aminobutyric acid (BABA) and its isomer named as γ-aminobutyric acid (GABA) can trigger defense responses in several plant species infected by pathogens of different lifestyles (Jakab et al., 2001; Justyna and Ewa, 2013; Cohen, 2002; Tarkowski et al., 2019; Cohen et al., 2016). Compelling evidence indicates that BABA was more efficient than GABA in reducing disease symptoms and efficiently boosting host defense responses for a larger number of host-pathogen interactions (Tarkowski et al., 2019; Cohen et al., 2016). For instance, severities of anthracnose, Phoma stem canker, and late blight in pepper, rapeseed, and tomato, respectively, besides downy mildew in cauliflower, grapevines, lettuce, and sunflower were greatly reduced by BABA in contrast to GABA (Cohen et al., 2016; Justyna and Ewa, 2013). The amino group at position 3(β) against the terminal carboxyl group provides BABA with an outstanding efficiency to help plants to cope with infections caused by viruses, protista, bacteria, oomycetes, fungi, and nematodes (Cohen, 2001, 2002; Cohen et al., 2016; Jakab et al., 2001; Baccelli and Mauch-Mani, 2016; Justyna and Ewa, 2013). Interestingly, plants exposed to BABA are primed to react faster and robustly (*e.g.*, production of reactive oxygen species and higher glycolate oxidase activity) upon exposition to abiotic stress and infection by soilborne, foliar, and fruit pathogens besides the fact that primed defense responses are kept in the next plants generation (Slaughter et al., 2012; Cohen et al., 2016; Li et al., 2019). Experiments carried out with *Arabidopsis* and some crop plants (*e.g.*, grapevines, potato, and tobacco) confirmed that BABA-induced resistance resulted in multiple signaling pathways leading to activation of host defense depending mainly on pathogen lifestyle (*e.g.*, *Pseudomonas syringae* pv. *tomato*, *Botrytis cinerea*, *Phytophthora infestans*, *tobacco mosaic*

virus vs. systemic acquired resistance-associated features (salicylic acid (SA) production and functional NPR1/NIMI protein; *Plasmopora viticola vs.* jasmonic acid (JA)-regulated genes; *Hyaloperonospora arabidopsidis*, *Alternaria brassicicola*, and *Plectosphaerella cucumerina vs.* impaired SA-, JA-, and ethylene-dependent signaling pathways; and *P. cucumerina vs.* low production or sensitivity to abscisic acid) (Cohen et al., 2016). One fact distinguishing BABA as a unique inducer of resistance stimulus refers to reduction on diseases symptoms on apple, cauliflower, grapevines, lettuce, tomato, and tobacco plants exposed to it from 1 to 3 days after inoculation with *Alternaria alternata* f. sp. *mali*, *Peronospora parasitica*, *P. viticola*, *Bremia lactucae*, *P. infestans*, and *Peronospora tabacina*, respectively (Cohen, 2002; Cohen et al., 2016; Gur et al., 2021). Wheat is among the few plant species capable of synthesizing BABA (Thevenet et al., 2017). After BABA supply to wheat plants, the endogenous level of this peculiar *β*-amino acid rapidly increased and infections by *Fusarium graminearum*, *Heterodera avenae*, and *H. latipons* result in lower diseases intensities (Thevenet et al., 2016; Cohen et al., 2016). Wheat plants drenched with BABA showed enhanced resistance against Septoria tritici leaf blotch as noticed by reduced foliar area with necrotic lesions and fewer pycnidia produced per cm^2 of leaf (Bellameche et al., 2020). Moreover, germination of *Zymoseptoria tritici* conidia on leaves of BABA-treated plants was reduced and hypha from germinated conidia grew slowly (Bellameche et al., 2020).

Considering blast as a very destructive disease capable of greatly reduce yield and lower grains quality, this study tested the hypothesis that wheat plants sprayed with BABA and GABA could have their resistance potentiated and, therefore, displaying lower blast symptoms. Therefore, to shed light on the possible induced resistance mediated by BABA and GABA, an in-depth analysis of the physiological and biochemical changes occurring in plants exposed to these two induced resistance stimuli and challenged or not with *P. oryzae* was performed.

Material and Methods

Plant growth

Wheat seeds from cultivar BRS Guamirim, susceptible to blast (Cruz et al., 2010), were surface sterilized in 10% (vol/vol) NaOCl for 2 min, rinsed in sterilized water for 3 min, and sown in plastic pots filled with 1 kg of substrate (Tropstrato, Vida Verde, Mogi Mirim, SP, Brazil). A total of 1.63 g of calcium phosphate monobasic was added to each plastic pot. Seven seeds were sown per pot and at five days after seedlings emergence, each pot was thinned to five seedlings. Substrate in each pot was weekly fertilized with a nutrient solution prepared with deionized water and containing, in g L^{-1}, 6.4 KCl, 3.48 K_2SO_4, 5.01 $MgSO_4.7H_2O$, 2.03 $(NH_2)_2CO$, 0.009 $NH_4MO_7O_{24}.4H_2O$, 0.054 H_3BO_3, 0.222 $ZnSO_4.7H_2O$, 0.058 $CuSO_4.5H_2O$, and 0.137 $MnCl_2.4H_2O$ (Xavier Filha et al., 2011). A volume of 15 mL of nutrient solution containing 0.27 g of $FeSO_4.7H_2O$ and 0.37 g of ethylenediaminetetraacetic acid (EDTA) disodium L^{-1} was also applied after seedlings emergence. Plants in each pot received 30 mL of the nutrient weekly starting after seedlings emergence. Plants were watered as needed. Plants were grown in a greenhouse (temperature of 25 ± 2°C, relative humidity of 70 ± 5%, and natural photosynthetically active radiation of 950 ± 50 µmol photons m^{-2} s^{-1}) during 45 days.

Application of inducers

Solutions of BABA and GABA (Sigma-Aldrich A4420 and A5835, respectively; São Paulo, Brazil), at 100 mM concentration, were prepared using distilled sterile water. Plants were sprayed with BABA and GABA solutions (10 ml per plant) at 48 h before being inoculated with *P. oryzae* as a fine mist to leaves of each plant by using a VL Airbrush atomizer (Paasche Airbrush Co., Chicago, IL, USA). Plants sprayed with water served as a control treatment.

Inoculum production and plant inoculation

The isolate UFV/DFP *Po*-12 of *P. oryzae* obtained from spikes of wheat plants from cultivar BR-18 was used to inoculate the plants (Debona et al., 2012). Disks of filter paper containing fungal mycelia were transferred to Petri dishes containing oat-agar medium. After fungal mycelia growth, plugs of the medium containing fungal mycelia were transferred to new Petri dishes containing the same medium. The dishes were incubated in a growth chamber at 25°C with a 24 h photoperiod for eight days. After this period, conidia were carefully removed from the dishes with a soft bristle brush using water containing gelatin (1% wt/vol). The conidial suspension was calibrated with a hemacytometer to obtain a concentration of 1×10^5 conidia/ml. The conidial suspension was sprayed on the adaxial surface of the leaves of plants (Zadoks et al., 1974) with the aid of a VL Airbrush atomizer. After inoculation, plants were kept in a mist chamber at 25°C for 24 h at darkness. Thereafter, plants were transferred to a greenhouse (temperature of 25 ± 3°C, relative humidity of 80 ± 5%, and photoperiod of 12 hours) during the experiments.

Experimental design

A 3 × 2 factorial experiment, consisting of three treatments (water (control), BABA e GABA) and plant inoculation (non-inoculated and inoculated plants), was arranged in a completely randomized design with four replications. Each experimental unit consisted of one plastic pot containing five plants.

Blast assessments

Blast severity was assessed on fourth and fifth leaves, from base to top, of each plant per replication of each treatment at 48, 72, and 96 hai using the diagrammatic scale proposed by Rios et al. (2013).

Imaging and quantification of chlorophyll (Chl) *a* fluorescence parameters

Images and parameters of Chl *a* fluorescence were obtained from fourth leaf, from base to top, of each plant per replication of each treatment at 48, 72, and 96 hai using the MAXI version of the Imaging-PAM fluorometer and the Imaging Win software (Heinz Walz GmbH, Effeltrich, Germany). The Chl *a* fluorescence emission transients were captured by a CCD (charge-coupled device) camera with a resolution of 640 × 480 pixels in a visible sample area of 24 × 32 mm on each leaf. The leaves were initially adapted to darkness for 30 min, after which they were carefully and individually fixed in a support at a distance of 18.5 cm from the CCD camera. The leaves were then exposed to a weak, modulated measuring beam (0.5 μmol m^{-2} s^{-1}, 100 μs, 1 Hz) to determine the initial fluorescence (F_0) when all the photosystem II (PSII) reaction centers were "open". Next, a saturating white light pulse of 2,400 μmol m^{-2} s^{-1} (10 Hz) was applied for 0.8 s to ensure maximum fluorescence emission (F_m) when all the PSII reaction centers are expected to be "closed". From these initial measurements, maximum PSII photochemical efficiency of the dark-adapted leaves was estimated through the variable-to-maximum Chl fluorescence ratio as follow: $F_v/F_m = [((F_m - F_0)/F_m)]$. The leaf tissues were subsequently exposed to actinic photon irradiance (110 μmol m^{-2} s^{-1}) for 120 s to obtain the steady-state fluorescence yield (F_s), after which a saturating white light pulse (2,400 μmol m^{-2} s^{-1}; 0.8 s) was applied to achieve the light-adapted maximum fluorescence (F'_m). Following the calculations of Kramer et al. (2004), the energy absorbed by the PSII for the following two yield components for dissipative processes was determined: the yield of photochemistry [YII = $((F'_m - F)/F'_m)$], the yield for dissipation by down-regulation [$Y(NPQ) = (F_s/F'_m) – (F_s/F_m)$], and the yield for other non-photochemical (non-regulated) losses [$Y(NO) = F_s/F_m$]. The parameters of Chl *a* fluorescence were determined by selecting the circular option on the Imaging Win software (area of ≈ 0.5 cm^2) on the leaves evaluated.

Determining Chl *a*, Chl *b*, and carotenoids concentrations

The concentrations of Chl *a*, Chl *b*, and carotenoids were determined using dimethyl sulfoxide (DMSO) as the solvent (Santos et al., 2008). Five leaf discs (1 cm^2 each) were obtained from fourth leaf, from base to top, of each plant per replication of each treatment at 48, 72, and 96 hai. The collected discs were immersed in glass tubes containing 5 ml of saturated DMSO solution and calcium carbonate ($CaCO_3$) (5 g/L) (Wellburn, 1994) and kept in the dark at room temperature for 24 h. The absorbances of the extracts were read at 480, 649, and 665 nm using a saturated solution of DMSO and $CaCO_3$ as a blank.

Biochemical assays

For all biochemical assays, fourth and fifth leaves, from base to top, of each plant per replication of each treatment were collected at 48, 72, and 96 hai. Leaves were also collected from non-inoculated plants at these same sampling times. Leaf samples were kept in liquid nitrogen during sampling and stored at -80ºC until further analysis.

Determining antioxidant enzymes activities

To determine the activities of ascorbate peroxidase (APX) (EC 1.11.1.11), catalase (CAT) (EC 1.11.1.6), peroxidase (POX) (EC 1.11.1.7), superoxide dismutase (SOD) (EC 1.15.1.1), and glutathione reductase (GR) (EC 1.8.1.7) a total of 0.2 g of leaf tissues was ground into a fine powder using a vibration ball mill (Retsch, Haan, Germany) with liquid nitrogen. The fine powder was homogenized in 2 ml of a solution containing 50 mM of potassium phosphate buffer (pH 6.8), 0.1 mM EDTA, 1 mM phenylmethylsulfonyl fluoride (PMSF), and 2% (w/v) polyvinylpyrrolidone (PVP). The homogenized material was centrifuged at 12,000 *g* for 15 min at 4°C and the supernatant was used as the crude enzyme extract. The SOD activity was determined by measuring its ability to photochemically reduce nitroblue tetrazolium (NBT) as

described by Beauchamp and Fridovich (1971). The reaction was initiated by adding the crude enzyme extract to a mixture containing 50 mM potassium phosphate buffer (pH 7.8), 14 mM methionine, 75 µM NBT, 0.1 mM EDTA, and 2 µM riboflavin. Samples were light-exposed for 7 min, and the production of formazan blue, resulting from the photoreduction of NBT, was measured at 560 nm with a spectrophotometer (Giannopolitis and Ries, 1977). Samples kept in the dark for 7 min served as a blank. One unit of SOD was defined as the amount of enzyme necessary to inhibit NBT photoreduction by 50%. The CAT activity was determined by adding the crude enzyme extract to a reaction mixture containing 50 mM potassium phosphate buffer (pH 7.0) and 20 mM hydrogen peroxide (H_2O_2). The determination of CAT activity was based on the rate of H_2O_2 decomposition measured in the spectrophotometer at 240 nm for 1 min at 25°C (Cakmak and Marschner, 1992). An extinction coefficient of 36 M^{-1} cm^{-1} was used to calculate CAT activity (Anderson et al., 1995). The POX activity was assayed by determining the pyrogallol oxidation as proposed by Kar and Mishra (1976). The reaction was started after the addition of the crude enzyme extract to a reaction mixture containing 25 mM potassium phosphate (pH 6.8), 20 mM pyrogallol, and 20 mM H_2O_2. The POX activity was determined by the absorbance of colored purpurogallin recorded for 1 min at 420 nm at 25°C. The extinction coefficient of 2.47 mM^{-1} cm^{-1} (Chance and Maehly, 1955) was used to calculate POX activity. The APX activity assay followed that described by Nakano and Asada (1981). The crude enzyme extract was added to a mixture containing 50 mM phosphate buffer (pH 7.0), 0.5 mM ascorbic acid, and 0.1 mM H_2O_2. The rate of ascorbate oxidation was measured by recording the absorbance at 290 nm for 1 min. The extinction coefficient of 2.8 mM^{-1} cm^{-1} (Nakano and Asada, 1981) was used to calculate APX activity. In order to determine GR activity, the reaction was started after the addition of the crude enzyme extract to a mixture containing 50 mM potassium phosphate (pH 7.8), 1 mM oxidized glutathione (GSSG), and 0.75 mM NADPH prepared in 0.5 mM Tris-HCl buffer (pH 7.5) according to Carlberg and

Mannervik (1985). The decrease in absorbance was determined at 340 nm for 1 min at 30°C. The extinction coefficient of 6.22 mM^{-1} cm^{-1} was used to calculate GR activity (Foyer and Halliwell, 1976). The activities of these enzymes were expressed in a protein-basis whose concentration was determined according to Bradford (1976).

Determining defense-related enzymes activities

A total of 0.2 g of leaf tissues was ground into a fine powder as described above to determine chitinase (CHI) (EC 3.2.1.14), *β*-1,3-glucanase (GLU) (EC 3.2.1.39), phenylalanine ammonia-lyase (PAL) (EC 4.3.1.5), polyphenoloxidase (PPO), and lipoxygenase (LOX) (EC 1.13.11.12) activities. The fine powder was homogenized in 2 ml of a solution containing 50 mM potassium phosphate buffer (pH 6.8), 1 mM EDTA, 1 mM PMSF, and 2% (w/v) PVP. The homogenate was centrifuged at 12,000 *g* for 15 min at 4°C and the supernatant was collected to be used to determine enzymes activity. The CHI activity was determined by adding the crude enzyme extract to a reaction mixture containing 50 mM sodium acetate buffer (pH 5.0) and 0.1 mM *p*-nitrophenyl-β-*D-N-N'*-diacetylchitobiose (Harman et al., 1993). The reaction mixture was incubated in a water bath at 37°C for 2 h and the reaction was terminated by the addition of 0.2 M sodium carbonate. For the control samples, the sodium carbonate was added soon after the addition of the crude enzyme extract to the reaction mixture. The absorbance of the product released by CHI was measured at 410 nm. The extinction coefficient of 7×10^3 mM^{-1} cm^{-1} was used to calculate CHI activity. The GLU activity was determined after adding the crude enzyme extract to a reaction mixture containing 50 mM sodium acetate buffer (pH 5.0) and laminarin (1 mg/mL) (Lever, 1972). The reaction mixture was incubated in a water bath for 30 min at 45°C. Afterward, this mixture was added to a reaction mixture of dinitrosalicylic acid (DNS). This reaction mixture was then incubated in a water bath for 10 min at 90°C and then cooled in an ice bath until it reached 25°C. The absorbance was measured at 540 nm. A similar procedure

was used for the control samples except that the first incubation was excluded. For PAL activity, the crude enzyme extract reacted with a reaction mixture containing 25 mM Tris-HCl buffer (pH 8.8) and 25 mM *L*-phenylalanine. The reaction mixture was incubated at 40°C for 3 h. For the control samples, the extract was replaced by the Tris-HCl buffer. The reaction was stopped by adding 6 N HCl. The absorbance of *trans*-cinnamic acid derivatives was recorded at 290 nm. The extinction coefficient of 100 M^{-1} cm^{-1} was used to calculate PAL activity (Guo et al., 2007). The PPO activity was determined using the same procedure as for POX, but H_2O_2 was omitted from the reaction mixture. The LOX activity was determined by adding the crude enzyme extract to a reaction mixture containing 50 mM sodium phosphate buffer (pH 6.5) and 50 µM sodium linoleate. The reaction mixture was incubated at 25°C, and the absorbance of the product released by LOX for 1 min was measured at 234 nm. The extinction coefficient of 25000 M^{-1} cm^{-1} was used to calculate LOX activity (Axelrod et al., 1981). These enzyme activities were expressed on a protein basis and protein concentration was determined according to Bradford (1976).

Determining concentrations of total soluble phenolics (TSP) and lignin-thioglycolic acid (LTGA) derivatives

A total of 0.1 g of leaf tissues was ground into a fine powder as described above and homogenized in 1 mL of 80% (v/v) methanol solution. The crude extract was shaken at 300 rpm at 25°C for 2 h and the mixture was centrifuged at 17,000 *g* for 30 min. The TSP concentration was determined in the methanolic extract and the pellet was used to determine the LTGA derivatives concentration with a few modifications (Tatagiba et al., 2014).

Determining malondialdehyde (MDA) concentration

Oxidative damage in the leaf tissues was estimated as the concentration of total 2-thiobarbituric acid (TBA) reactive substances and expressed as equivalents of MDA (Cakmak and Horst, 1991). A total of 0.1 g of leaf tissues was ground into a fine powder as described above and homogenized in 2 ml of 0.1% (w/v) trichloroacetic acid (TCA) solution in an ice bath. The homogenate was centrifuged at 12,000 *g* for 15 min at 4°C. After centrifugation, a total of 250 µl of the supernatant was reacted with 750 µl of TBA solution (0.5% in 20% TCA) for 60 min in a boiling water bath at 95°C. After this period, the reaction was stopped in an ice bath. The non-specific absorbance was estimated at 600 nm and subtracted from the specific absorbance value. The extinction coefficient of 155 mM^{-1} cm^{-1} (Heath and Packer, 1968) was used to calculate MDA concentration.

Determining H_2O_2 concentration

A total of 0.1 g of leaf tissues was ground into a fine powder as described above and homogenized in 2 ml of 0.1% (w/v) of TCA. The homogenate was centrifuged at 12,000 *g* for 15 min at 4°C and the supernatant was used as the crude extract to determine H_2O_2 concentration. The supernatant was added to a reaction mixture containing 10 mM potassium buffer (pH 7.0) and 1 M of iodide solution and incubated for 10 min. The oxidation product formed was measure a 390 nm (Velikova et al., 2000). A standard curve for H_2O_2 (Sigma-Aldrich, São Paulo, Brazil) was used to determine the H_2O_2 concentration.

Determining superoxide anion radical ($O_2^{\bullet-}$) concentration

A total of 0.2 g of leaf tissues was ground into a fine powder as described above and homogenized in 2 ml of a solution containing 100 mM sodium phosphate buffer (pH 7.2), and 1 mM sodium diethyldithiocarbamate. The homogenate was centrifuged at 22,000 *g* for 20 min

at 4°C and the supernatant was used to determine $O_2^{\bullet-}$ concentration according to Chaitanya and Naithani (1994).

Data analysis

Data for all variables and parameters evaluated were subjected to analysis of variance and the treatments means were compared by *F* test ($P \leq 0.05$). Principal components analysis (PCA) was performed aiming to determine the relationship between the variables and parameters evaluated. Data were analyzed using the Minitab software (version 18, Minitab Corporation).

Results

Analysis of variance

The factors inducers of resistance (IR) and plant inoculation (PI) as well as the IR × PI interaction were significant for most of the variables and parameters evaluated (Table 1).

Blast symptoms, severity, and AUBPC

In the leaves of plants from control and GABA treatments, there were many coalesced necrotic lesions. By contrast, lesions were of reduced size, with less coalescence, and in less number in the leaves of plants from BABA treatment (Fig. 1A). Blast severity was significantly higher by 67 and 52% at 48 hai, by 45 and 50% at 72 hai, and by 51 and 42% at 96 hai for plants from control and GABA treatments, respectively, compared to plants from BABA treatment (Fig. 1B). The AUBPC was significantly higher by 52 and 47% for plants from control and GABA treatments, respectively, compared to plants from BABA treatment (Fig. 1C).

Images of Chl *a* fluorescence

For non-inoculated plants, there was no distinct difference in the color pattern of Chl *a* fluorescence images regardless of parameters evaluated and treatments. The first visual changes in Chl *a* fluorescence images from leaves of inoculated plants started at 48 hai regardless of treatment (Fig. 2). There was progressive loss of the photosynthetic capacity of infected leaves for plants from control and GABA treatments in contrast to infected leaves of plants from BABA treatment as indicated by black areas in the images for F_v/F_m, Y(II), Y(NPQ), and Y(NO) from 48 to 96 hai (Fig. 2).

Parameters of Chl *a* fluorescence

Inducers vs. non-inoculated plants

The parameters F_v/F_m, Y(II), Y(NPQ), and Y(NO) were not affected by control, GABA, and BABA treatments regardless of evaluation time (Fig. 3A, C, E, and G).

Inducers vs. inoculated plants

The F_v/F_m was significantly lower by 5 and 3% at 48 hai, by 18 and 11% at 72 hai, and by 34 and 30% at 96 hai for plants from control and GABA treatments, respectively, compared to plants from BABA treatment. The Y(II) was significantly lower by 26 and 25% at 48 hai, by 31 and 25% at 72 hai, and by 67 and 66% at 96 hai for plants from control and GABA treatments, respectively, compared to plants from BABA treatment. For plants from control and GABA treatments, Y(NPQ) was significantly lower by 31 and 37% at 48 hai, by 26 and 19% at 72 hai, and by 49 and 36% at 96 hai, respectively, compared to plants from BABA treatment. The Y(NO) was significantly higher by 32 and 33% at 48 hai, by 44 and 47% at 72 hai, and by 41 and 39% at 96 hai for plants from control and GABA treatments, respectively, compared to plants from BABA treatment (Fig. 3B, D, F, and H).

Non-inoculated vs. inoculated plants

For F_v/F_m, there were significant reductions of 6 and 5% at 48 hai, of 15 and 11% at 72 hai, and of 39 and 35% at 96 hai, respectively, for inoculated plants from control and GABA treatments compared to their non-inoculated counterparts. At 48 hai, F_v/F_m was significantly lower by 3% for inoculated plants from BABA treatment compared to non-inoculated plants from this same treatment (Fig. 3A-B). For inoculated plants, Y(II) was significantly lower by 18% at 48 hai for control treatment as well as by 41 and 34% at 72 hai, and of 68 and 66% at 96 hai, respectively, for control and GABA treatments compared to their non-inoculated counterparts (Fig. 3C-D).

For inoculated plants, Y(NPQ) was significantly lower by 26% at 72 hai for control treatment and by 41 and 25% at 96 hai for control and GABA treatments, respectively, compared to their non-inoculated counterparts (Fig. 3E-F). For inoculated plants, Y(NO) was significantly higher by 41 and 42% at 48 hai for control and GABA treatments, respectively, by 16% at 72 hai for GABA treatment as well as by 57, 50, and 29% at 96 hai for control, GABA, and BABA treatments, respectively, compared to their non-inoculated counterparts. At 48 hai, Y(NO) was significantly lower by 38% for inoculated plants from BABA treatment compared to non-inoculated plants from this same treatment (Fig. 3G-H).

Concentrations of photosynthetic pigments

Inducers vs. non-inoculated plants

At 48 hai, Chl *a+b* concentration was significantly lower by 15 and 17% for plants from control and GABA treatments, respectively, compared to BABA treatment (Fig. 4A). There was no significant effect of control, GABA, and BABA treatments for carotenoids concentration regardless of evaluation time (Fig. 4C).

Inducers vs. inoculated plants

Concentration of Chl *a+b* was significantly lower by 35 and 33% at 72 hai and by 41 and 38% at 96 hai for plants from control and GABA treatments, respectively, compared to BABA treatment (Fig. 4B). Concentration of carotenoids was significantly lower by 38 and 59% at 48 hai and by 51 and 70% at 96 hai for plants from control and GABA treatments, respectively, compared to BABA treatment (Fig. 4D). At 72 hai, concentration of carotenoids was significantly lower by 45% for plants from GABA treatment compared to BABA treatment (Fig. 4D).

Non-inoculated vs. inoculated plants

At 96 hai, Chl *a+b* concentration was significantly lower by 42 and 45% for inoculated plants from control and GABA treatments, respectively, compared to their non-inoculated counterparts. The Chl *a+b* concentration was significantly lower by 26% at 72 hai for inoculated plants from GABA treatment compared to non-inoculated plants from this same treatment. For inoculated plants, carotenoids concentration was significantly lower by 27 and 43% at 72 hai and by 60 and 72% at 96 hai for control and GABA treatments, respectively, compared to their non-inoculated counterparts (Fig. 4A-D).

Concentrations of MDA, H_2O_2, and $O_2^{\bullet-}$

Inducers vs. non-inoculated plants

Concentrations of MDA, H_2O_2, and $O_2^{\bullet-}$ were not affected by control, GABA, and BABA treatments regardless of evaluation time (Fig. 5A, C, and E).

Inducers vs. inoculated plants

At 96 hai, there were significant reductions of 30 and 24% for MDA concentration and of 44 and 38% for H_2O_2 concentration for plants from control and GABA treatments, respectively, compared to BABA treatment (Fig. 5F and D). For $O_2^{\bullet-}$ concentration, there were significant reductions of 37 and 28% at 72 hai and of 32 and 26% at 96 hai for plants from control and GABA treatments, respectively, compared to BABA treatment (Fig. 5F).

Non-inoculated vs. inoculated plants

At 96 hai, MDA and H_2O_2 concentrations were significantly higher by 38 and 49%, respectively, for inoculated plants from BABA treatment compared to non-inoculated plants from this same treatment (Fig. 5A-D). The $O_2^{\bullet-}$ concentration was significantly higher by 41

and 49% at 48 hai for inoculated plants from control and GABA treatments, respectively, by 40, 36, and 60% at 72 hai, and by 46, 32, and 60% at 96 hai for inoculated plants from control, GABA, and BABA treatments, respectively, compared to their non-inoculated counterparts (Fig. 5E-F).

Activities of antioxidant enzymes

Inducers vs. non-inoculated plants

The SOD, CAT, APX, and GR activities were not affected by control, GABA, and BABA treatments regardless of evaluation time (Fig. 6A, C, E, and G).

Inducers vs. inoculated plants

At 48 hai, CAT activity was significantly lower by 35 and 46% for plants from GABA and BABA treatments, respectively, compared to control treatment while APX activity was significantly lower for 55 and 32% for plants from control and BABA treatments, respectively, compared to GABA treatment (Fig. 6D and F). There were significant reductions of 33 and 37% for SOD activity, of 24 and 36% for CAT activity, and of 56 and 68% for APX activity for plants from control and GABA treatments, respectively, compared to BABA treatment at 96 hai (Fig. 6B, D, and F). Significant increases of 36 and 44% for CAT activity at 72 hai as well as of 40 and 46% at 72 hai and of 38 and 44% at 96 hai for GR activity were obtained for plants from control and GABA treatments, respectively, compared to plants from BABA treatment (Fig. 6D and H).

Non-inoculated vs. inoculated plants

At 96 hai, SOD activity was significantly higher by 28 and 43% for inoculated plants from GABA and BABA treatments, respectively, compared to their non-inoculated counterparts

(Fig. 6A-B). For inoculated plants from control treatment, there were significant increases for CAT (65, 58, and 25% at 48, 72, and 96 hai, respectively), APX (40% at 72 hai), and GR (57% at 96 hai) activities compared to non-inoculated plants from this same treatment (Fig. 6C-H). The activities of CAT (32, 57, and 27% at 48, 72, and 96 hai, respectively), APX (50 and 44% at 48 and 72 hai, respectively), and GR (42, 31, and 73% at 48, 72, and 96 hai, respectively) were significantly higher for inoculated plants from GABA treatment compared to non-inoculated plants from this same treatment (Fig. 6C-H). At 96 hai, SOD, CAT, APX, and GR activities were significantly higher by 43, 40, 57, and 37%, respectively, for plants from BABA treatment compared to non-inoculated plants from this same treatment (Fig. 6A-H). The GR activity was significantly lower for inoculated plants from BABA treatment compared to non-inoculated plants from this same treatment at 72 hai (Fig. 6G-H).

Activities of defense enzymes

Inducers vs. non-inoculated plants

The GLU activity was significantly higher by 85 and 77% at 48 hai, by 75 and 80% at 72 hai, and by 69 and 74% at 96 hai for plants from GABA and BABA treatments, respectively, compared to control treatment (Fig. 7C). The CHI, POX, PAL, PPO, and LOX activities were not affected by control, GABA, and BABA treatments regardless of evaluation time (Fig. 7A, E, G, I, and K).

Inducers vs. inoculated plants

The CHI activity was significantly higher by 55% for plants from BABA treatment compared to GABA treatment at 72 hai and significantly lower by 49 and 45% for plants from control and GABA treatments, respectively, compared to BABA treatment at 96 hai (Fig. 7B). At 96 hai, GLU activity was significantly higher by 54 and 70% for plants from control and BABA

treatments, respectively, compared to plants from GABA treatment (Fig. 7D). For POX activity, there were significant reductions of 50 and 70% for plants from control and GABA treatments, respectively, compared to BABA treatment at 72 hai and significant increases of 59 and 41% for plants from control and GABA treatments, respectively, compared to plants from BABA treatment at 96 hai (Fig. 7F). At 48 hai, PAL activity was significantly higher by 72 and 74% for plants from control and GABA treatments, respectively, compared to BABA treatment (Fig. 7H). There were significant reductions for PAL activity of 51 and 66% for plants from GABA and BABA treatments, respectively, compared to plants from control treatment at 72 hai and of 37 and 48% for plants from control and GABA treatments, respectively, compared to plants from BABA treatment at 96 hai (Fig. 7H). For PPO activity, there were significant increases of 22 and 31% for plants from control and GABA treatments, respectively, compared to BABA treatment at 72 hai and significant decreases of 20 and 23% for plants from control and GABA treatments, respectively, compared to BABA treatment at 96 hai (Fig. 7J). The LOX activity was significantly lower by 36 and 48% for plants from control and GABA treatments, respectively, compared to plants from BABA treatment at 96 hai (Fig. 7L).

Non-inoculated vs. inoculated plants

For inoculated plants from control treatment, there were significant increases for GLU (87% regardless of evaluation time), POX (59, 78, and 89% at 48, 72, and 96 hai, respectively), PAL (84, 94, and 94% at 48, 72, and 96 hai, respectively), PPO (50, 67, and 83% at 48, 72, and 96 hai, respectively), and LOX (71, 93, and 94% at 48, 72, and 96 hai, respectively) activities compared to non-inoculated plants from this same treatment (Fig. 7C-L). The activities of GLU (42 and 41% at 48 and 72 hai, respectively), POX (65 and 77% at 48 and 96 hai, respectively), PAL (75, 84, and 93% at 48, 72, and 96 hai, respectively), PPO (65, 77, and 82% at 48, 72, and 96 hai, respectively), and LOX (65, 85, and 87% at 48, 72, and 96 hai, respectively) were

significantly higher for inoculated plants from GABA treatment compared to non-inoculated plants from this same treatment (Fig. 7C-L). The activities of CHI (44 and 41% at 72 and 96 hai, respectively), GLU (49 and 68% at 48 and 96 hai, respectively), POX (62, 80, and 60% at 48, 72, and 96 hai, respectively), PAL (73 and 95% at 72 and 96 hai, respectively), PPO (72, 67, and 83% at 48, 72, and 96 hai, respectively), and LOX (80 and 95% at 72 and 96 hai, respectively) were significantly higher for inoculated plants from BABA treatment compared to non-inoculated plants from this same treatment (Fig. 7A-L).

Concentrations of TSP and LTGA derivatives

Inducers vs. non-inoculated plants

The concentrations of TSP and LTGA derivatives were not affected by control, GABA, and BABA treatments regardless of evaluation time (Fig. 8A and C).

Inducers vs. inoculated plants

Concentration of TSP was significantly lower by 59 and 62% at 72 hai and by 64 and 67% at 96 hai for plants from control and GABA treatments, respectively, compared to BABA treatment (Fig. 8B). Concentration of LTGA derivatives was significantly lower by 28 and 35% at 48 hai and by 40 and 38% at 96 hai for plants from control and GABA treatments, respectively, compared to BABA treatment (Fig. 8D). At 72 hai, concentration of LTGA derivatives was significantly lower by 21% for plants from GABA treatment compared to BABA treatment (Fig. 8D).

Non-inoculated vs. inoculated plants

Concentration of TSP was significantly higher by 41 and 43% at 72 and 96 hai, respectively, for inoculated plants from BABA treatment compared to non-inoculated plants from this same

treatment. Concentration of LTGA derivatives was significantly higher for inoculated plants from control (29% at 48 hai), GABA (32% at 72 hai), and BABA (34, 32, and 38% at 48, 72, and 96 hai, respectively) treatments compared to their non-inoculated counterparts (Fig. 8A-D).

PCA analysis

Distinct separation occurred between non-inoculated and inoculated plants and the one principal component (PC) explained most of data variation (PC1 and PC2 = 54 and 41%, respectively) (Fig. 9A-B). According to cluster analysis with complete linkage and Pearson distance, three clusters (C) were generated: C1 (non-inoculated plants from control, BABA, and GABA treatments), C2 (inoculated plants from BABA treatment), and C3 (inoculated plants from control and GABA treatments) (Fig. 9). The first PC resulted in negative scores for photosynthetic parameters (F_v/F_m, Y(NPQ), and Y(II)) and photosynthetic pigments (Chl *a*+*b* and Car). Positive scores were obtained for disease severity, Y(NO), antioxidant (APX, SOD, CAT, and GR) and defense (CHI, GLU, LOX, PAL, PPO, and POX) enzymes activities, and concentrations of metabolites (MDA, H_2O_2, and $O_2^{\bullet-}$) as well as TSP and LTGA derivatives (Fig. 9B).

Discussion

Some reports highlight the potential of BABA to induce resistance in many plant species against infection by a plethora of pathogens (Cohen et al., 2016; Tarkowski et al., 2019). Notably for wheat-*P. oryzae* interaction, the present study is the first to bring novel insights at both physiological and biochemical levels for using BABA to reduce blast symptoms in an attempt to shed light on the mechanisms implicated in BABA-induced wheat resistance against blast. Interestingly, blast development (less chlorosis, lesions of reduced size, and lower disease severity) was negatively impacted for plants sprayed with BABA compared to GABA. This finding indicates that an isomer specificity of the aminobutyric acid plays an important role in attaining a desirable level of blast control in wheat. Some studies have been key in emphasizing that GABA is less effective than BABA to reduce symptoms of some diseases (Cohen et al., 2016; Jakab et al., 2001; Baccelli and Mauch-Mani, 2016; Justyna and Ewa, 2013) giving support to the findings of the present study. Considering the fact that GABA is a source of nitrogen for some pathogens and is involved in some aspects of their physiology (Bouché and Fromm, 2004; Kumar and Punekar, 1997; Oliver and Solomon, 2004), disease development can be dramatically favored in plants exposed it. In contrast to BABA, GABA is rapidly metabolized in plant tissues and less cytotoxic whether sprayed at higher rates (Cohen and Gisi, 1994; Justyna and Ewa, 2013), raising the possibility of its less efficiency in keeping plants in a prolonged state of induction.

Photosynthesis is the crucial physiological process in plants that can be directly or indirectly affected by foliar and vascular pathogens, respectively (Tatagiba et al., 2015; Bispo et al., 2016; Dallagnol et al., 2011; Debona et al., 2014). In this regard, examining alterations of Chl *a* fluorescence parameters can provide helpful insights regarding the spatial-temporal impairment in the photosynthetic performance of infected plants (Tatagiba et al., 2015; Rolfe and Scholes, 2010). In the present study, neither BABA nor GABA perturbed the

photosynthetic rates of wheat leaves not infected by *P. oryzae*. Tomato plants sprayed with BABA or GABA did not show perturbations in photosynthesis based on incorporation of $^{14}CO_2$ into sugars (Cohen, 2002). Interestingly, inhibition of the photosynthetic process on leaves of BABA-sprayed plants was less impaired during the infection by *P. oryzae*. Values of F_v/F_m, Y(II), and Y(NPQ) were kept higher during the infection process of *P. oryzae* in the leaves of BABA-sprayed plants reflecting great photoprotection of the photosynthetic apparatus due to less photooxidative damage. On the other hand, leaves of water and GABA-sprayed plants showed reduced photosynthetic performance and less capacity for photoprotection (lower F_v/F_m, Y(II), and Y(NPQ) values and great Y(NO) values) as a result of higher blast severity. In contrast to GABA-sprayed plants, infected leaf tissues of BABA-sprayed plants displayed lower Y(NO) values suggesting that both excitation energy directed to photochemical conversion and regulation mechanisms of protection become more effective. The Y(NO) indicates that the fraction of energy could be passively dissipated in the form of heat and fluorescence mainly due to closed PSII reaction centers (Klughammer and Schreiber, 2008). Discrete reductions in F_v/F_m and Y(II) and an increase in Y(NPQ) are noticed at the beginning of the infection process of foliar pathogens, followed by dramatically decreases in the values of these parameters at advanced stage of infection due to severe perturbations in the photosynthetic apparatus and reduced photosynthetic pigments concentration (Tatagiba et al., 2015; Rolfe and Scholes, 2010; Bermúdez-Cardona et al., 2015; Silveira et al., 2015; Aucique-Pérez et al., 2014, 2020). By examining leaf gas exchange and Chl *a* fluorescence parameters, many studies demonstrated that wheat leaves infected by *P. oryzae* had their photosynthetic process, mainly at the photochemical phase, impaired linked to reduced biochemical capacity for carbon fixation due to lower RuBisCO activity (Aucique-Pérez et al., 2014; Debona et al., 2014; Rios et al., 2017; Rodrigues et al., 2020). The pools of photosynthetic pigments (Chl *a*+*b* and carotenoids) were kept higher for BABA-sprayed plants during *P. oryzae* infection process

than water and GABA-sprayed plant as a result of preservation of the functionality of the photosynthetic apparatus. Considering that photosynthetic pigments are closely associated with light-harvesting complexes (Akhtar et al., 2015), more energy transfer to PSII due to their less degradation in leaves of BABA-sprayed plants resulted in a more robust photosynthetic apparatus. Destruction of photosynthetic pigments in the chloroplasts is one of the major cytologic features associated with infection by hemibiotrophic and necrotrophic pathogens causing foliar diseases in different crops, including *P. oryzae* in wheat (Bermúdez-Cardona et al., 2015; Silveira et al., 2015; Rodrigues et al., 2015; Aucique-Pérez et al., 2014, 2020; Debona et al., 2014; Rios et al., 2017; Rodrigues et al., 2020). Increased resistance of tomato and lettuce plants to late blight and downy mildew, respectively, after exposition to BABA and grown under continuous light, was linked to great H_2O_2 production and enhanced photosynthetic capacity (Cohen et al., 2016).

Surprisingly, MDA concentration for infected BABA-sprayed plants was great at 96 hai. It is plausible to postulate that great MDA concentration, a well-known biomarker for the peroxidation of polyunsaturated lipids of cell membranes formed in response to stress (Yamauchi et al., 2008), could be feasible involved in BABA-inducing resistance. There was no visual effect of phytotoxicity caused by BABA before plant inoculation with *P. oryzae* and changes in the photosynthetic apparatus (based on F_v/F_m, Y(II), and Y(NPQ) values) even for not infected BABA-sprayed plants were not noticed. Moreover, higher H_2O_2 production (at 96 hai) and $O_2^{\bullet-}$ (at 72 and 96 hai) along well with great LOX activity (96 hai) for BABA-sprayed plants infected by *P. oyrzae* could be linked to their increased resistance against blast. Siegrist et al. (2000) reported the appearance of microscopical hypersensitive reaction-like lesions in tobacco leaves sprayed with BABA indicating cell death (confirmed by histochemical staining with trypan blue and Evans blue) associated with great production of MDA, H_2O_2, and $O_2^{\bullet-}$. These authors stressed that BABA-mediated lesion formation in tobacco leaves involved a

complex regulation of cell death to activate host-defense responses against *Tobacco mosaic virus* infection. Indeed, reactive oxygen species (ROS) generated in plant tissues exposed to BABA may facilitate its cross-linking with cell wall matrix (Cohen et al., 2011). Elsherbiny et al. (2021) reported increased MDA concentration and lower total lipid content from mycelia of *Penicillium digitatum* during 96 h of exposure to BABA, indicating its direct antifungal activity. It is interesting to point out that LOX is an important enzyme for JA biosynthesis, a linolenic acid-derived cyclopentanone involved in systemic acquired resistance (SAR) of some plant species in response to pathogens infection (Mueller, 1997; Halim et al., 2008). The substrate for JA production is originated from di-, mono-, and tri-unsaturated fatty acids in the cell membrane, including chloroplast membrane and peroxisomes (León and Sánchez-Serrano, 1999). It is plausible to speculate that an increase in MDA concentration could be linked to higher LOX activity with the participation of ROS as reported by Elsherbiny and Taher (2018), and, therefore, resulting in boosted resistance of wheat plants against blast. Rios et al. (2014) reported that higher LOX activity in the leaves of JA-sprayed wheat plants resulted in less blast symptoms. For the grapevines-downy mildew interaction, BABA-induced resistance involved JA signaling pathway and intense callose deposition at pathogen infection sites (Hamiduzzaman et al., 2005). More than a negative effect of ROS in stressed plants, increasing pieces of evidence highlights the role of ROS, especially H_2O_2, as signaling molecules for activation of host-defense responses against pathogens infection, especially with the occurrence of SAR (Veluchamy et al., 2012; Camejo et al., 2016; Pitzschke et al., 2006; Low and Merida, 1996; Turkan, 2018; Wang et al., 2014; Mignolet-Spruyt et al., 2016). In lettuce leaves sprayed with BABA, colonization by *B. lactucae* was hampered by intense callose depositions around the primary and secondary vesicles and great production of H_2O_2 in the penetrated epidermal cells indicated by DAB staining (Cohen et al., 2010).

An orchestrated enzymatic system take place in plants facing abiotic stress and also to counteract against infection by pathogens to remove the excess of ROS produced in the apoplast, endoplasmic reticulum, chloroplasts, mitochondria, cell wall, plasm membranes, and peroxisomes that cause oxidative damage to DNA, lipids, and proteins (You and Chan, 2015; Das and Roychoudhury, 2014). In this system, SOD converts $O_2^{\bullet-}$ into O_2 and H_2O_2, while higher APX, CAT, and POX activities lower H_2O_2 produced in the stressed plant tissues (Sharma et al., 2012; Das and Roychoudhury, 2014). The GR, mainly found in chloroplasts and barely in the mitochondria and cytosol, uses NADPH as a reductant to reduce GSSG to reduced glutathione, preventing thiol groups from getting oxidized and react with singlet oxygen and hydroxyl radical (Das and Roychoudhury, 2014). In general, SOD, CAT, and APX activities were greater for BABA-sprayed plants at 96 hai helping alleviating H_2O_2 and $O_2^{\bullet-}$ generation. On the other hand, lower GR activity for BABA-sprayed plants was possibly linked to less production of other ROS (singlet oxygen and hydroxyl radical) during the infection process of *P. oryzae* in contrast to its higher activity for water and GABA-sprayed plants from 72 to 96 hai. Infection of wheat leaves by *P. oryzae* increased production of H_2O_2 and $O_2^{\bullet-}$ requiring a more robust antioxidative system (great APX, CAT, POX, and glutathione S-transferase activities) to overcome the harmful effect of fungal infection (Debona et al., 2012). In general, different plant species exposed to BABA and challenged by both abiotic stresses and pathogens infection exhibited increased activities of APX, CAT, SOD, and guaiacol peroxidase (Justyna and Ewa, 2013).

The increased resistance of BABA-sprayed plants against *P. oryzae* infection was closely linked to great CHI, GLU, POX, PPO, and PAL activities. The great photosynthetic capacity of BABA-sprayed plants was of remarkable importance to counteract the infection by *P. oryzae* either by influencing their overall energy status, reduced power of cells, and ROS production. Moreover, the nutrition of *P. oryzae* colonizing the leaf tissues of wheat plants is an additional

drain on plant energy, considering that their defense mechanisms operate at a high cost and that energy needed originates from photosynthesis or through reserves (Neilson et al., 2013; Rodrigues et al., 2020). The spray of BABA to blueberry leaves decreased leaf spot (*Pestalotiopsis microspora*) symptoms due to increased activities of PAL, POX, and PPO (Yi-Lan et al., 2021). Great PAL, POX, and PPO activities occurred in orange fruits exposed to BABA and infected by *P. digitatum,* resulting in less incidence and reduced severity of green mold (Elsherbiny et al., 2021). The CHI, GLU, POX, PPO, and PAL have different roles in the response of plants against pathogens infection. The colonization of plant tissues by fungi is hampered when chitin and *β*-1,3-glucan in their cell wall are intensively hydrolyzed by the mutual action of CHI and GLU, respectively (Sánchez-Vallet et al., 2015). The PAL is a keystone enzyme in the phenylpropanoid pathway from which an array of phenolics is produced, which are further oxidated to quinones or used to form lignin polymers with the participation of both POX and PPO (Dixon et al., 2002; Ojaghian et al., 2014). In the leaves of BABA-sprayed plants, an enhancement of TSP production was linked to higher PAL activity followed by an increase in the pool of LTGA derivatives due to great POX and PPO activities ending up in less blast symptoms. It is well known that some soluble phenolics in the cytosol and those stored in vacuoles of cells infected by pathogens of several lifestyles may exerts antimicrobial effect against them (Daayf et al., 2012; Lattanzio et al., 2008). Moreover, phenolics polymerization leading to lignin production following deposition in cell wall become a structural obstacle to hamper the colonization of plant tissues by pathogens and the diffusion of hydrolytic enzymes and non-host selective toxins produced by them (Daayf et al., 2012; Lattanzio et al., 2008, Jiang et al., 2019; Hassan and Abo-Elyousr, 2013; Zhang et al., 2013). Interestingly, great CHI, GLU, PAL, POX, and PPO activities were linked with the increased resistance of many other crops against diseases in response to BABA (Justyna and Ewa, 2013; Li et al., 2019). Plants exposed to BABA responded against pathogens infection activating

defense mechanisms of different physical and biochemical natures. Depending on the host-pathogen interaction, BABA triggers the deposition of callose (boosted tricarboxylic acid cycle and mobilization of starch reserves for callose synthesis) and lignin, papillae formation, and expression of defense-related genes (*e.g.*, *CHS* (chalcone synthase), *DFR* (dichydroflavonol-4-reductase), *PAL*, *LOX9*, *STS* (stilbene synthase), *C4H* (cinnamate-4-hydroxylase), *POX*, *CHI*, *GLU*, *PR1*, *PR2*, *PR4*, *PR5*, and *PDF1.2*), and antimicrobial compounds (*e.g.*, phenolics, phytoalexins (capsidiol, furocoumarins, and pisatin), terpenoids, and ROS) in the infected tissues (Cohen, 2002; Cohen et al., 2016; Justyna and Ewa, 2013; Tarkowski et al., 2020). Hae-Keun et al. (1999) sprayed tobacco plants with SA and BABA and showed differential *PR1* expression indicating that BABA acted through the SA-independent pathway. However, this effect is dependent on the plant species and the challenging pathogen. Zimmerli et al. (2000) demonstrated that Arabidopsis plants expressing the *NahG* gene (degradation of SA to catechol) exhibited less symptoms of downy mildew (*P. parasitica*) due to rapid papilla formation after being sprayed with BABA but were susceptible to infection by *P. syringae* pv. *tomato*. Moreover, BABA spray reduced gray mold symptoms, caused by *B. cinerea* infection, in Arabidopsis plants and mutants in JA and ethylene pathways rather than on mutants impaired in the SA pathway, indicating that SA and *NPR1* gene were involved in BABA-induced resistance (Zimmerli et al., 2001).

Overall, the present study brings novel physiological and biochemical shreds of evidence demonstrating the potential of BABA to reduce blast symptoms on wheat. Based on the PCA analysis, the isolation of the cluster inoculated BABA-sprayed plants from the others clusters (non-inoculated plants from control, BABA, and GABA treatments as well as inoculated plants from control and GABA treatments) highlights the peculiar effect of BABA on the outcome of variables and parameters investigated in the present study. In this scenario, BABA boosted wheat resistance against *P. oryzae* infection linked to a more robust antioxidant metabolism and

preservation of the photosynthetic apparatus. In a visionary context, BABA supply to wheat plants under field conditions may help decrease auto- and allo-infections by *P. oryzae* and, therefore, slow blast epidemic rate and ensure less yield losses caused by this very destructive disease.

References

Akhtar P, Dorogi M, Pawlak K, Kovács L, Bóta A, Kiss T, Garab G, Lambrev PH (2015) Pigment interactions in light-harvesting complex II in different molecular environments. The Journal of Biological Chemistry 290:4877-4886.

Anderson MD, Prasad TK, Stewart CR (1995) Changes in isozyme profiles of catalase, peroxidase, and glutathione reductase during acclimation to chilling in mesocotyls of maize seedlings. Plant Physiology 109:1247-1257.

Anh VL, Inoue Y, Asuke S, Vy TTP, Anh NT, Wang S, Chuma I, Tosa Y (2018) *Rmg8* and *Rmg7*, wheat genes for resistance to the wheat blast fungus, recognize the same avirulence gene *AVR-Rmg8*. Molecular Plant Pathology 19:1252-1256.

Aucique-Pérez CE, Rios VS, Neto LBC, Rios JA, Martins SCV, Rodrigues FA (2020) Photosynthetic changes in wheat cultivars with contrasting levels of resistance to blast. Journal of Phytopathology 168:721-729.

Aucique-Pérez CE, Rodrigues FA, Moreira WR, DaMatta FM (2014) Leaf gas exchange and chlorophyll *a* fluorescence in wheat plants supplied with silicon and infected with *Pyricularia oryzae*. Phytopathology 104:143-149.

Axelrod B, Cheesbrough TM, Laasko S (1981) Lipoxygenases from soybeans. Methods in Enzymology 71:441-451.

Baccelli I, Mauch-Mani B (2016) β-aminobutyric acid priming of plant defense: the role of ABA and other hormones. Plant Molecular Biology 91:703-707.

Beauchamp C, Fridovich I (1971) Superoxide dismutase: improved assays and an assay applicable to acrylamide gels. Analytical Biochemistry 44:276-287.

Bellameche F, Pedrazzini C, Mauch-Mani B, Mascher (2020) Efficiency of biological and chemical inducers for controlling Septoria tritici leaf blotch (STB) on wheat (*Triticum aestivum* L.). European Journal of Plant Pathology 158:99-109.

Bermúdez-Cardona MB, Wordell Filho JA, Rodrigues FA (2015) Leaf gas exchange and chlorophyll *a* fluorescence in maize leaves infected with *Stenocarpella macrospora*. Phytopathology 105:26-34.

Bispo WMS, Araujo L, Moreira WR, Silva LC, Rodrigues FA (2016) Differential leaf gas exchange performance of mango cultivars infected by different isolates of *Ceratocystis fimbriata*. Scientia Agricola 73:150-158.

Bouché N, Fromm H (2004) GABA in plants: just a metabolite?. Trends in Plant Science 9:110-115.

Bradford MN (1976) A rapid and sensitive method for the quantitation of microgram quantities of protein utilizing the principle of protein-dye binding. Analytical Biochemistry 72:248-254.

Cakmak I, Horst WJ (1991) Effect of aluminium on lipid peroxidation, superoxide dismutase, catalase, and peroxidase activities in root tips of soybean (*Glycine max*). Physiologia Plantarum 83:463-468.

Cakmak I, Marschner H (1992) Magnesium deficiency and high light intensity enhance activities of superoxide dismutase, ascorbate peroxidase, and glutathione reductase in bean leaves. Plant Physiology 98:1222-1227.

Camejo D, Guzmán-Cedeño A, Moreno A (2016) Reactive oxygen species, essential molecules, during plant-pathogen interactions. Plant Physiology and Biochemistry 103:10-23.

Carlberg I, Mannervik B (1985) Glutathione reductase. Methods in Enzymology 113:484-490.

Castroagudín VL, Ceresini PC, Oliveira SC, Reges JT, Maciel JL, Bonato AL, Dorigan AF, McDonald BA (2015) Resistance to QoI fungicides is widespread in Brazilian populations of the wheat blast pathogen *Magnaporthe oryzae*. Phytopathology 105:284-294.

Ceresini PC, Castroagudín VL, Rodrigues FA, Rios JA, Aucique-Pérez CE, Moreira SI, Alves E, Croll D, Maciel JLN (2018) Wheat blast: past, present, and future. Annual Review of Phytopathology 56:427-456.

Chaitanya KSK, Naithani SC (1994) Role of superoxide, lipid peroxidation and superoxide dismutase in membrane perturbation during loss of viability in seeds of *Shorea robusta* Gaertn.f. New Phytologist 126:623-627.

Chance B, Maehly AC (1955) Assay of catalase and peroxidase. Methods in Enzymology 2:764-775.

Cohen Y (2002) *β*-aminobutyric acid-induced resistance against plant pathogens. Plant Disease 86:448-457.

Cohen, Y (2001) The BABA story of induced resistance. Phytoparasitica 29:375-378.

Cohen Y, Gisi U (1994) Systemic translocation of 14C-DL3-aminobutyric acid in tomato plants in relation to induced resistance against *Phytophthora infestans*. Physiological and Molecular Plant Pathology 45:441-446.

Cohen Y, Rubin AE, Kilfin G (2010) Mechanisms of induced resistance in lettuce against *Bremia lactucae* by DL-*β*-amino-butyric acid (BABA). European Journal of Plant Pathology 126:553-573.

Cohen Y, Rubin AE, Vaknin M (2011) Post infection application of DL-3-amino-butyric acid (BABA) induces multiple forms of resistance against *Bremia lactucae* in lettuce. European Journal of Plant Pathology 130:13-27.

Cohen Y, Vaknin M, Mauch-Mani B (2016) BABA-induced resistance: milestones along a 55-year journey. Phytoparasitica 44:513-538.

Conrath U, Beckers GJ, Langenbach CJ, Jaskiewicz MR (2015) Priming for enhanced defense. Annual Review of Phytopathology 53:97-119.

Cruz MFA, Prestes AR, Maciel JL, Scheeren P (2010) Resistência parcial à brusone de genótipos de trigo comum e sintético nos estádios de planta jovem e de planta adulta. Tropical Plant Pathology 25:24-25.

Daayf F, El Hadrami A, El-Bebany AF, Henriquez MA, Yao Z, Derksen H, El-Hadrami I, Adam LR (2012) Phenolic compounds in plant defense and pathogen counter-defense mechanisms. In: Cheynier V, Sarni-Manchado P, Quideau S (Eds.). Recent Advances in Polyphenol Research. vol. 3., Wiley-Blackwell, Oxford. pp. 191-208.

Dallagnol LJ, Rodrigues FA, Martins SCV, Cavatte PC, DaMatta FM (2011) Alterations on rice leaf physiology during infection by *Bipolaris oryzae*. Australasian Plant Pathology 40:360-365.

Das K, Roychoudhury A (2014) Reactive oxygen species (ROS) and response of antioxidants as ROS-scavengers during environmental stress in plants. Frontiers in Environmental Science 2:53.

Debona D, Rodrigues FA, Rios JA, Martins SCV, Pereira LF, DaMatta FM (2014) Limitations to photosynthesis in leaves of wheat plants infected by *Pyricularia oryzae*. Phytopathology 104:33-39.

Debona D, Rodrigues FA, Rios JA, Nascimento KJT (2012) Biochemical changes in the leaves of wheat plants infected by *Pyricularia oryzae*. Phytopathology 102:1121-1129.

Dixon RA, Achnine L, Kota P, Liu CJ, Reddy MSS, Wang L (2002) The phenylpropanoid pathway and plant defence - a genomics perspective. Molecular Plant Pathology 3:371-390.

Elsherbiny EA, Dawood DH, Safwat NA (2021) Antifungal action and induction of resistance by *β*-aminobutyric acid against *Penicillium digitatum* to control green mold in orange fruit. Pesticide Biochemistry and Physiology 171:104721.

Elsherbiny EA, Taher MA (2018) Silicon induces resistance to postharvest rot of carrot caused by *Sclerotinia sclerotiorum* and the possible of defense mechanisms. Postharvest Biology and Technology 140:11-17.

FAO (2020) Crop prospects and food situation. Available at: http://www.fao.org/3/ca9803en/ca9803en.pdf. Accessed on August 30, 2021.

Fisher MC, Henk DA, Briggs CJ, Brownstein JS, Madoff LC, McCraw SL, Gurr SJ (2012) Emerging fungal threats to animal, plant and ecosystem health. Nature 484:186-194.

Foyer CH, Halliwell B (1976) The presence of glutathione and glutathione reductase in chloroplasts: a proposed role in ascorbic acid metabolism. Planta 133:21-25.

Giannopolitis CN, Ries SK (1977) Superoxide dismutases I. Occurrence in higher plants. Plant Physiology 59:309-314.

Guo Y, Liu L, Zhao J, Bi Y (2007) Use of silicon oxide and sodium silicate for controlling *Trichothecium roseum* postharvest rot in Chinese cantaloupe (*Cucumis mel*o L.). International Journal of Food Science & Technology 42:1012-1018.

Gur L, Reuveni M, Cohen Y (2021) *β*-Aminobutyric acid induced resistance against Alternaria fruit rot in apple fruits. Journal of Fungi 7:564.

Hae-Keun Y, So-Young Y, Seung-Heun Y, Doil C (1999) Cloning of pathogenesis-related protein-1 gene from *Nicotians glutinosa* L. and its salicylic acid-independent induction by copper and *β*-aminobutyric acid. Journal of Plant Physiology 154:327-333.

Halim VA, Vess A, Schell D, Rosahl S (2008) The role of salicylic acid and jasmonic acid in pathogen defence. Plant Biology 8:307-313.

Hamiduzzaman MM, Jakab G, Barnavon L, Neuhaus J-M, MauchMani B (2005) *β*-aminobutyric acid-induced resistance against downy mildew in grapevine acts through the potentiation of callose formation and jasmonic acid signaling. Molecular Plant-Microbe Interactions 18:819-829.

Harman GE, Hayes CK, Lorito M, Broadway RM, Di Pietro A, Peterbauer C, Tronsmo A (1993) Chitinolytic enzymes of *Trichoderma harzianum*: purification of chitobiosidase and endochitinase. Phytopathology 83:313-318.

Hassan MAE, Abo-Elyousr KAM (2013) Activation of tomato plant defence responses against bacterial wilt caused by *Ralstonia solanacearum* using DL-3-aminobutyric acid (BABA). European Journal of Plant Pathology 136:145-157.

Heath RL, Packer L (1968) Photoperoxidation in isolated chloroplasts I. Kinetics and stoichiometry of fatty acid peroxidation. Archives of Biochemistry and Biophysics 125:189-198.

Jakab G, Cottier V, Toquin V, Rigoli G, Zimmerli L, Métraux J-P, Mauch-Mani B (2001) *β*-aminobutyric acid-induced resistance in plants. European Journal of Plant Pathology 107:29-37.

Jiang S, Han S, He D, Cao G, Fang K, Xiao X, Yi J, Wan X (2019) The accumulation of phenolic compounds and increased activities of related enzymes contribute to early defense against walnut blight. Physiological and Molecular Plant Pathology 108:101433.

Jones JDG, Dangl JL (2006) The plant immune system. Nature 444:323-332.

Justyna PG, Ewa K (2013) Induction of resistance against pathogens by *β*-aminobutyric acid. Acta Physiologiae Plantarum 35:1735-1748.

Kar M, Mishra D (1976) Catalase, peroxidase, and polyphenol oxidase activities during rice leaf senescence. Plant Physiology 57:315-319.

Kesel J, Conrath U, Flors V, Luna E, Mageroy MH, Mauch-Mani B, Pastor V, Pozo MJ, Pieterse CMJ, Ton J, Kyndt T (2021) The induced resistance lexicon: do's and don'ts. Trends in Plant Science 26:685-691.

Klughammer C, Schreiber U (2008) Complementary PS II yields calculated from simple fluorescence parameters measured by PAM fluorometry and the Saturation Pulse method. PAM Application Notes 1:27-35.

Kramer DM, Johnson G, Kiirats O, Edwards GE (2004) New fluorescence parameters for the determination of Q_A redox state and excitation energy fluxes. Photosynthesis Research 79:209-218.

Kumar S, Punekar NS (1997) The metabolism of 4-aminobutyrate (GABA) in fungi. Mycological Research 101:403-409.

Lattanzio V, Kroon PA, Quideau S, Treutter D (2008) Plant phenolics - secondary metabolites with diverse functions. In: Daayf F, Lattanzio V (Eds.). Recent Advances in Polyphenol Research. vol. 1., Wiley-Blackwell, Oxford. pp. 1-35.

León J, Sánchez-Serrano JJ (1999) Molecular biology of jasmonic acid biosynthesis in plants. Plant Physiology and Biochemistry 37:373-380.

Lever M (1972) A new reaction for colorimetric determination of carbohydrates. Analytical Biochemistry 47:273-279.

Li G, Meng F, Wei X, Lin M (2019) Postharvest dipping treatment with BABA induced resistance against rot caused by *Gilbertella persicaria* in red pitaya fruit. Scientia Horticulturae 257:108713.

Low PS, Merida JR (1996) The oxidative burst in plant defense: function and signal transduction. Physiologia Plantarum 96:533-542.

Mauch-Mani B, Baccelli I, Luna E, Flors V (2017) Defense priming: an adaptive part of induced resistance. Annual Review of Plant Biology 68:485-512.

Mueller MJ (1997) Enzymes involved in jasmonic acid biosynthesis. Physiologia Plantarum 100:653-663.

Mignolet-Spruyt L, Xu E, Idänheimo N, Hoeberichts FA, Mühlenbock P, Brosché M, Van Breusegem F, Kangasjärvi J (2016) Spreading the news: subcellular and organellar reactive oxygen species production and signalling. Journal of Experimental Botany 67:3831-3844.

Nakano Y, Asada K (1981) Hydrogen peroxide is scavenged by ascorbate-specific peroxidase in spinach chloroplasts. Plant and Cell Physiology 22:867-880.

Neilson EH, Goodger JQ, Woodrow IE, Møller BL (2013) Plant chemical defense: at what cost?. Trends in Plant Science 18:250-258.

Ojaghian MR, Wang L, Cui Zq, Yang C, Zhongyun T, Xie GL (2014) Antifungal and SAR potential of crude extracts derived from neem and ginger against storage carrot rot caused by *Sclerotinia sclerotiorum*. Industrial Crops and Products 55:130-139.

Oliver RP, Solomon PS (2004) Does the oxidative stress used by plants for defence provide a source of nutrients for pathogenic fungi?. Trends in Plant Science 9:472-473.

Pagani APS, Dianese AC, Café-Filho AC (2014) Management of wheat blast with synthetic fungicides, partial resistance and silicate and phosphite minerals. Phytoparasitica 42:609-617.

Pitzschke A, Forzani C, Hirt H (2006) Reactive oxygen species signaling in plants. Antioxidants & Redox Signaling 8:1757-1764.

Reglinski T, Dann E, Deverall B (2007) Integration of induced resistance in crop production. In: Walters D, Newton A, Lyon G (Eds.). Induced Resistance for Plant Defence: a Sustainable Approach to Crop Protection. Blackwell Publishing, Oxford. pp. 201-228.

Rios JA, Debona D, Duarte HSS, Rodrigues FA (2013) Development and validation of a standard area diagram set to assess blast severity on wheat leaves. European Journal of Plant Pathology 136:603-611.

Rios JA, Rios VS, Aucique-Pérez CE, Cruz MFA, Morais LE, DaMatta FM, Rodrigues FA (2017) The photosynthetic performance and source-sink relationships are altered on wheat plants infected by *Pyricularia oryzae*. Plant Pathology 66:1496-1507.

Rios JA, Rodrigues FA, Debona D, Resende RS, Moreira WR, Andrade CCL (2014) Induction of resistance to *Pyricularia oryzae* in wheat by acibenzolar-S-methyl, ethylene and jasmonic acid. Tropical Plant Pathology 39:224-233.

Rodrigues FA, Aucique-Pérez CE, Debona D, Rios JA (2020) Effect of blast on wheat physiology. In: Kumar S, Kashyap PL, Singh GP (Eds.). Wheat Blast. CRC Press, Boca Raton. 1st Edition. pp. 131-148.

Rodrigues FA, Rios JA, Debona D, Aucique-Pérez CE (2017) *Pyricularia oryzae*-wheat interaction: physiological changes and disease management using mineral nutrition and fungicides. Tropical Plant Pathology 42:223-229.

Rolfe SA, Scholes JD (2010) Chlorophyll fluorescence imaging of plant-pathogen interactions. Protoplasma 247:163-175.

Sánchez-Vallet A, Mesters JR, Thomma BPHJ (2015) The battle for chitin recognition in plant-microbe interactions. FEMS Microbiology Reviews 39:171-183.

Santos RP, Cruz, ACF, Iarema L, Kuki KN, Otoni WC (2008) Protocolo para extração de pigmentos foliares em porta-enxertos de videira micropropagados. Ceres 55:356-364.

Sharma P, Jha AB, Dubey RS, Pessarakli M (2012) Reactive oxygen species, oxidative damage, and antioxidative defense mechanism in plants under stressful conditions. Journal of Botany 2012:1-26.

Siegrist J, Orober M, Buchenauer H (2000) β-aminobutyric acid-mediated enhancement of resistance in tobacco to tobacco mosaic virus depends on the accumulation of salicylic acid. Physiological and Molecular Plant Pathology 56:95-106.

Silveira PR, Nascimento KJT, Andrade CCL, Bispo WMS, Oliveira JR, Rodrigues FA, (2015) Physiological changes in tomato leaves arising from *Xanthomonas gardneri* infection. Physiological and Molecular Plant Pathology 92:130-138.

Slaughter A, Daniel X, Flors V, Luna E, John B, Mauch-Mani B (2012) Descendants of primed *Arabidopsis* plants exhibit resistance to biotic stress. Plant Physiology 158:835-843.

Spoel SH, Dong X (2012) How do plants achieve immunity? Defense without specialized immune cells. Nature Reviews Immunology 12:89-100.

Tarkowski LP, Signorelli S, Höfte M (2020) γ-Aminobutyric acid and related amino acids in plant immune responses: Emerging mechanisms of action. Plant, Cell & Environment 43:1103-1116.

Tarkowski LP, Van de Poel B, Höfte M, Van den Ende W (2019) Sweet immunity: inulin boosts resistance of lettuce (*Lactuca sativa*) against grey mold (*Botrytis cinerea*) in an ethylene-dependent manner. International Journal of Molecular Sciences 20:1052.

Tatagiba SD, Rodrigues FA, DaMatta FM (2015) Leaf gas exchange and chlorophyll *a* fluorescence imaging of rice leaves infected with *Monographella albescens*. Phytopathology 105:180-188.

Tatagiba SD, Rodrigues FA, Filippi MCC, Silva GB, Silva LC (2014) Physiological responses of rice plants supplied with silicon to *Monographella albescens* infection. Journal of Phytopathology 162:596-606.

Thevenet D, Pastor V, Baccelli I, Balmer A, Vallat A, Neier R, Glauser G, Mauch-Mani B (2017) The priming molecule *β*-aminobutyric acid is naturally present in plants and is induced by stress. New Phytologist 213:552-559.

Turkan I (2018) ROS and RNS: key signalling molecules in plants. Journal of Experimental Botany 69:3313-3315.

Urashima AS, Grosso CRF, Stabili A, Freitas EG, Silva CP, Netto DCS, Franco I, Merola Bottan JH (2009) Effect of *Magnaporthe grisea* on seed germination, yield and quality of wheat. In: Wang GL, Valent B (Eds.). Advances in Genetics, Genomics and Control of Rice Blast Disease. Springer, Berlin. pp. 267-77.

Velikova V, Yordanov I, Edreva A (2000) Oxidative stress and some antioxidant systems in acid rain-treated bean plants: protective role of exogenous polyamines. Plant Science 151:59-66.

Veluchamy S, Williams B, Kim K, Dickman MB (2012) The CuZn superoxide dismutase from *Sclerotinia sclerotiorum* is involved with oxidative stress tolerance, virulence, and oxalate production. Physiological and Molecular Plant Pathology 78:14-23.

Wang C, El-Shetehy M, Shine MB, Yu K, Navarre D, Wendehenne D, Kachroo A, Kachroo P (2014) Free radicals mediate systemic acquired resistance. Cell Reports 7:348-355.

Wang S, Asuke S, Vy TTP, Inoue Y, Chuma I, Win J, Kato K, Tosa Y (2018) A new resistance gene in combination with *Rmg8* confers strong resistance against *Triticum* isolates of *Pyricularia oryzae* in a common wheat landrace. Phytopathology 108:1299-1306.

Wellburn AR (1994) The spectral determination of chlorophylls *a* and *b,* as well as total carotenoids, using various solvents with spectrophotometers of different resolution. Journal of Plant Physiology 144:307-313.

Xavier Filha MS, Rodrigues FA, Domiciano GP, Oliveira HV, Silveira PR, Moreira WR (2011) Wheat resistance to leaf blast mediated by silicon. Australasian Plant Pathology 40:28-38.

Yamauchi Y, Furutera A, Seki K, Toyoda Y, Tanaka K, Sugimoto Y (2008) Malondialdehyde generated from peroxidized linolenic acid causes protein modification in heat-stressed plant. Plant Physiology and Biochemistry 46:786-793.

Yi-Lan J, Shi-Long J, Xuan-Li J (2021) Disease-resistant identification and analysis to transcriptome differences of blueberry leaf spot induced by beta-aminobutyric acid. Archives of Microbiology 203:3623-3632.

You J, Chan Z (2015) ROS regulation during abiotic stress responses in crop plants. Frontiers in Plant Science 6:1092.

Zadoks JC, Chang TT, Konzak CF (1974) A decimal code for the growth stages of cereals. Weed Research 14:415-421.

Zhang G, Cui Y, Ding X, Dai Q (2013) Stimulation of phenolic metabolism by silicon contributes to rice resistance to sheath blight. Journal of Nutrition and Soil Science 176:118-124.

Zimmerli L, Jakab C, Metraux JP, Mauch-Mani B (2000) Potentiation of pathogen-specific defense mechanisms in *Arabidopsis* by β-aminobutyric acid. Proceedings of the National Academy of Sciences of the United States America 97:12920-12925.

Zimmerli L, Metraux JP, MauchMani B (2001) *β*-aminobutyric acid-induced protection of Arabidopsis against the necrotrophic fungus *Botrytis cinerea*. Plant Physiology 126:517-523.

Tables and Figures

Table 1. Analysis of variance for the effects of inducers of resistance (IR), plant inoculation (PI), and the IR × PI interaction for blast severity (Sev), area under blast progress curve (AUBPC), variable-to-maximum chlorophyll *a* fluorescence ratio (F_v/F_m), photochemical yield (Y(II)), yield for dissipation by down-regulation (Y(NPQ)), yield for non-regulated dissipation (Y(NO)), concentrations of chlorophylls *a*+*b* (Chl *a*+*b*) and carotenoids (Car), activities of superoxide dismutase (SOD), catalase (CAT), ascorbate peroxidase (APX), glutathione reductase (GR), chitinase (CHI), *β*-1,3-glucanase (GLU), peroxidase (POX), phenylalanine ammonia-lyase (PAL), polyphenoloxidase (PPO), and lipoxygenase (LOX) as well as concentrations of malondialdehyde (MDA), hydrogen peroxide (H_2O_2), superoxide anion radical ($O_2^{\bullet-}$), total soluble phenolics (TSP), and lignin-thioglycolic acid (LTGA) derivatives.

Variables/Parameters	IR	PI	IR × PI
Sev	**< 0.001**	-	-
AUBPC	**< 0.001**	-	-
F_v/F_m	**0.002**	**< 0.001**	**0.005**
Y(II)	**< 0.001**	**< 0.001**	**0.002**
Y(NPQ)	**< 0.001**	**< 0.001**	**0.015**
Y(NO)	**< 0.001**	**< 0.001**	**< 0.001**
Chl *a*+*b*	**< 0.001**	**< 0.001**	0.121
Car	**< 0.001**	**< 0.001**	**< 0.001**
SOD	0.069	**0.006**	0.876
CAT	0.427	**< 0.001**	**0.013**
APX	**0.010**	**< 0.001**	0.335
GR	0.122	**< 0.001**	**0.002**
CHI	0.065	0.297	**0.016**
GLU	**0.010**	**< 0.001**	**0.013**
POX	0.773	**< 0.001**	0.401
PAL	0.658	**< 0.001**	0.626
PPO	0.960	**< 0.001**	0.586
LOX	0.564	**< 0.001**	0.488
MDA	**0.016**	**0.008**	0.096
H_2O_2	0.161	0.056	**0.016**
$O_2^{\bullet-}$	**0.002**	**< 0.001**	**0.007**
TSP	**< 0.001**	0.618	**< 0.001**
LTGA derivatives	**< 0.001**	**< 0.001**	**0.002**

[a] Bold values are significant ($P \leq 0.05$).

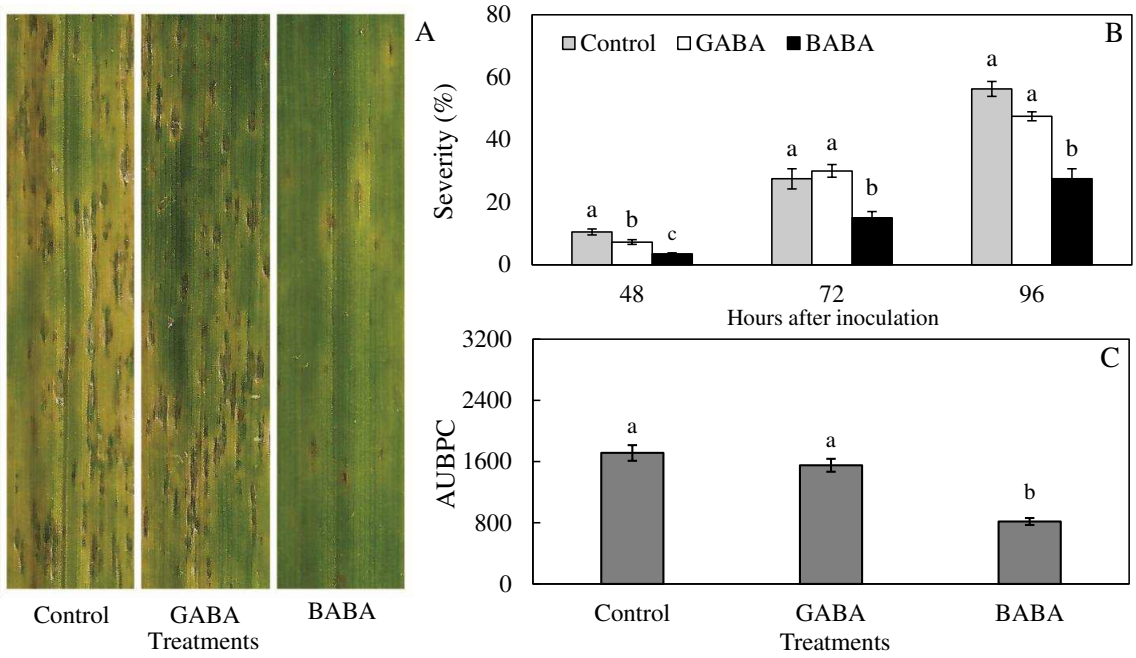

Figure 1. Symptoms of blast at 96 hours after inoculation with *Pyricularia oryzae* (A), severity of blast (B), and area under blast progress curve (AUBPC) (C) determined on the leaves of wheat plants that were sprayed with water (control) or with solutions of γ-aminobutyric acid (GABA) and *β*-aminobutyric acid (BABA). Means followed by different letters in graphics B (at each evaluation time) and C are significantly different ($P \leq 0.05$) according to Tukey's test. Bars represent the standard error of the means.

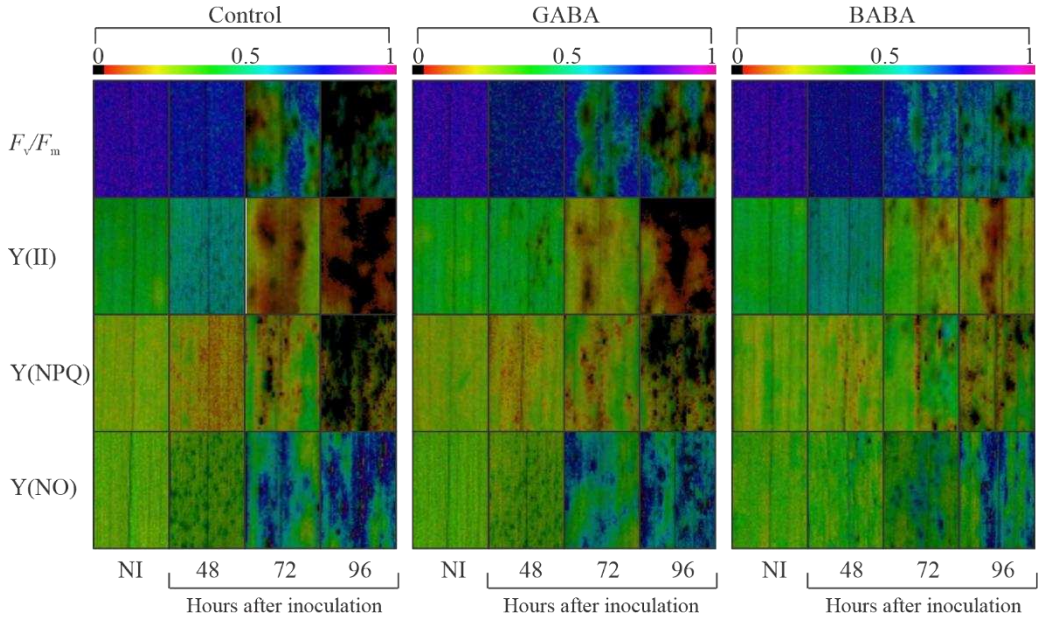

Figure 2. Images of chlorophyll *a* fluorescence parameters: variable-to-maximum chlorophyll a fluorescence ratio (F_v/F_m), photochemical yield (Y(II)), yield for dissipation by downregulation (Y(NPQ)), and yield for non-regulated dissipation (Y(NO)) determined on the leaves of wheat plants that were sprayed with water (control) or with solutions of γ-aminobutyric acid (GABA) and *β*-aminobutyric acid (BABA) and non-inoculated (NI) or at different times after inoculation with *Pyricularia oryzae*.

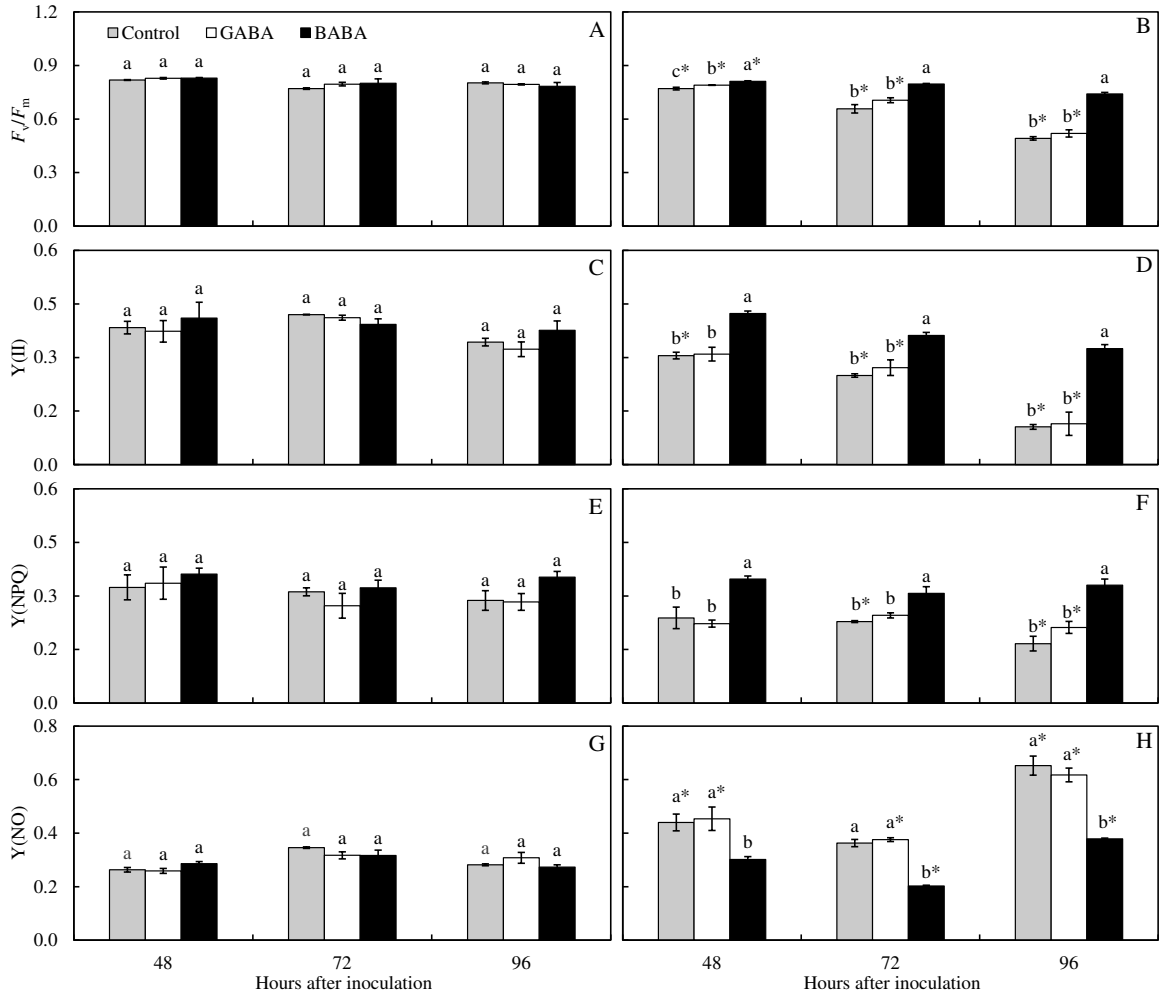

Figure 3. Quantification of chlorophyll *a* parameters: variable-to-maximum chlorophyll *a* fluorescence ratio (F_v/F_m) (A and B), photochemical yield (Y(II)) (C and D), yield for dissipation by down-regulation (Y(NPQ)) (E and F), and yield for non-regulated dissipation (Y(NO) (G and H) on the leaves of wheat plants that were sprayed with water (control) or with solutions of γ-aminobutyric acid (GABA) and *β*-aminobutyric acid (BABA) and non-inoculated (A, C, E, and G) or inoculated (B, D, F, and H) with *Pyricularia oryzae*. For each evaluation time, means from treatments followed by different letters and for non-inoculated and inoculated plants, for each treatment, followed by an asterisk (*) are significantly different ($P \leq 0.05$) according to *F* and Tukey tests, respectively. Bars represent the standard error of the means.

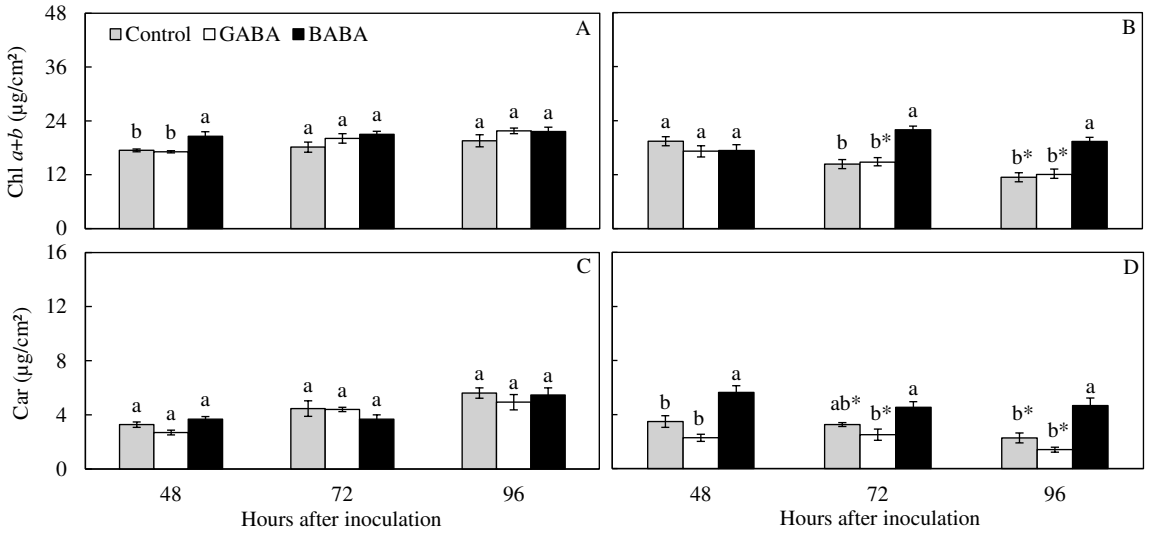

Figure 4. Concentrations of chlorophylls *a+b* (Chl *a+b*) (A and B) and carotenoids (Car) (C and D) determined on the leaves of wheat plants that were sprayed with water (control) or with solutions of γ-aminobutyric acid (GABA) and *β*-aminobutyric acid (BABA) and non-inoculated (A and C) or inoculated (B and D) with *Pyricularia oryzae*. For each evaluation time, means from treatments followed by different letters and for non-inoculated and inoculated plants, for each treatment, followed by an asterisk (*) are significantly different ($P \leq 0.05$) according to *F* and Tukey tests, respectively. Bars represent the standard error of the means.

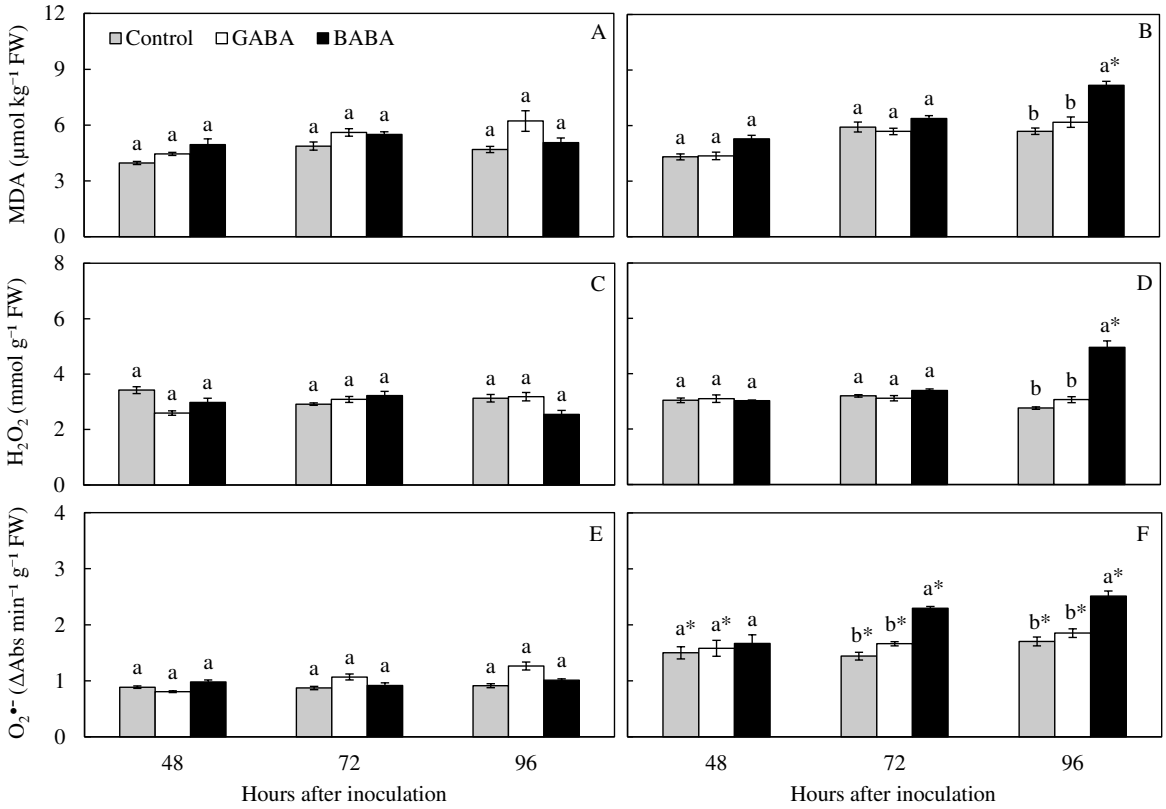

Figure 5. Concentrations of malondialdehyde (MDA) (A and B), hydrogen peroxide (H_2O_2) (C and D), and superoxide anion radical ($O_2^{\bullet-}$) (E and F) determined on the leaves of wheat plants that were sprayed with water (control) or with solutions of γ-aminobutyric acid (GABA) and *β*-aminobutyric acid (BABA) and non-inoculated (A, C, and E) or inoculated (B, D, and F) with *Pyricularia oryzae*. For each evaluation time, means from treatments followed by different letters and for non-inoculated and inoculated plants, for each treatment, followed by an asterisk (*) are significantly different ($P \leq 0.05$) according to *F* and Tukey tests, respectively. Bars represent the standard error of the means. FW = fresh weight.

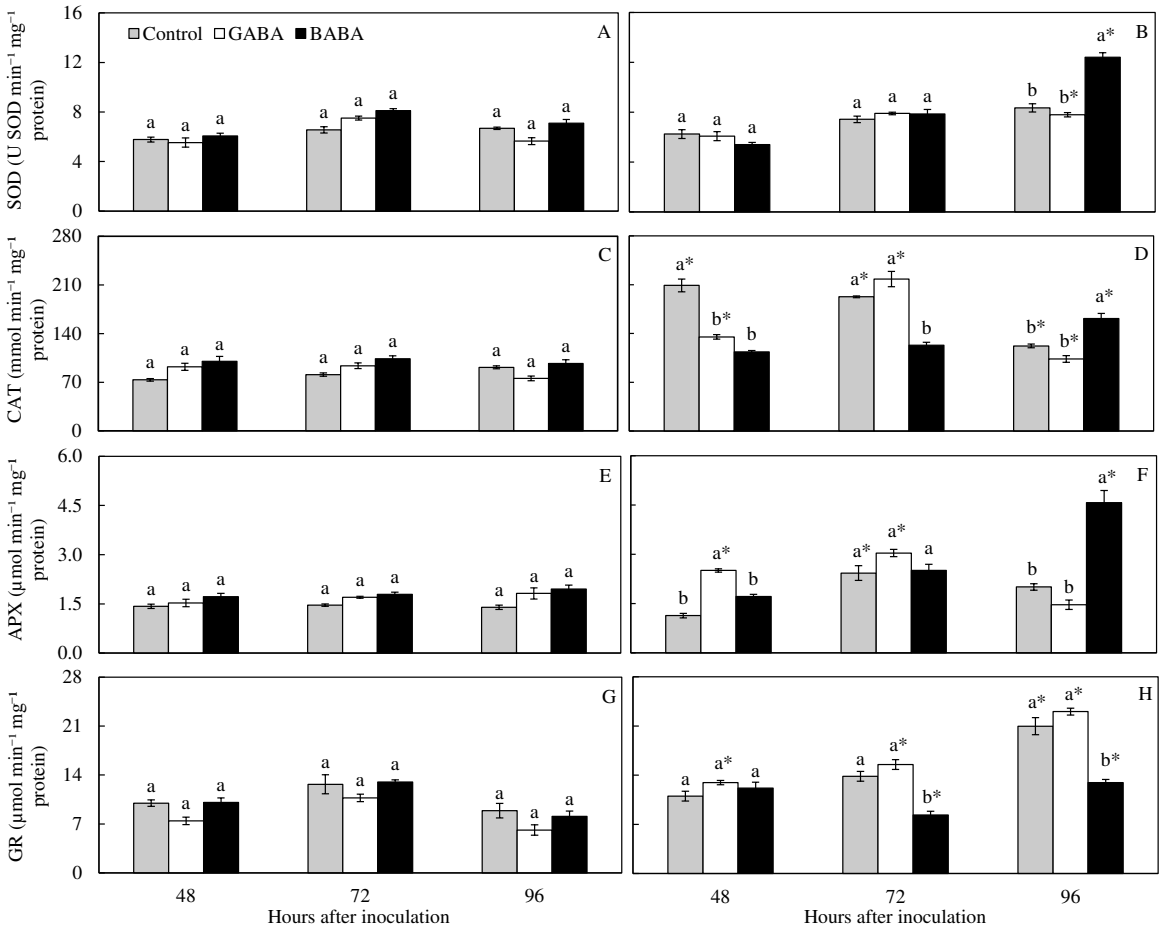

Figure 6. Activities of superoxide dismutase (SOD) (A and B), catalase (CAT) (C and D), ascorbate peroxidase (APX) (E and F), and glutathione reductase (GR) (G and H) determined on the leaves of wheat plants that were sprayed with water (control) or with solutions of γ-aminobutyric acid (GABA) and *β*-aminobutyric acid (BABA) and non-inoculated (A, C, E, and G) or inoculated (B, D, F, and H) with *Pyricularia oryzae*. For each evaluation time, means from treatments followed by different letters and for non-inoculated and inoculated plants, for each treatment, followed by an asterisk (*) are significantly different ($P \leq 0.05$) according to *F* and Tukey tests, respectively. Bars represent the standard error of the means.

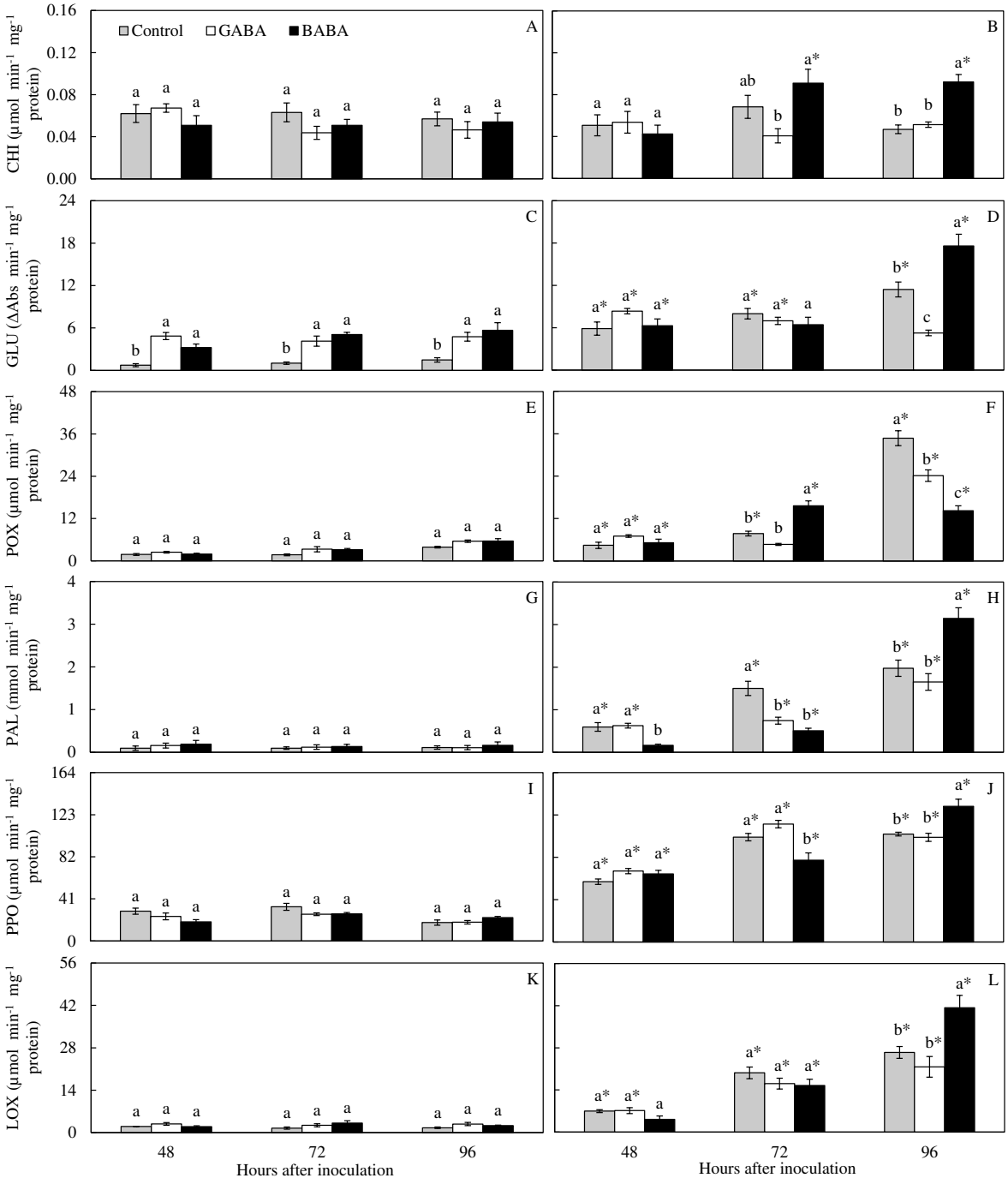

Figure 7. Activities of chitinase (CHI) (A and B), *β*-1,3-glucanase (GLU) (C and D), peroxidase (POX) (E and F), phenylalanine ammonia-lyase (PAL) (G and H), polyphenoloxidase (PPO) (I and J), and lipoxygenase (LOX) (K and L) determined on the leaves of wheat plants that were sprayed with water (control) or with solutions of γ-aminobutyric acid (GABA) and *β*-aminobutyric acid (BABA) and non-inoculated (A, C, E, G, I, and K) or inoculated (B, D, F, H, J, and L) with *Pyricularia oryzae*. For each evaluation time, means from treatments followed

by different letters and for non-inoculated and inoculated plants, for each treatment, followed by an asterisk (*) are significantly different ($P \leq 0.05$) according to F and Tukey tests, respectively. Bars represent the standard error of the means.

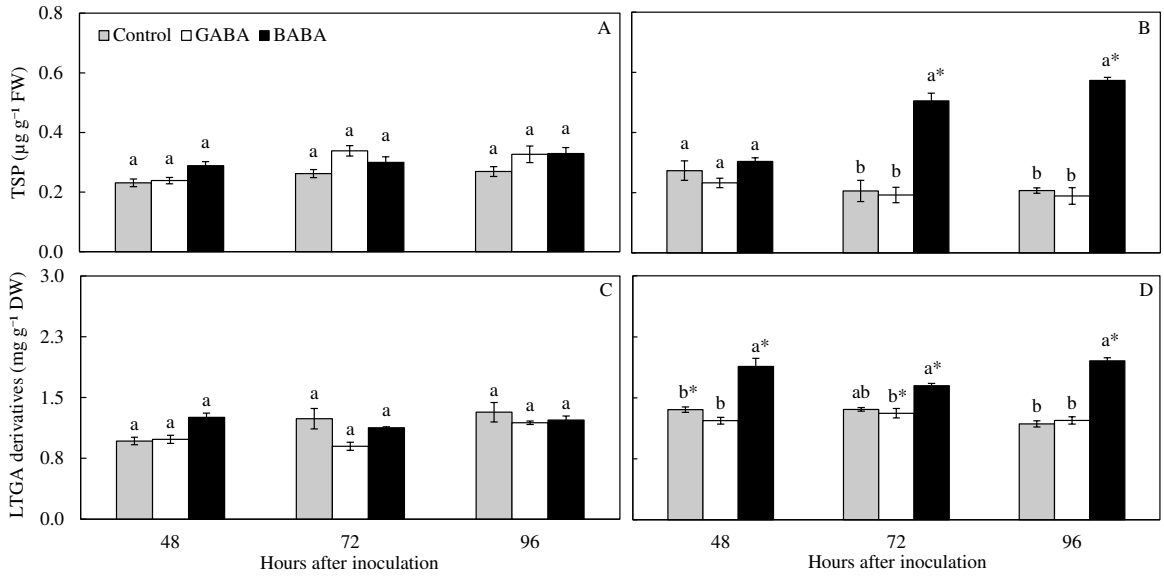

Figure 8. Concentrations of total soluble phenolics (TSP) (A and B) and lignin-thioglycolic acid (LTGA) derivatives (C and D) determined on the leaves of wheat plants that were sprayed with water (control) or with solutions of γ-aminobutyric acid (GABA) and *β*-aminobutyric acid (BABA) and non-inoculated (A and C) or inoculated (B and D) with *Pyricularia oryzae*. For each evaluation time, means from treatments followed by different letters and for non-inoculated and inoculated plants, for each treatment, followed by an asterisk (*) are significantly different ($P \leq 0.05$) according to *F* and Tukey tests, respectively. FW and DW = fresh weight and dry weight, respectively.

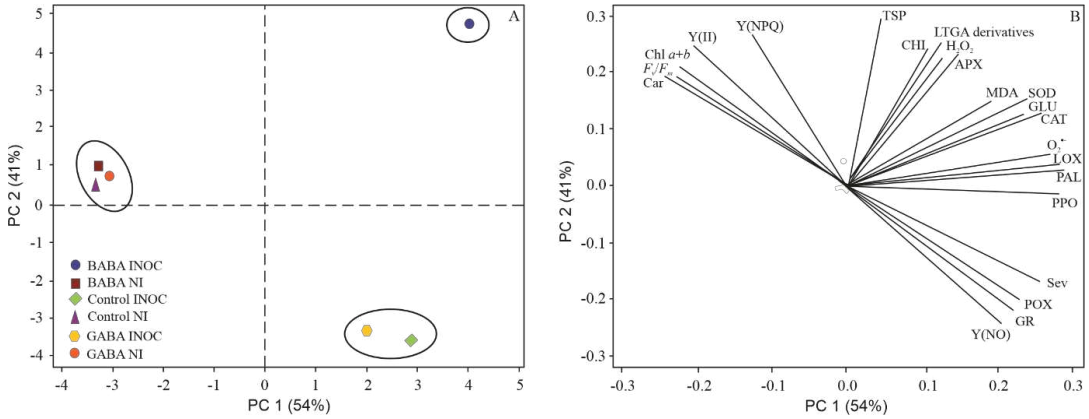

Figure 9. Principal components analysis showing score plot (A) and loading values (B) in the principal component analysis for blast severity (Sev), area under blast progress curve (AUBPC), variable-to-maximum chlorophyll *a* fluorescence ratio (F_v/F_m), photochemical yield (Y(II)), yield for dissipation by down-regulation (Y(NPQ)), yield for non-regulated dissipation (Y(NO)), concentrations of chlorophylls *a*+*b* (Chl *a*+*b*) and carotenoids (Car), activities of superoxide dismutase (SOD), catalase (CAT), ascorbate peroxidase (APX), glutathione reductase (GR), chitinase (CHI), *β*-1,3-glucanase (GLU), peroxidase (POX), phenylalanine ammonia-lyase (PAL), polyphenoloxidase (PPO), and lipoxygenase (LOX) as well as concentrations of malondialdehyde (MDA), hydrogen peroxide (H_2O_2), superoxide anion radical ($O_2^{\bullet-}$), total soluble phenolics (TSP), and lignin-thioglycolic acid (LTGA) derivatives for wheat plants that were sprayed with water (control) or with solutions of γ-aminobutyric acid (GABA) and *β*-aminobutyric acid (BABA) and non-inoculated (NI) or inoculated (INOC) with *Pyricularia oryzae*. Groups were generated from cluster analysis with complete linkage and Pearson distance.